REPORT DOCUMENTATION PAGE

Public reporting burden for this collection of information is estimated to average 1 hour per response, including the time for reviewing instructions, searching existing data sources, gathering and maintaining the data needed, and completing and reviewing the collection of information. Send comments regarding this burden estimate or any other aspect of this collection of information, including suggestions for reducing this burden, to Washington Headquarters Services, Directorate for Information Operations and Reports, 1215 Jefferson Davis Highway, Suite 1204, Arlington, VA 22202-4302, and to the Office of Management and Budget, Paperwork Reduction Project (0704-0188), Washington, DC 20503.

1. AGENCY USE ONLY (Leave blank)	2. REPORT DATE	3. REPORT TYPE AND DATES COVERED
	10 Sep 95	

4. TITLE AND SUBTITLE
A Study of The Cloud-To-Ground Lightning Characteristics During The 21-23 Novermber 1992 Widespread Severe Weather Outbreak

5. FUNDING NUMBERS

6. AUTHOR(S)

William John Carle

7. PERFORMING ORGANIZATION NAME(S) AND ADDRESS(ES)

AFIT Students Attending:

Texas A&M University

8. PERFORMING ORGANIZATION REPORT NUMBER

95-103

9. SPONSORING/MONITORING AGENCY NAME(S) AND ADDRESS(ES)
DEPARTMENT OF THE AIR FORCE
AFIT/CI
2950 P STREET, BLDG 125
WRIGHT-PATTERSON AFB OH 45433-7765

10. SPONSORING/MONITORING AGENCY REPORT NUMBER

11. SUPPLEMENTARY NOTES

12a. DISTRIBUTION/AVAILABILITY STATEMENT
Approved for Public Release IAW AFR 190-1
Distribution Unlimited
BRIAN D. GAUTHIER, MSgt, USAF
Chief of Administration

12b. DISTRIBUTION CODE

13. ABSTRACT (Maximum 200 words)

DTIC
SELECTED
OCT 18 1995
B

19951017 154

DTIC QUALITY INSPECTED 8

14. SUBJECT TERMS

15. NUMBER OF PAGES
109

16. PRICE CODE

17. SECURITY CLASSIFICATION OF REPORT	18. SECURITY CLASSIFICATION OF THIS PAGE	19. SECURITY CLASSIFICATION OF ABSTRACT	20. LIMITATION OF ABSTRACT

A STUDY OF THE CLOUD-TO-GROUND LIGHTNING

CHARACTERISTICS DURING THE 21-23 NOVEMBER 1992 WIDESPREAD

SEVERE WEATHER OUTBREAK

A Thesis

by

WILLIAM JOHN CARLE

Submitted to the Office of Graduate Studies of
Texas A&M University
in partial fulfillment of the requirements for the degree of

MASTER OF SCIENCE

August 1995

Major Subject: Meteorology

A STUDY OF THE CLOUD-TO-GROUND LIGHTNING

CHARACTERISTICS DURING THE 21-23 NOVEMBER 1992 WIDESPREAD

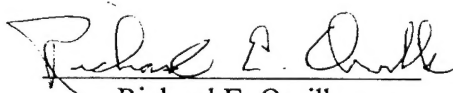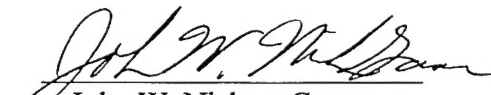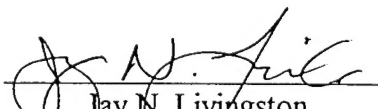# SEVERE WEATHER OUTBREAK

A Thesis

by

WILLIAM JOHN CARLE

Submitted to Texas A&M University
in partial fulfillment of the requirements
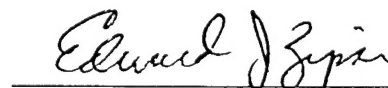for the degree of

MASTER OF SCIENCE

Approved as to style and content by:

Richard E. Orville
(Chair of Committee)

John W. Nielsen-Gammon
(Member)

Jay N. Livingston
(Member)

Edward J. Zipser
(Head of Department)

August 1995

Major Subject: Meteorology

ABSTRACT

A Study of the Cloud-to-Ground Lightning Characteristics During the

21-23 November 1992 Widespread Severe Weather Outbreak. (August 1995)

William John Carle, B.S., United States Air Force Academy;

B.S., Texas A&M University

Chair of Advisory Committee: Dr. Richard E. Orville

A synoptic low pressure system developed in Texas on 21 November 1992 and

propagated to the Great Lakes region on 23 November 1992. Over 90 tornadoes

were spawned throughout the Southeast and parts of the Ohio River Valley. The

cloud-to-ground (CG) lightning characteristics for the system were studied in a storm

relative coordinate system. Results indicate that a moderate negative correlation exists

between the positive flash rate and the median first stroke peak current. A higher

order correlation exists between the negative flash rate and the mean multiplicity.

Maxima of the positive flash density were almost always displaced to the north or east

of the maxima in the negative flash density. The effects of shear on bipolar lightning

patterns indicate that 13 of the 18 bipolar patterns are most closely oriented with the

shear vector associated with the 700 mb-surface layer. A correlation between the

magnitude of the shear vector and the length of the bipolar pattern was not found. No

correlation was found between the percentage of positive lightning and 31 cases of hail

greater than or equal to 0.75 inches. Many of the hail cases were predominantly

associated with negative lightning. The lightning characteristics of 21 F3 and F4 tornadoes studied indicate a possible lag time between the peak in the total, positive, and negative CG flash rates of approximately 10 minutes. Large boxed areas were not the most suitable means of associating CG lightning with the tornadic storms due to varying amounts of contamination of the CG flash rate. Two Houston area cases, for which the CG lightning was isolated to the parent supercell storms, both show a zero CG flash rate just prior (F4 case) and within 10 minutes (F3 case) of the touchdown of the tornadoes. A polarity reversal in the CG flash rate was not observed in any of the cases. No correlation exists between the total storm flash rate and the duration or intensity of any of the tornadic storms studied here.

DEDICATION

This thesis is dedicated to the Savior and Lord of my life, Jesus Christ, and to my wonderful wife Julie and our son Jonathan who faithfully supported me with love and encouragement. This thesis is also dedicated to my family who never gave up on me.

ACKNOWLEDGMENTS

I would first like to thank God who made everything possible. I would also like to thank the members of my committee Dr. Richard E. Orville, Dr. John Nielsen-Gammon, and Dr. Jay Livingston for their invaluable guidance and support during my research. Additionally, I acknowledge the United States Air Force for financially supporting me through my graduate studies while at Texas A&M University.

Special thanks are extended to the members of the Lightning Research Group (Luis Rios, Al Silver, Steve Barnaby, Eric Livingston, Aaron Studwell, Keith Aclin, , and Randy Bass). I am also indebted to Antony Perez and his research on lightning and tornadoes. I would like to acknowledge my good friends and Air Force peers Greg Giondomenica, Tony Moninski, and Scott Saul for their assistance and support. I would also like to thank all of the graduate students and faculty in the Meteorology Department who provided help in a variety of ways, specifically Marion Alcorn, Mike Morgan, Matt Gilmore, Matt Wandishin, Justin Shaw, Magda Hashem, Svetla Veleva, Mike Kay, and many others whom by my negligence have forgotten to properly acknowledge. Also, thanks to some very helpful members of the National Weather Service, specifically William Read, John Livingston, Steve Allen, and Rusty Pfost.

Finally, I am greatly and entirely indebted to the absolute support and love of my family who never gave up on me. Their encouragement helped me to persevere through the many long and stressful hours. Thanks to my brother Dave and sister Grace for their timely assistance in typing and proofreading of this thesis.

TABLE OF CONTENTS

LIST OF FIGURES

LIST OF TABLES

CHAPTER I

INTRODUCTION

The existence of virtually complete spatial coverage of cloud-to-ground (CG) lightning by detection networks in the United States and the availability of this real-time data to operational weather forecasters highlight the importance of lightning research in facilitating its operational use as a possible prognostic tool. While traditional means of forecasting severe weather have improved in recent years, added knowledge gained from the research of CG lightning characteristics of severe storms should enhance future forecast accuracy and provide a greater understanding of convective systems as well as of lightning. Even though CG lightning accounts for only one-third of the total number of electrical discharges from convective clouds in the midlatitudes (Prentice and Mackerras 1977), a comprehensive intracloud (IC) lightning network does not exist. Therefore, studies that are limited to CG flashes should, nonetheless, prove valuable to understanding the interaction between storm kinematics and electrical activity until IC lightning data are available. Most studies concentrate on CG lightning and its relationship to particular weather phenomena by isolating specific cases from various storm systems. The approach of this study is to examine the lightning characteristics of a specific synoptic-scale event.

A powerful storm system, occurring 21-23 November 1992, tore a path of

---

The style is that of the *Monthly Weather Review.*

destruction from Texas through the Southeast, as well as through parts of the Ohio River Valley. During these 40 plus hours of nearly continuous severe weather, 94 known tornadoes were spawned (Natural Disaster Survey Report 1993). Approximately 66% of the tornadoes reported for November were associated with this storm system, including six of seven F4 tornadoes (Goodge 1992). Indiana reported a November state record of 15 tornadoes (Natural Disaster Survey Report 1992). Also noteworthy were the 12 tornadoes reported, including one F3 and one F4, within 130 km of the Houston-Galveston WSR-88D radar (Guerrero and Read 1993). There have only been two other incidents when F4 tornadoes are known to have ever occurred in Southeast Texas (Grazulis 1991).

The goal of this research is to gain a better understanding of the lightning characteristics in severe weather systems by: 1) examining the temporal and spatial lightning patterns of all 21 F3 and F4 tornado occurrences during this outbreak; 2) studying the percentage of positive lightning associated with hail greater than or equal to 0.75 inches in diameter; 3) correlating vertical windshear to bipolar lightning patterns; and 4) examining the lightning characteristics of the 21-23 November 1992 widespread severe weather outbreak relative to the position of the synoptic low pressure system.

Chapter II provides a survey of applicable published literature, and an overview of the synoptic weather conditions associated with the 21-23 November 1992 severe weather outbreak. Chapter III covers the data and its sources, and the methodology for each part of this study. Chapter IV is an overview of the CG lightning relative to

the synoptic storm system. Chapter V deals with the effects of shear on bipolar

lightning patterns. Chapter VI is on the percentage of positive lightning and large hail.

Chapter VII is concerned with the relationship between CG lightning and tornadic

storms. Chapter VIII is the conclusions and recommendations for further research.

CHAPTER II

BACKGROUND

1. Survey of Literature

A number of published studies have suggested a relationship between lightning characteristics and storm severity, including tornadic storms. The results differ from case to case. Early studies of lightning measurements associated with tornadic storms were based on the electromagnetic noise produced by lightning, known as sferics. As noted by MacGorman (1993) many of these early studies found a tendency for sferic rates in the 150 kHz range to peak during severe weather and eventually subside towards the end of the severe weather event. While MacGorman (1993) points out that many of the sferics studies showed a clear tendency for lightning associated with tornadic storms to evolve in characteristic patterns, there are still some inherent uncertainties related to this type of study, one of which is determining the lightning type and flash rate. Later studies which mapped lightning positions were able to alleviate some of these discrepancies and provide better information. A few of these studies will be discussed.

Using data obtained from the National Lightning Detection Network (NLDN), Kane (1991) found a relationship between the 5-min CG lightning flash rate and the occurrence of severe weather. Besides intense downbursts and large hail, Kane (1991) studied two cases of F1 tornadic activity which occurred from 27-28 August 1988, in a region north of the New York-Pennsylvania border. A 10 to 15 minute time lag was

observed between the peak in the 5-min lightning rate of total CG flashes and the onset of the tornadoes.

MacGorman and Nielsen (1991) studied a tornadic supercell storm which occurred on 8 May 1986. Three tornadoes were associated with this storm, including an F3 tornado in Edmond, Oklahoma. They found positive CG lightning activity began just prior to the occurrence of tornadoes and the associated flash rates peaked during the tornadic periods of the storm. They also found negative CG flash rates were positively correlated to the intensity of the low-level cyclonic shear in the mesocyclone vortex. Cyclonic shear is a measure of the mesocyclone rotation, which is equal to half the vertical vorticity for a vertical cylinder rotating as a solid body. Due to significant dissimilarities in the lightning characteristics, MacGorman and Nielsen compared their results of the Edmond tornado to an earlier study conducted by MacGorman et al. (1989), which focused on a tornadic supercell storm that occurred on 22 May 1981. Five tornadoes were associated with this storm, including an F4 near the town of Binger, Oklahoma. Contrary to the previous study, total CG lightning flash rates were found to be negatively correlated with the cyclonic shear in the mesocyclone. MacGorman et al. did find a preference for total CG strikes to be located near the largest reflectivity core during the lifetime of the Binger tornado. Additionally, negative CG flash rates increased after the tornadic storms dissipated. Intracloud (IC) lightning data (not available for the Edmond tornado) were found to dominate during the Binger tornado. MacGorman et al. hypothesized that stronger updrafts in the Binger storm were responsible for the predominance of IC lightning and lack of CG

lightning during the most severe tornado. Stronger updrafts in the Binger storm versus the Edmond storm were deduced from the storm structure, as depicted by Doppler radar reflectivity and wind fields, and also from differences in helicity values and bulk Richardson numbers. Stronger updrafts in the Binger storm caused the main negative charge region to be much higher, producing conditions more favorable to IC discharges than CG flashes (MacGorman et al. 1989).

Seimon (1993) studied an F5 tornado-producing supercell that occurred near Plainfield, Illinois on 28 August 1990. This storm, unlike those previously mentioned, was initially dominated by positive CG lightning (IC flash data were not available). Besides a 20 min lag between the peak in the 5-min flash interval and the time of tornado touchdown, a dramatic change in polarity from positive to negative coincided with the onset of the F5 tornado. Incidentally, there was a 2.5 min interval during the polarity reversal when zero CG flashes were detected. Seimon also notes a steady decline in the peak current of the positive flashes up to the time of the tornado touchdown and an increase in the magnitude of the peak current of the negative flashes until the tornado retraction. CG flash density was also observed to be highly concentrated and frequent along the tornado path.

To further understand the tenable relationship between tornadoes and lightning, other recent studies relate positive CG lightning to specific types of supercells in an attempt to specify the apparent link found between positive lightning and severe weather by a number of investigators (e.g., Rust et al. 1985; Reap and MacGorman 1989; MacGorman and Nielsen 1991). Branick and Doswell (1992) relate high

positive CG lightning rates to low-precipitation (LP) supercell storms and low positive CG lightning rates to high-precipitation (HP) supercells. Those storms dominated by positive flashes produced the most intense tornadoes. They also noticed a tendency for tornadic storms of a particular polarity to be restricted to a given geographical region. This suggests environmental conditions were important in influencing the lightning characteristics of the storms. Curran and Rust (1992) propose that the environments with stronger vertical speed shear influence, in some way, the production of LP storms versus HP storms. They studied an LP storm that evolved into a classic supercell. Positive CG flashes were the dominant polarity during the LP phase, while negative CG flashes dominated during the classic supercell phase. The onset of a tornado coincided with the change in flash polarity, similar to the observations of Seimon (1993). Incidentally, Doswell and Brooks (1993) propose the observed polarity reversal by Seimon was due to a change in supercell type -- from classic to HP supercell storm.

To further understand the conditions under which positive flashes occur in severe storms, MacGorman and Burgess (1994) studied 15 storms. Twelve of these storms produced weak to severe tornadoes, while others produced hail. In general, they found the dominant polarities of storms to coincide with specific geographical regions for a particular day. Polarities tended to change within specific locations for subsequent storms traversing into those regions, similar to the findings of Branick and Doswell (1992). Changes in the dominant polarities also tended to coincide with a change in the storm type. While most storms dominated by positive flashes were

either classic or LP supercell storms, those supercell storms whose dominant polarity switched to negative became either classic or HP supercells. The majority of the storms dominated by positive flashes spawned tornadoes. In every case studied, the most violent tornadoes corresponded to the time of the dominant CG polarity shift from positive to negative flashes when there was a positive flash rate greater than 1.5 min^{-1}. MacGorman and Burgess conclude that while severe weather also occurs in the more common storms dominated by negative CG flashes, those storms dominated by positive flashes tend to produce severe weather more frequently than those dominated by negative flashes.

In an attempt to classify lightning traits common to violent tornadoes, Perez et al. (1995) investigated the flash rates of 42 F4 and F5 tornadoes which occurred from January 1989 through November 1992. In over 70% of the cases a peak in the total CG flash rate was observed to occur prior to the tornado touchdown; however, the time of the overall flash rate maxima occurred prior, during, and after the tornadoes' lifetimes for 17, 14, and 11 cases, respectively. Eleven tornadic storms exhibited an association with high percent positive CG flashes for most of their lifetimes, or revealed a polarity shift coincident to the time of the tornado touchdown. These storms were associated with either long-track tornadoes (mean value of 34.6 miles), F5 damage, or severe weather outbreaks. Furthermore, they found no correlation between the number of flashes and the tornado intensity. Perez et al. conclude that while a viable relationship exists between the CG flash rate and tornadogenesis, further

studies that include both IC and CG lightning data are needed to further understand the apparent relationship between lightning and storm dynamics.

Not only have studies focused on the lightning characteristics of tornadic storms, but they have also concentrated on the occurrence of positive CG lightning in general. It is felt by some researchers that CG polarity may be an important indicator of certain phenomena associated with thunderstorms (Brook et al. 1989). Brook et al. (1982), studying wintertime thunderstorms along the Hokuriku coast of Japan, first noted a possible threshold value of $1.5 \ m \ s^{-1} \ km^{-1}$ in the magnitude of the vertical wind shear for the occurrence of positive CG lightning. An increase in the horizontal winds aloft is believed to create a tilted dipole in the vertical cloud charge structure. They proposed that as positively charged particles located in the upper region of the cloud are sheared or advected away from the cloud's lower region, a pathway is created between the cloud's positive charge region and the ground. This provides an enhanced probability for the occurrence of positive CG lightning. Curran and Rust (1992) also found shear to be a possible contributor to positive lightning. Rust et al. (1985) cited a $2 \ m \ s^{-1} \ km^{-1}$ threshold for the occurrence of positive lightning for the 850-300 mb layer of the environment for springtime storms.

Orville et al. (1988) first noted a tendency for storms to produce a spatial distribution of predominantly positive CG lightning to the northeast and a negatively dominated region to the southwest. The resultant ensemble of positive and negative lightning strikes is known as a bipolar pattern. This pattern was found to be aligned with the upper level geostrophic winds. Typical lengths between the positive and

negative CG flash density centers were larger than the individual cloud sizes and ranged from 60 to 200 km. They hypothesized that besides microphysical charge separation mechanisms, the occurrence of the bipolar pattern was due to the advection of positively charge particles from the upper region of the cloud structure away from the lower negative charge region by the geostrophic wind. They also noticed a tendency for the surface cold front to intersect the center of the bipolar pattern.

Other studies have found analogous results. Rutledge and MacGorman (1988) found an apparent affinity for positive CG lightning to occur from the stratiform region of mesoscale convective systems (MCSs) while negative CG lightning was associated with the convective region. Rutledge and MacGorman noted the possibility of positive charge advection as a contributor to the occurrence of positive CG lightning. While Orville et al.'s (1988) advection theory is based on the large scale motion of the geostrophic wind, Rutledge and MacGorman base their advection of positive charges on the smaller scale storm relative winds. Therefore, Rutledge and MacGorman's bipolar patterns are aligned differently than those observed by Orville et al. Instead of the positive region to the northeast and the negative region to the southwest as described by Orville et al., those observed by Rutledge and MacGorman show the positive strike region to be downshear of the negative strike region for a linear squall line.

Engholm et al. (1990) studied six winter and three summer bipolar patterns. While the winter bipolar patterns showed the same southwest to northeast orientation and approximate lengths as Orville et al. (1988), they did not find the same preferential

location with respect to the surface fronts. They did find the wintertime bipolar patterns aligned with the geostrophic wind, and the summertime bipolar patterns aligned with the vertical wind shear. While their results are consistent with the tilted dipole theory, they also found the stratiform region in squall lines was electrified independently from the deep convective region. Additionally, they found shallow top clouds were more favorable for positive lightning. They conclude that the tilted dipole theory alone does not account for the occurrence of positive lightning; therefore, they recognize the possibility of more than one mechanism.

The results of other research imply a link between lightning and the occurrence of hail. Reap and MacGorman (1989) not only found high positive flash density to be associated with severe weather, but also with the occurrence of large hail. The results of Curran and Rust (1992) support this possibility. Seimon (1993) also noticed large hail (greater than 7 cm in diameter) corresponded to periods predominated with positive lightning. MacGorman and Burgess (1994) found that hail reports generally coincided with the period when positive CG flashes were dominant. They also found the frequency and reported hail size to typically decrease after the negative CG flash rate became the dominant polarity.

There are, however, some exceptions to the general link between positive lightning and large hail. Contrary to aforementioned findings, Nielsen et al. (1994) noted in their study the tendency of a storm to continue to produce large hail even after the dominant polarity of CG flashes reversed to negative. Additionally, a study conducted by Changnon (1994) found *zero* instances of positive lightning occurring in or adjacent

to any of the 48 hailstreaks examined during the summer over the Midwest. Hailstreaks are defined as "the surface embodiment (4.5 km long by 1.3 km wide) of a single volume of hail generated aloft." He notes that previous studies have related negative lightning to deep convection. Therefore, due to the deep convective nature of hail storms, positive flashes are not expected. He also notes that only 23% of the defined lightning centers were associated with the 48 cases of damaging hail.

To further study the nature of positive lightning, Stolzenburg (1994) studied 24 selected summertime thunderstorms in the Great Plains region of the United States. These storms showed high percent positive flashes (hourly averages of 75%-100%) and high flash densities (>0.01 km^{-2} h^{-1}) during the beginning of active CG lightning periods. This differs with many published studies which typically reveal positive CG flash densities as being low (maximum values on the order of 0.01 km^{-2} h^{-1}) when compared to negative CG flash densities (Orville et al. 1988; Rutledge and MacGorman 1988; Brook et al. 1989; and MacGorman and Nielsen 1991). Stolzenburg hypothesized that the high percentage, flash rate, and flash density of positive CG lightning in these storms are possibly associated with a period of rapid increase in cloud top height as depicted by radar echoes and are related to the production of hail. Interestingly, work done by Orville (1994) showed high positive flash densities and percent positive values for the years 1989-91 were favored in the region studied by Stolzenburg (1994).

2. Synoptic Overview

The synoptic overview section primarily focuses on the weather conditions during the period between Saturday morning, 1200 UTC 21 November 1992, and Monday morning, 1200 UTC 23 November 1992. Infrared satellite imagery is shown in Fig. 2.1, National Meteorological Center (NMC) surface weather analyses are shown in Fig. 2.2, and 500-mb and 850-mb analyses are shown in Figs. 2.3 and 2.4, respectively.

a. Initial development

A large, disorganized region of cloud cover is located over the central and southern Rockies as depicted on infrared satellite imagery at 0000 UTC 21 November 1992 (Fig. 2.1a). A visible dry slot in the cloud mass over east central Arizona is associated with a strong 500-mb low and a 100 kt wind maximum on the backside of the 500-mb trough axis (not shown). Over the next 12 hours the storm system becomes better organized as seen in the satellite imagery (Fig. 2.1b). Note the beginning of a line of convection in central Texas (see circled region in Fig. 2.1b) just ahead of the position of the surface low (Fig. 2.2a). During the next 48 hours, as the system intensifies, most of the severe weather develops along and ahead of this initial line of convection.

At the 500 mb level, a pocket of cold air (-31°C) is associated with the low pressure center at 500 mb level (Fig. 2.3a). A strong jet is evident to the southwest of the low in conjunction with an area of divergence located over west central Texas.
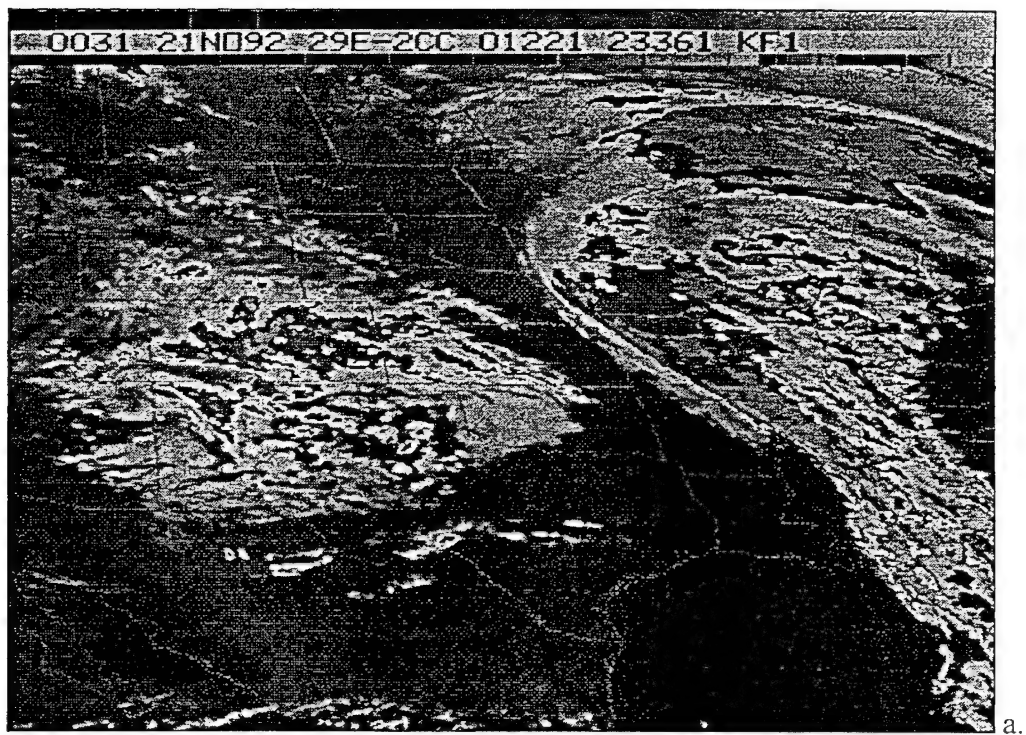
Fig. 2.1. Infrared satellite imagery of central United States for (a) 0031 UTC 21 November 1992, (b) 1231 UTC 21 November 1992 (see text for description of encircled region), (c) 0031 UTC 22 November 1992, (d) 1231 UTC 22 November 1992, (e) 0001 UTC 23 November 1992, (f) 1201 UTC 23 November 1992.

c.

d.

Fig. 2.1 (Continued).

0001 23N092 29E=4ZA 01032 23081 CC1

e.

f.
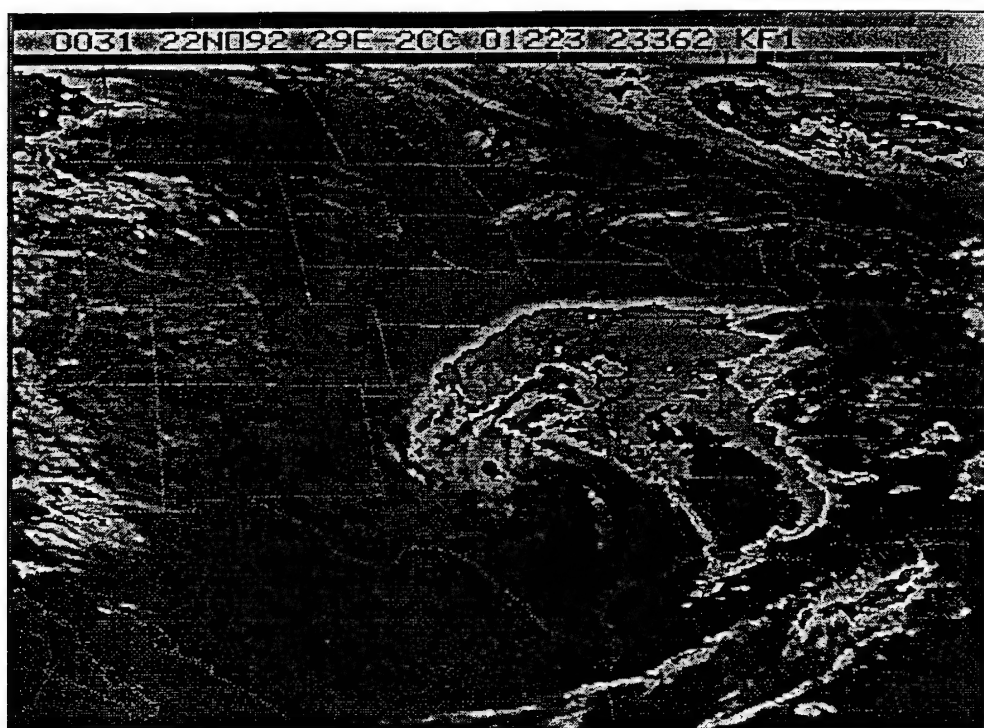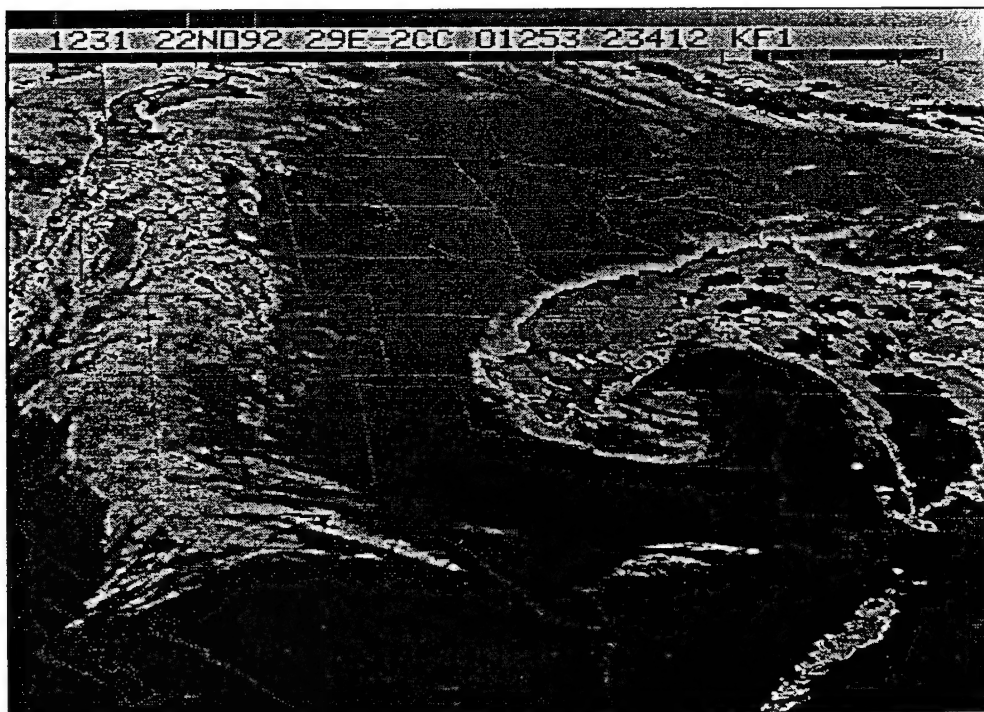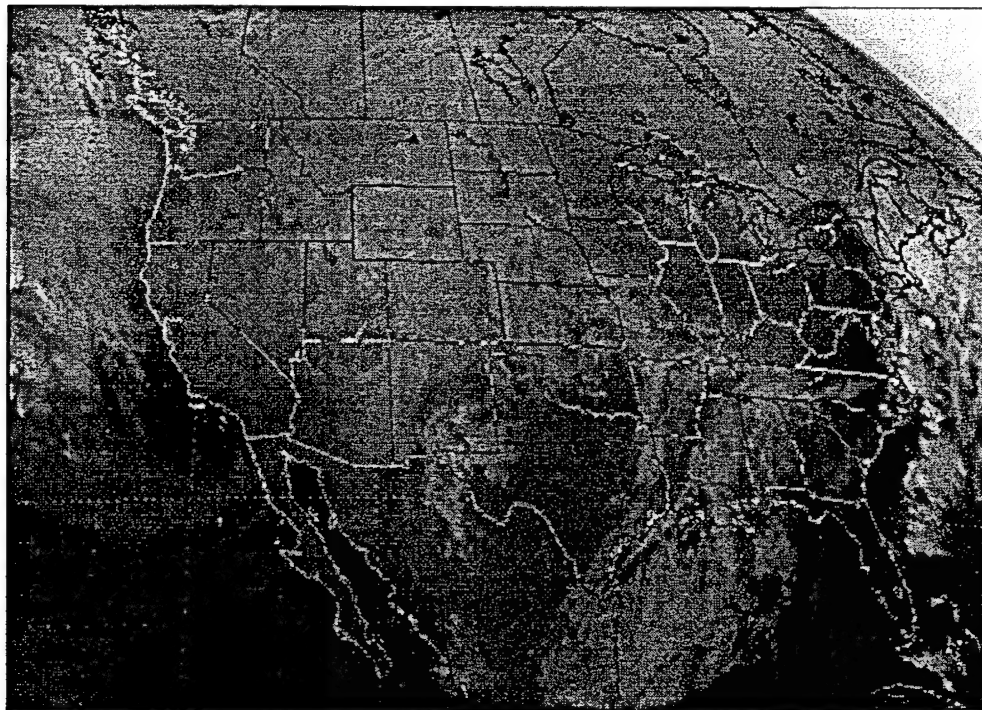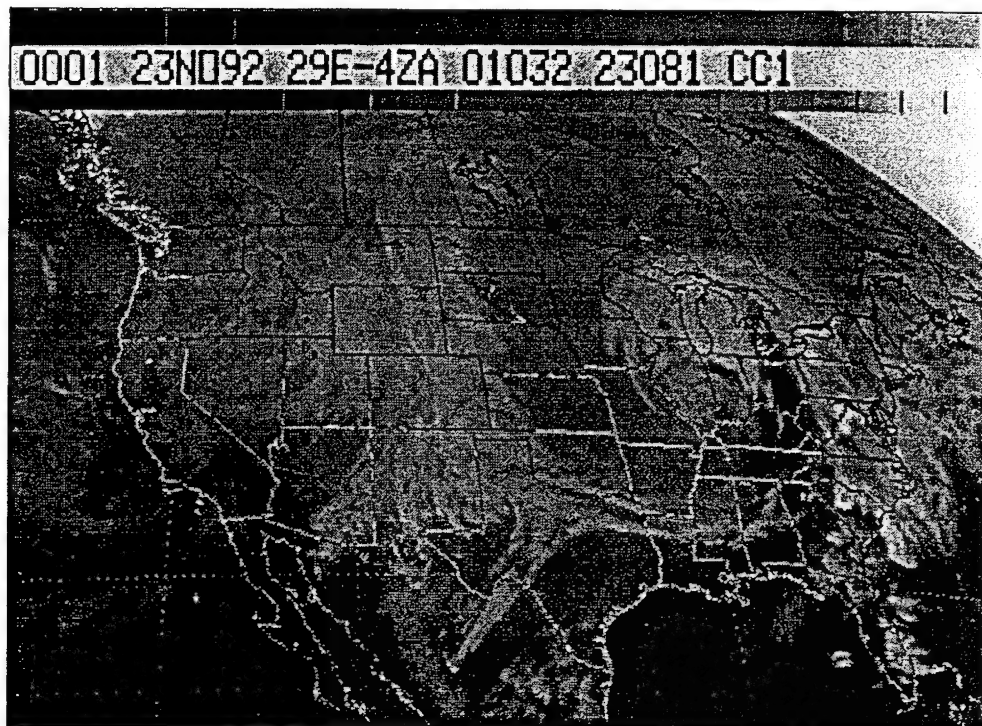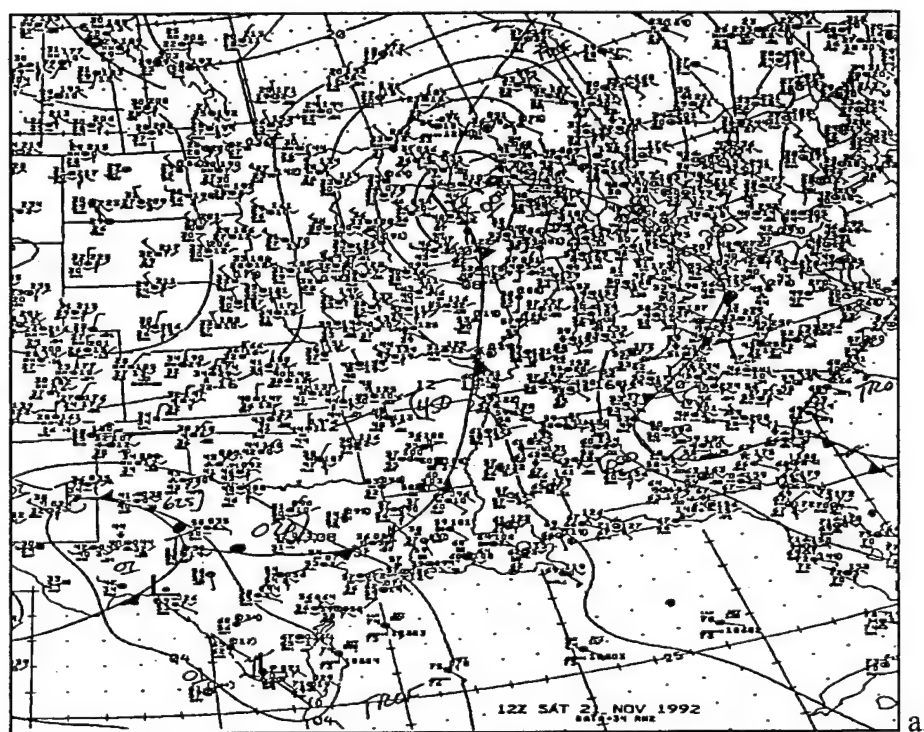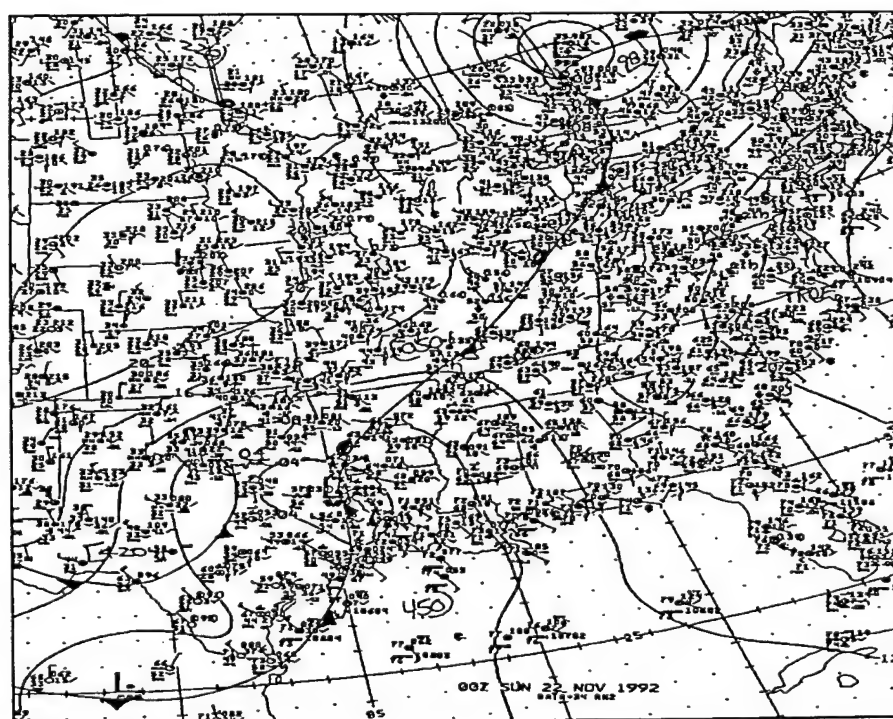
Fig. 2.1 (Continued).

Fig. 2.2. Surface weather analysis valid for (a) 1200 UTC 21 November 1992, (b) 0000 UTC 22 November 1992, (c) 1200 UTC 22 November 1992, (d) 0000 UTC 23 November 1992.

c.

d.
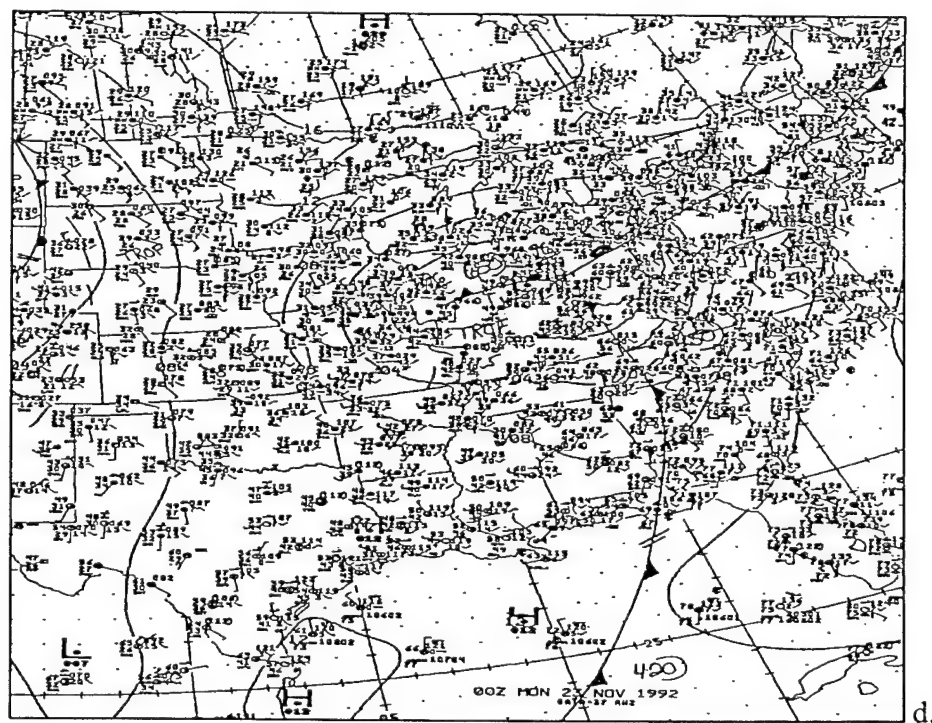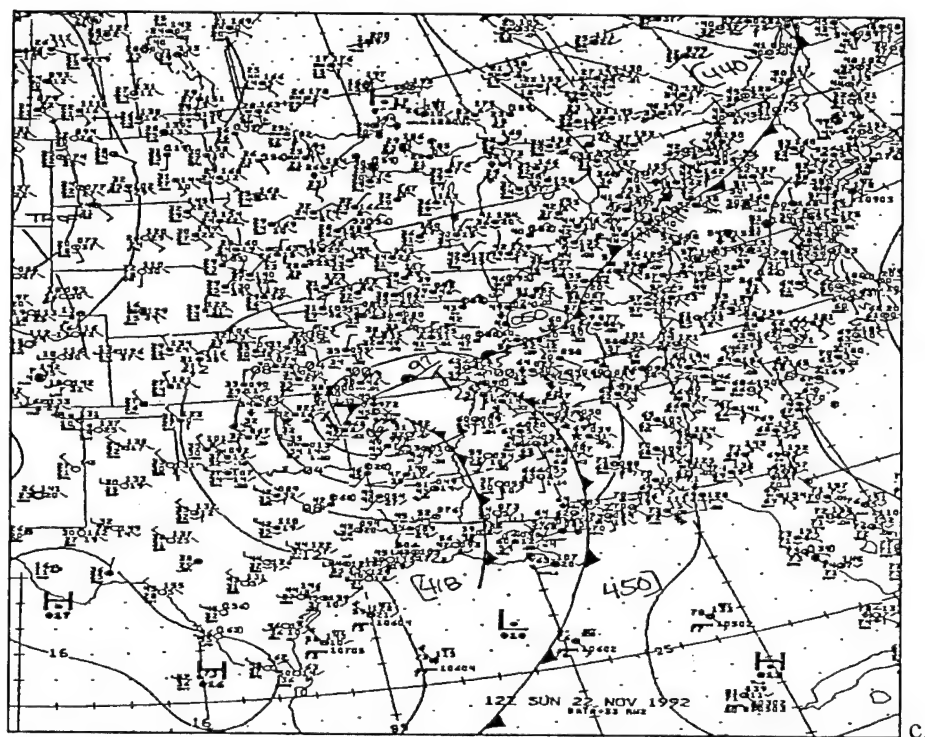
Fig. 2.2 (Continued).
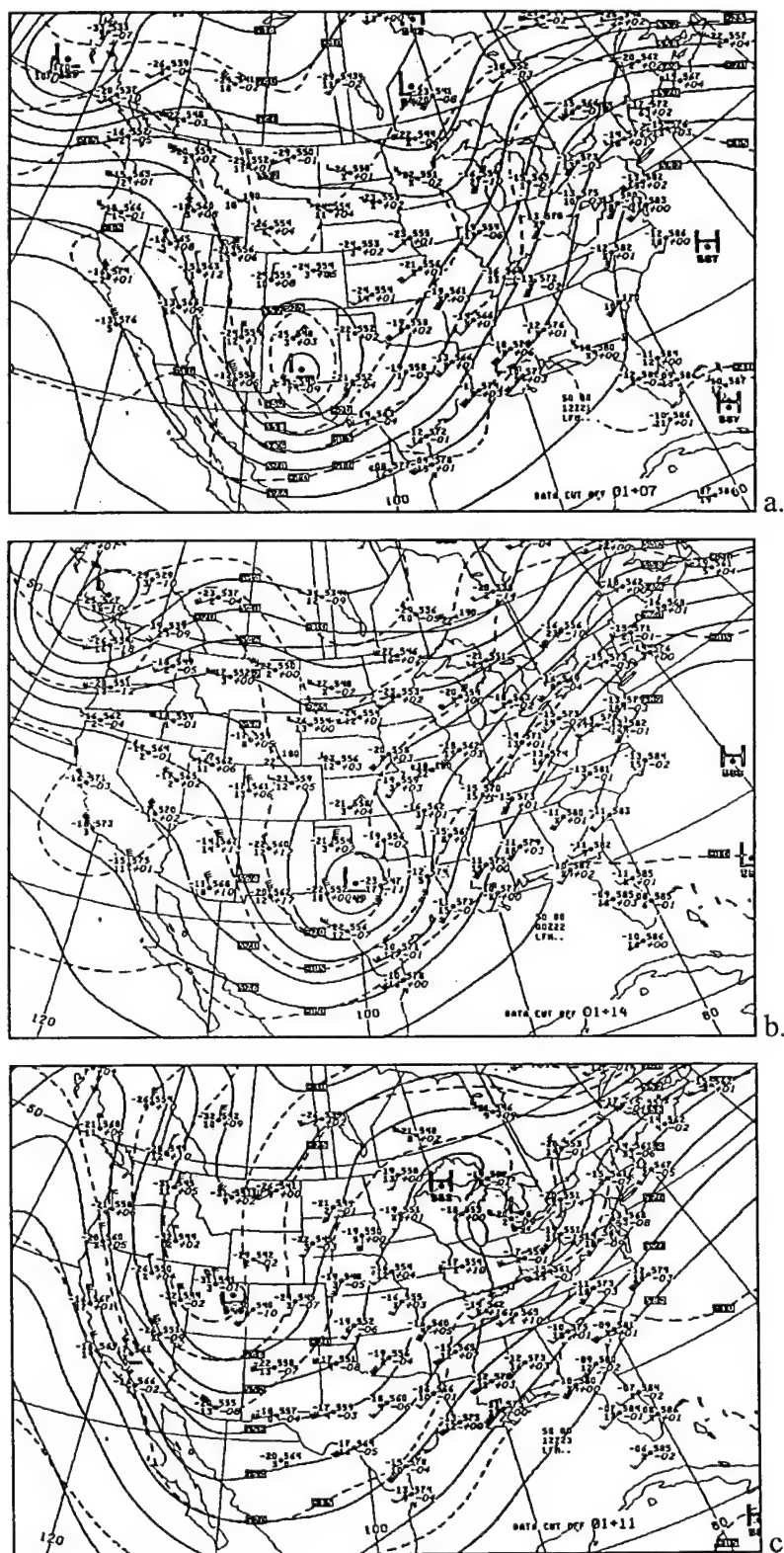
Fig. 2.3. 500 mb analysis valid for (a) 1200 UTC 21 November 1992, (b) 0000 UTC
22 November 1992, (c) 1200 UTC 23 November 1992.
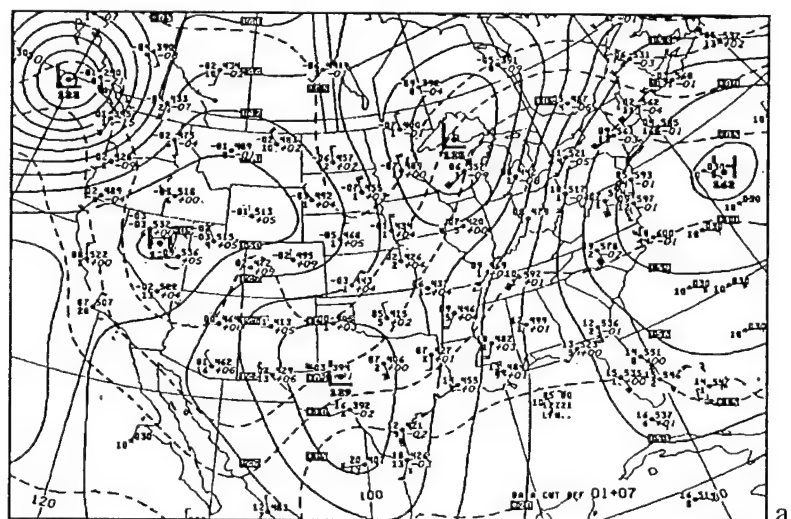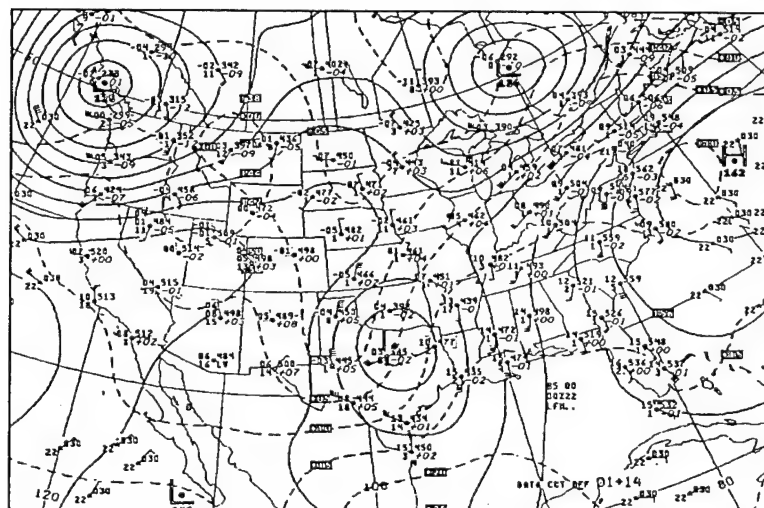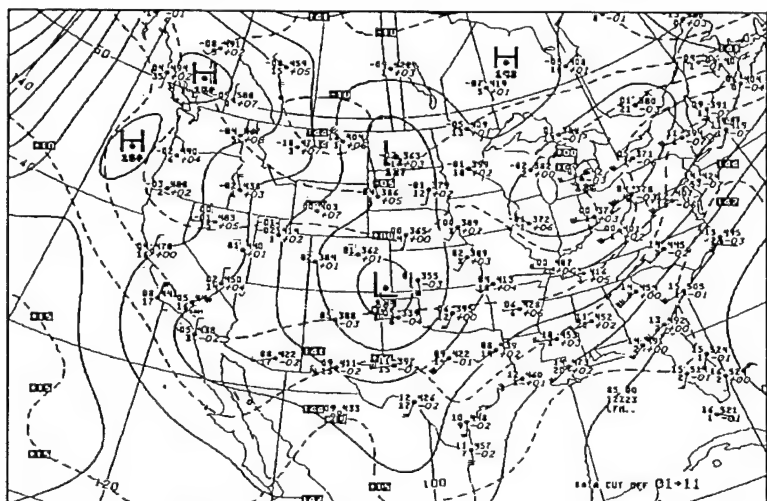
Fig. 2.4. 850 mb analysis valid for (a) 1200 UTC 21 November 1992, (b) 0000 UTC
22 November 1992, (c) 1200 UTC 23 November 1992.

In the lower levels, 50 kt winds over southern Texas at 850 mb reveal the presence of a strong low-level jet (Fig. 2.4a). Warm moist air from the Gulf of Mexico is advected over the eastern portion of the state by the low-level jet.

At the surface, the incipient low pressure center is located under the 500-mb divergence area (Fig. 2.2a). The winds along the Texas coast are mostly onshore advecting warm moist air ahead of the developing low center. Another surface cyclone is located over Wisconsin with a trailing cold front becoming a warm front associated with the developing low in western Texas.

b. Synoptic evolution

The storm system reaches the mature stage by 0000 UTC 22 November 1992 (Fig. 2.1c). Figures 2.1d-f illustrate the continued evolution of the storm system.

The strongest and deepest convection occurs at the beginning of the 12-hr period between 0000 UTC 22 November 1992 and 1200 UTC 22 November 1992. Strong winds of at least 70 kts at 500 mb are associated with the principal vorticity maximum and are advecting cold air from the base of the short-wave trough (Fig 2.3a). Diverging winds at 500 mb over Louisiana reflect the exist region of an upper level jet streak. The resulting deep convection is visible at 0031 UTC 22 November 1992 (Fig. 2.1c) over Louisiana ahead of the surface cold front. All the tornadoes associated with the widespread outbreak occur along or ahead of the cold front (Riordan et al. 1993). The associated surface low pressure center located over northeastern Texas has developed into the main low pressure center, while another low is situated over Oklahoma with a weak frontal boundary extending through central Texas (Fig. 2.2b).

Rain and snow are reported over northern Texas through Missouri, while snow is reported over western Nebraska and the Oklahoma panhandle. Low-level moisture from the Gulf of Mexico continues to be advected ahead of the surface cold front. Strong low-level shear also exists ahead of this front.

Between 1200 UTC 22 November 1992 and 0000 UTC 23 November 1992, two separate tornado outbreaks occur in association with regions of strong upper level divergence (not shown) over the Midwest and over the Southeast. Additionally, the majority of the severe weather is noted to occur near the 850 mb jet (Natural Disaster Survey Report 1992) (Figs. 2.4b, c). Winds as high as 65 kts are over Illinois at 1200 UTC 22 November 1992 (not shown) before the time of the outbreak over the Ohio River Valley region, and are as high as 50 kts over the southeastern United States during tornadic storms over this region. Unstable, warm moist air from the Gulf of Mexico is advected by the low-level jet ahead of the low pressure center throughout the period.

The dominant surface feature at the beginning of this period is the 995 mb low pressure center over southern Missouri with a trailing cold front through western Alabama (Fig. 2.2c). The secondary surface low pressure center (located previously over Oklahoma) with an associated weak trailing cold front has moved in tandem with the main low pressure center located over western Arkansas. The most severe tornadoes, F4's (refer to Appendix A for a description of the Fujita tornado intensity scale), occur in Georgia ahead of the main cold front, while a number of F3's and an F4 occur ahead of the triple point near the Ohio River Valley region.

By 0000 UTC 23 November 1992, the main low pressure center is located over Indiana with a trailing cold front extending through western Georgia (Fig. 2.2d). Some of the convection ahead of the southern portion of this front is beginning to interact with preexisting convection near and along the coast of Georgia and South Carolina. This convection can be seen on the infrared satellite imagery (Fig. 2.1e). A squall line is visible in western Ohio and through southern Michigan from NWS radar summaries (not shown).

By 1200 UTC 23 November 1992 much of the severe weather has subsided as the majority of the convection is now offshore (Fig. 2.1f). The closed 500-mb low center is now an open trough (Fig. 2.3c). The storm system is nearly vertically stacked with height with the low pressure center situated over Michigan and the triple point located in western New York (Figs. 2.3c and 2.4c). Two of the longest tornado tracks in this study occur in North Carolina, and from Georgia to South Carolina between the hours of approximately 0600 UTC until shortly after 1200 UTC.

CHAPTER III

DATA AND METHOD OF ANALYSIS

1. Data

The data for this research originated from a variety of sources. Unless otherwise noted, the period of the collected data is from 0000 UTC 21 November 1992 to 1200 UTC 23 November 1992. The following subsections provide information on the data and appropriate sources.

a. Meteorological data

Upper air and surface data were used to study the atmospheric environment of the storm system. Upper air sounding data were retrieved from the *Radiosonde Data of North America 1946-1992 version 1*, CD ROM. This CD is produced jointly by the Forecast Systems Lab, Boulder, Colorado, and the National Climatic Data Center, Asheville, North Carolina. NWS surface station data were obtained from Steve Finley, Department of Atmospheric Science, Colorado State University, Fort Collins, Colorado. A variety of NWS facsimile products were also used. The primary charts used include the upper air analyses, radar summaries, and surface analyses.

WSR-88D Doppler radar data were archived by the Houston-Galveston Weather Service Office (WSO). Hard copy prints of 0.5° radar reflectivity and radial velocity fields were also used.

b. Lightning data

The CG lightning data from the National Lightning Detection Network (NLDN) were obtained from GeoMET Data Services, Incorporated, Tucson, Arizona. At the time of this severe weather episode, the NLDN was composed of 132 magnetic direction finders (DF's) within the United States (Richard Pyle, GeoMET Data Services, Inc., personal communication 1995). Each (DF) is composed of an orthogonal magnetic-loop antenna and a flat-plate antenna. An algorithm discriminates between CG and IC lightning based on the lightning waveform. Only CG flashes are processed into the database. The NLDN has a detection efficiency of approximately 70% within a nominal range of 400 km from any given DF (Orville et al. 1988). Location errors are within 5-10 km (Orville 1994), while the proper detection of the polarity of the flash is accurate within a range of 600 km (Brook et al. 1989).

c. Tornado data

Tornado characteristics for the most severe tornadoes during this widespread outbreak were obtained from the National Severe Storms Forecast Center (NSSFC) (Hart 1993). Fifteen of these storms were rated as F3's, while 6 were rated as F4's on the Fujita Tornado Intensity Scale. See Appendix A for a table describing the Fujita scale. Characteristics available for the tornadic storms include touchdown time, location, number of segments, and Fujita scale classification. Tornado retraction times were taken from *Storm Data*, because of their absence from the NSSFC database. Tornado touchdown times are accurate within $\pm$ 15 minutes. Discrepancies were

found for seven touchdown times between the data stored in the NSSFC database and information published by *Storm Data*. These cases were all off by one hour and were located within the Eastern Time Zone. In all cases of disagreement, *Storm Data* was consistent with other publications, specifically the *Natural Disaster Survey Report 1992*. Therefore, *Storm Data* information was used over that of the NSSFC database when there were conflicts.

d. Hail data

Hail data were also obtained from the NSSFC database. Thirty-two reported occurrences of hail greater than or equal to 0.75 inches in diameter were originally extracted. Information used for each hail event was hail size, time, and location. Verification of each hail event was based on *Storm Data*. As was the case for the tornado data, there were some discrepancies between the NSSFC database and *Storm Data*. Only the intersection of the data found in the NSSFC data base and *Storm Data* were used. This eliminated only one case; therefore, 31 cases were used for this study.

2. Methodology

This section provides information on how the data were processed and analyzed. The following subsections provide information appropriate to specific portions of this study.

a. The CG lightning relative to the synoptic storm system

For the study period, CG flashes associated with the storm system of interest were isolated from other CG lightning which also occurred during the same period. The lightning flashes not associated with the storm system were initially unambiguous and

easy to identify due to the large spatial separation between CG lightning associated with the two major storm systems. However, as a frontal boundary along the East Coast stalled and the main storm system intensified and moved east, it became difficult to identify which CG flashes were directly associated with the main surface front and upper-level forcing. Therefore, in order to filter CG lightning not associated with the main storm system, surface data, upper air analyses, and radar summaries were used.

The storm system farther east of the main system, as described in the synoptic overview section, initially provided energy for coastal convection. This convection continued to develop and dissipate. After approximately 1900 UTC 23 November 1992 redevelopment of the convection over Georgia occurred. A diffluent region associated with the 500 mb trough at 0000 UTC 23 November 1992 appeared to have enhanced convection over Georgia. The first flashes occurred over this region at approximately 1950 UTC 22 November 1992. Prior to this time only CG lightning located within approximately 400 km ahead of the surface cold front were kept. After 1950 UTC all CG lightning ahead of the cold front were retained. CG lightning in the cold air sector of the storm system was easily traced to an associated forcing mechanism; therefore, no ambiguity was involved in isolating these flashes.

Figure 3.1a shows the location of the CG flashes before filtering, and Fig. 3.1b shows the location of the CG flashes after filtering. The number of CG flashes for the study period (1200 UTC 21 November 1992 through 1200 UTC 23 November 1992) were reduced from 49,774 to 43,397.
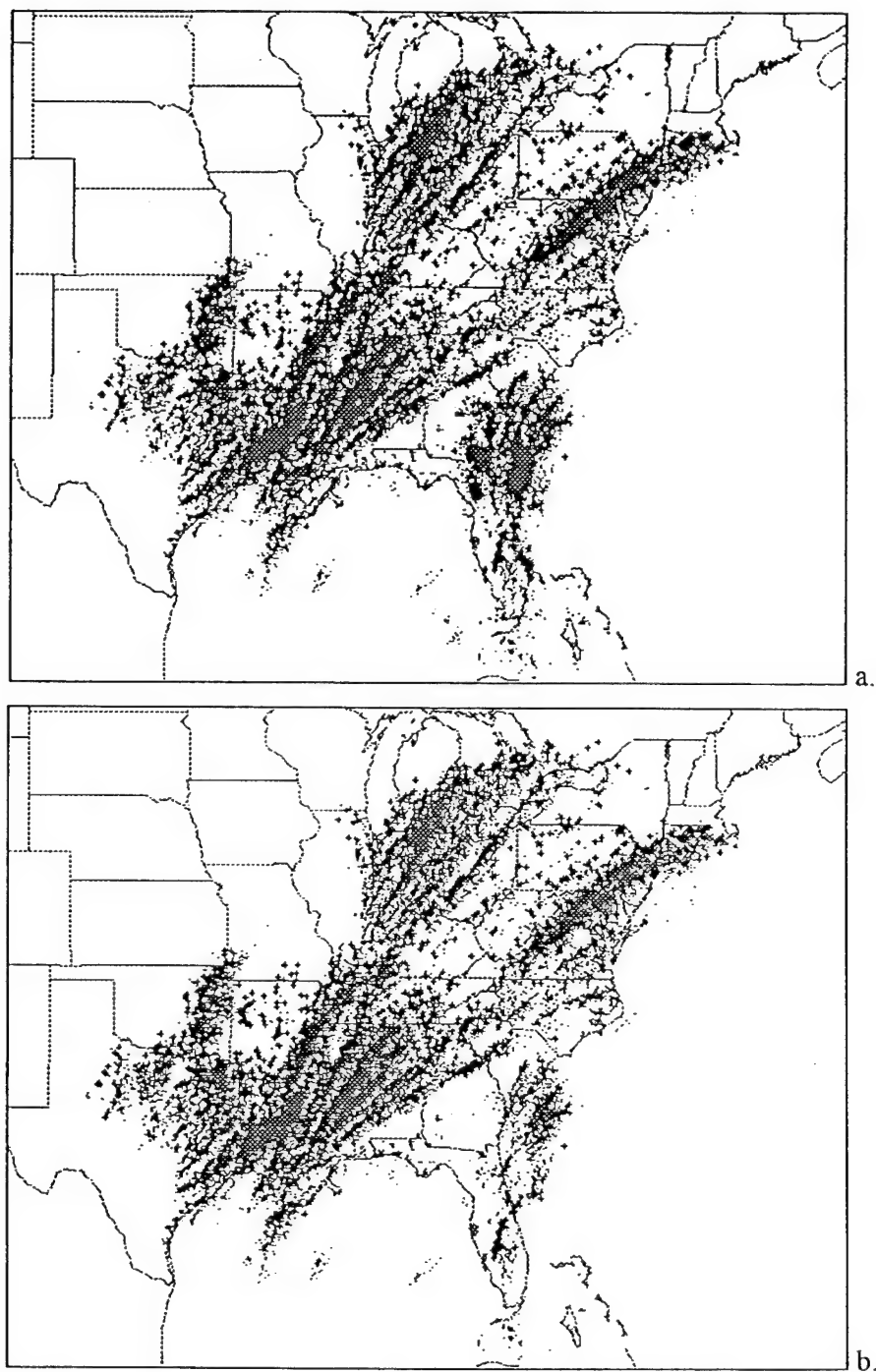
Fig. 3.1. CG lightning during 0000 UTC 22 November 1992 to 1200 UTC 23 November 1992 for (a) all CG lightning which occurred during this period, and (b) only the isolated CG lightning associated with storm system of interest. Dots are negative lightning and pluses are positive lightning. Note positive flashes are masked in high flash densities regions.

The latitude and longitude coordinates of each flash were then transformed from an earth relative to a storm relative coordinate system. The storm relative position was based on either the low-pressure center or the intersection of the frontal boundaries (triple point) from the NMC surface analyses every 12 hours. Intermediate positions were determined by linearly interpolating the storm's track. Figure 3.2 depicts the filtered storm relative CG lightning for the study period. The position of the storm system is plotted at 40° N and 90° W. The primary motivation for this method is the investigation of the effects of vertical wind shear on bipolar lightning patterns. Further details are provided in the next section. Nevertheless, having the data in this format provides a unique and untried way of examining the CG flashes associated with a midlatitude synoptic storm system.

Subsequently, ground flash densities of both positive and negative CG flashes were created for four 12-hr periods of lightning. Contours of the percentage of positive lightning were also created.

b. The effects of shear on bipolar lightning patterns

The effects of vertical wind shear on bipolar lightning patterns were studied for four layers: 300 mb to 500 mb, 300 mb to 700 mb, 500 mb to 700 mb, and 700 mb to the surface. This section discusses the methods used to interpolate the vertical windshear between each 12-hr period at which upper air soundings were taken, the method used to identify bipolar patterns, and finally, how the bipolar patterns were studied with respect to the vertical wind shear. In this study, vertical windshear, or
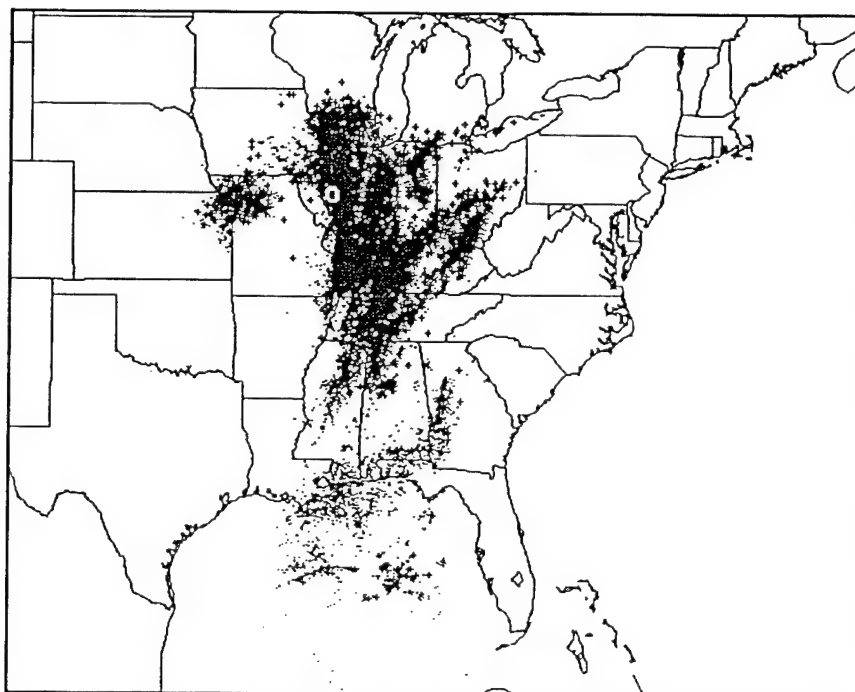
Fig. 3.2. Same as Fig. 3.1b except the coordinates of the CG lightning are storm relative. Flashes are plotted with respect to the storm system at 40° N, 90° W. Map is plotted to show scale.

shear vector, is defined as the difference between the corresponding wind vector at two separate levels.

When defining the layers for which vertical wind shear was calculated, important consideration was given to the microphysics of charge separation in a thunderstorm cloud. In recent years, it has been commonly theorized that thunderstorm electrification results from the noninductive charge transfer between colliding ice crystals and riming hailstones in the presence of supercooled water (Illingworth 1985). Laboratory experiments by Takahashi (1978), Jayaratne et al. (1983), and Saunders et al. (1991) have revealed charge reversal temperatures (the temperature at which riming graupel or hail begin to change sign during ice-ice noninductive processes) between $-10°$ C and $-20°$ C for supercooled liquid water contents between 1-2 g m^{-3}. Figure 3.3 illustrates the effect of colliding ice crystals and riming graupel and the role of the charge reversal temperature on building charge regions within a typical summertime thunderstorm cloud. The figure indicates that the center of the main positive and negative charge regions are at $-30°$ C and $-10°$ C, respectively. A smaller positive charge region is found at the base of the cloud. A compilation of a number of field experiments indicates the height of the main negative charge region to vary between the $-7°$ C and $-15°$ C temperature levels (Williams 1989). Field studies conducted in Florida show that the temperature level of the positive charge region is as cold as $-40°$ C to $-60°$ C (Saunders 1988).
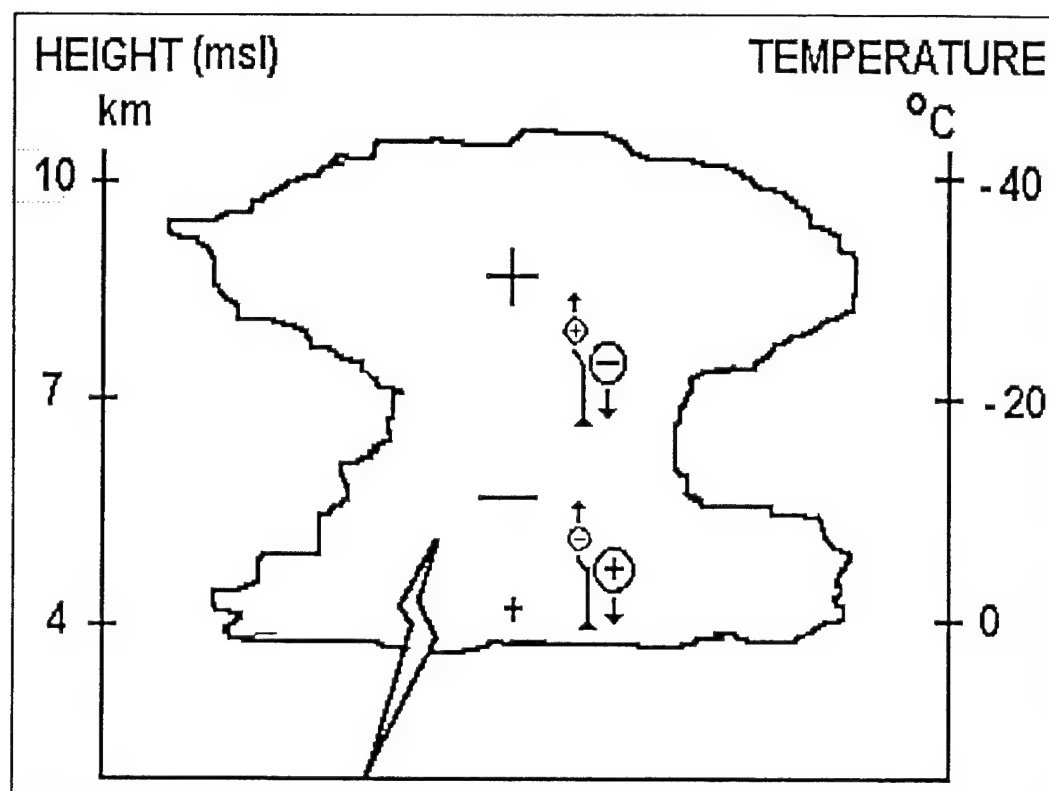
Fig. 3.3. Charge transfer between ice crystals and riming graupel leads to regions of opposite charge when the particles move apart in the updraft (adapted from Saunders 1988).

500 mb temperature analyses at the time of the upper air soundings for 21-23 November 1992 of this data set reveal CG lightning activity occurring in environmental temperatures roughly between -8° C and -20° C, while the temperatures at the 300 mb level are between -36° C and -46° C. Therefore, the 500 mb and 300 mb heights may then be the locations of the main negative and positive charge regions, respectively. As a result, the vertical windshear for the 300-500 mb layer was calculated for this study. The vertical windshear for the 300-700 mb layer was also calculated, because other studies such as Brook et al. (1982), have calculated the vertical windshear for the entire cloud layer. Additionally, the vertical windshear for the 500-700 mb layer was calculated for this study to address the possibility that the 500 mb level may also be the bottom of the main positive charge region. The logic behind choosing the previously mentioned levels is to ensure that shear exits between the height of the main negative and positive charge regions within the cloud structure. Finally, other studies have revealed the importance of low-level windshear on the development of convective storms (Rotunno and Klemp 1985; and Weisman and Klemp 1986); therefore, vertical windshear for the 700 mb-surface layer was also calculated.

To calculate vertical windshear, upper air data were first gridded onto a cartesian grid. The resolution of the grid is 3° longitude x 2° latitude. The Barnes objective map analysis scheme optimized for GEMPAK was used to grid the data (see Koch et al. (1983) for a full description of the Barnes scheme). In addition to the grid spacing, values were selected for delta-n, gamma, and the search radius. Delta-n is the data

spacing. Gamma is the numerical convergence parameter that ranges between 0.0 and 1.0. Greater detail is attained with a lower gamma value for a given delta-n. The search radius is the maximum distance from the grid point that a data point may be used in the analysis for that grid point. Values for delta-n, gamma, and the search radius used are 4°, 0.3, and 20 km, respectively. The domain of the grid covers the full evolution of the storm system and extends from 22°N to 50°N, and 116°W to 65°W.

Based on the initial assumption that the storm system evolves and travels in a linear fashion, the 12-hr locations of the surface low or the triple point were used as the reference points for hourly interpolations of the wind fields. The location of the surface low pressure center or the triple point was based on the NMC surface charts. The analyses of the NMC surface charts were also reviewed for validity. The location of the 12-hr surface low pressure centers or triple points were further adjusted so that their initial positions were located on a grid point. Gridded data associated with each of the 12-hr storm positions were then relocated with respect to the storm relative position (38°N and 89°W on the main grid) (Fig. 3.4). In this way, hourly interpolations of the wind fields occurred at the same grid coordinate with respect to the storm center for each 12-hr period. The hourly shear vectors and contours of their magnitude were plotted for each 12-hr period. This interpolation scheme seems reasonable due to the collocation of the shear maximum and minimum and the orientation of the wind vectors for each 12-hr period. Although interpolations based on adjusting the location of the storm system with respect to thermal surface

UPPER AIR GRID LOCATIONS
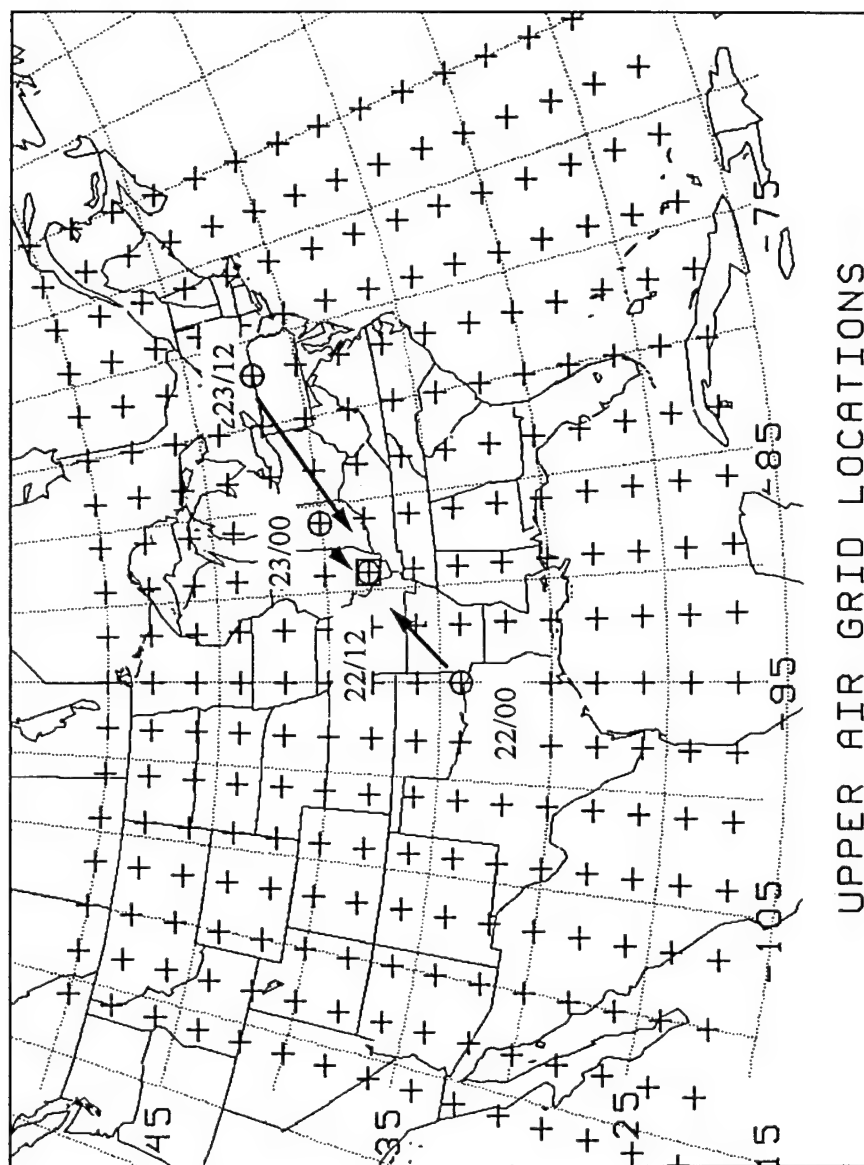
Fig. 3.4. Grid domain for the upper air sounding data. The grid locations of the 12-hr storm positions are designated by a circle. Corresponding times are given as day/hour (UTC). The boxed location is at 38°N, 89°W. Arrows indicate position where the 12-hr storm locations were transferred to. The data associated with each 12-hr storm position were also moved with respect to the storm location. The dotted lines represent latitude and longitude lines 5°.

boundaries were also tested, this technique did not work as well. Circulations in the wind field tended to migrate towards the adjusted location of the low pressure center near the 12-hr periods for each height, instead of keeping the main circulation around the axis of the storm relative location. As a further note, interpolations in the wind field were only accomplished between the period of 0000 UTC 22 November 1992 and 1200 UTC 23 November 1992. This was due to the proximity of the incipient low pressure center at 1200 UTC 21 November 1992 to the southern boundary of the grid and the lack of data near this region.

Previous studies have identified bipolar lightning patterns in a variety of ways. Engholm et al. (1990) selected six wintertime cases which had at least ten flashes per hour of both polarities. The length of the bipolar pattern was determined by the distance between the average location of the negative flashes to the positive flashes. Orville et al. (1988) measured the distance between the estimated centers of positive and negative CG flashes, which were based on the ground flash density centers. Stolzenburg (1990) used a similar technique. In this study, bipolar lightning patterns were initially identified by inspection based upon the criteria that there were at least five flashes per hour of each type of lightning. Careful examination in time of the positive and negative lightning clusters ensured continuity of the bipolar cases. If a classified bipolar pattern failed to met the minimum criteria for the number of flashes for a given period, but at a later period meet the requirements, then it was reclassified as a new case. Similar to Orville et al. (1988) the length of the bipolar pattern is defined as the distance between the positive and negative ground flash density maxima.

Orientation of the bipolar pattern is measured from the negative to the positive ground flash density centers. Eighteen cases were identified for this study.

After identifying bipolar patterns, storm relative CG lightning were overlaid with the hourly shear vectors and contours of their magnitude. CG lightning 30 minutes before and after the time of the vertical wind shear calculation were plotted for the four layers of interest. Length and orientation of the bipolar pattern with respect to an interpolated shear vector were calculated and compared. Duration of the bipolar pattern was also documented.

c. CG lightning and hail

This section explains the technique used to study the possible relationship between hail greater than or equal to 0.75 inches in diameter and positive lightning. In the study conducted by MacGorman and Burgess (1994), the occurrence of large hail was noted to be unambiguously coincident in time and location to regions dominated by positive flashes. Changnon (1994) noted that the CG lightning associated with hail occurred 10 minutes before the hail reached the ground at the leading edge of the hailstreak. Additionally, Changnon (1994) limited the CG lightning sample to within 30 km and 30 minutes before and after each hail streak. Due to the paucity of the hail data available to this study, it is virtually impossible to accurately construct a hailstreak. Therefore, based on the previous studies and because the motivation of this study was to determine if positive lightning and large hail are positively correlated, a circle was created for each hail report to sample the CG lightning associated with it. The radius was defined as the distance traveled by the cell in 10 minutes, where the

speed was taken from the radar summaries. Therefore a normalized radius for each hail event was used to sample the largest number of CG flashes around each hail event, which are presumed to be associated with the main updraft of the storm cell. The location of each hail report was assumed to be the center of a hailstreak. The radius of the circle around each hail report is approximately twice the median length of the hailstreaks sampled by Changnon. This technique was also applied for a 15 minute period, and therefore a larger circle. An even larger circle with a 250 km radius was also created for each case. This circle was assumed to sample CG lightning associated with large hail, small hail, and nonhail producing storms. A comparison of the percentage of positive lightning within the hail circle and within the 250 km circle was then performed.

d. CG lightning and tornadic activity

Lightning flashes associated with the region of each tornadic event were selected by creating a box around the corresponding tornado path. This technique is similar to Perez et al. (1995). The box was generated by using the end points of the tornado's path. From each point, distances of 100 km east (or west) and 100 km south (or north) were used to create the sides (Fig. 3.5). Temporally, lightning flashes 30 minutes before confirmed touchdown time and 30 minutes after retraction time were used. Perez et al. (1995) further filtered the CG lightning by accepting lightning only along the path of the tornado. In this part of the study, the CG lightning were not further filtered. This simplified approach was investigated in order to determine if it may be useful to operational weather forecasters.
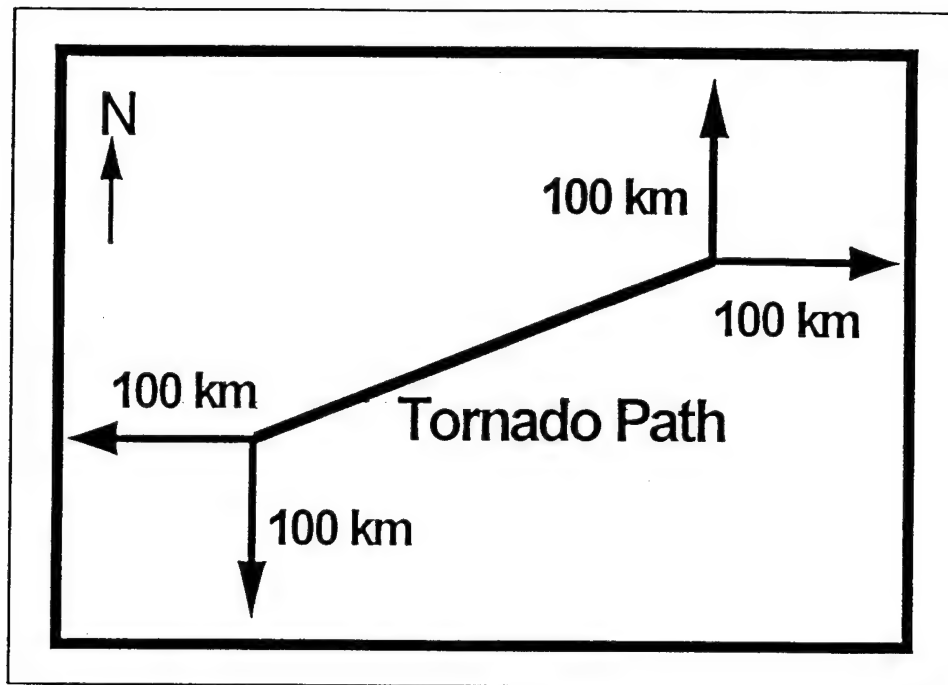
Fig. 3.5. CG lightning sample region for tornado cases. Data collected 30 minutes prior and after tornado touchdown and retraction times.

Histograms of the 5-min flash rate for the total, positive, and negative CG lightning were used to determine the tendencies of the respective flash rates and the time of the peak in the flash rate. When more than one pronounced peak was evident, the peak with the largest change from the previous or following interval was selected. Lag times in the flash rate were determined by counting the number of 5-min intervals between the peak and the 5-min interval in which the tornado touched down. The flash rate tendency prior to tornado touchdown and the total flash rate tendency during the tornado's lifetime were examined.

In order to determine whether the selected peak in the 5-min flash rate was meaningful, each time series was tested to determine whether a distinguishable pattern or a serial (temporal) correlation existed. If neither existed, the data set was said to be white noise as defined by Newton (1988). The white noise test utilized in this study uses the sample correlogram (autocorrelation plot) and the cumulative periodogram (spectral density curve). The autocorrelation function is defined as $\rho(v)$, where v is the lag, or time increment. For such a purpose, 95% confidence bounds are superimposed on both graphs. In other words, if more than 5% of the autocorrelations $\rho(v)$ for $v=0,1,...,M$ (M is no greater than one less the number of data points), or the points in the cumulative periodogram fall outside the bounds, then the white noise hypothesis is rejected. For this study, serial correlations about 40 minutes are more meaningful than serial correlations on the order of 10 minutes. Low frequency serial correlations indicate less ambiguity in the relationship between a peak in the CG flash rate and the tornado touchdown.

In the aforementioned lightning sample technique it is recognized that some contamination of the CG lightning signature occurred. Therefore, two cases (an F4 and an F3) which occurred near the Houston WSR-88D Doppler radar were further analyzed. By visually selecting each flash associated with the supercell storms as depicted by the radar reflectivity fields, the CG lightning for each supercell was isolated. Because a running 5-min average total CG flash rate was determined to have better flash rate tendency resolution, it was plotted and examined for both cases. Individual flash rates for positive or negative lightning were not accomplished, since only a very small fraction of positive flashes occurred in either case. The white noise test was also performed on the time series plots for these two cases. The flash rate results of these two isolated cases were then compared to their respective boxed cases.

CHAPTER IV

OVERVIEW OF THE CG LIGHTNING WITH RESPECT TO THE STORM

SYSTEM

This chapter details the evolution of the CG lightning characteristics with respect to

the location of the surface low pressure center or the triple point between 1200 UTC

21 November 1992 and 1200 UTC 23 November 1992. As previously mentioned,

there were a total of 43,397 flashes during this period, of which 3,981 (or 9.2%) were

positive flashes. This value is similar to the 9.4% found by Silver and Orville (1995)

for the entire month of November 1992 for the continental United States, although

slightly less than the 1989-1994 November average value of 10.5% (Alan Silver,

personal communication 1995) and more than twice the annual value of 4% found by

Orville (1994).

Figure 4.1a is a plot of the number of negative flashes per hour with respect to their

median first stroke peak current, while Fig. 4.1b is the same except for positive

flashes. Only Fig. 4.1b shows a moderate level of linear correlation, with a correlation

coefficient of 0.65. This may be attributed to a limit in the positive charge area within

the cloud and the rate at which it is regenerated after a discharge occurs. For example,

after a positive flash depletes a highly positive charge region, the time required to

redevelop another charge region with a large enough magnitude for another electric

potential breakdown (which is related to existing meteorological conditions) to occur,

may subsequently limit the flash rate. But once the charge is regenerated and
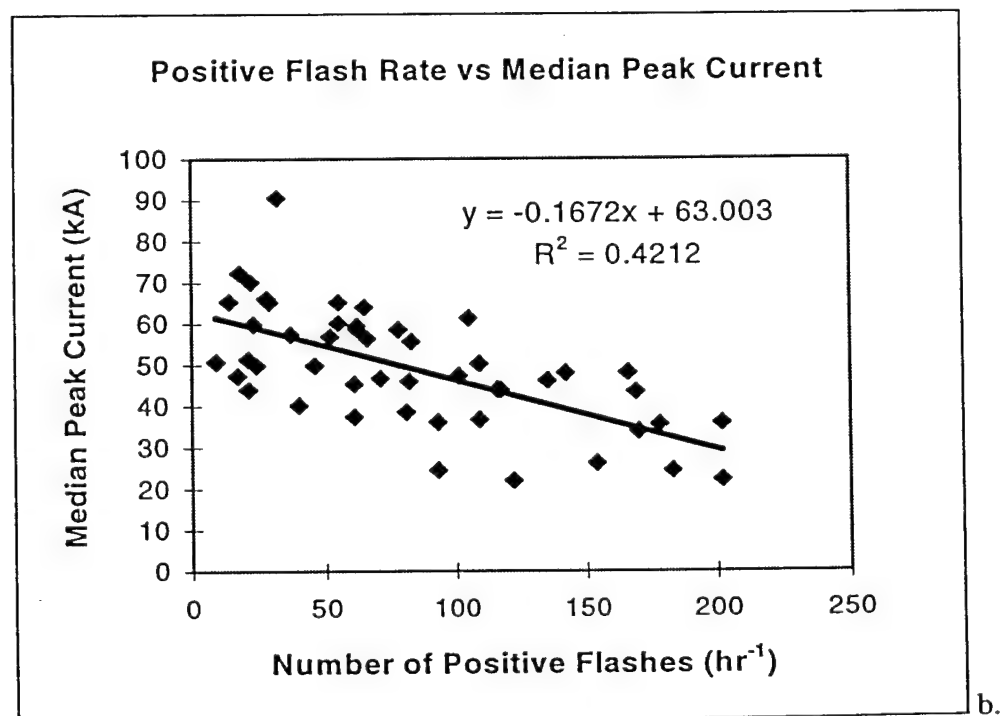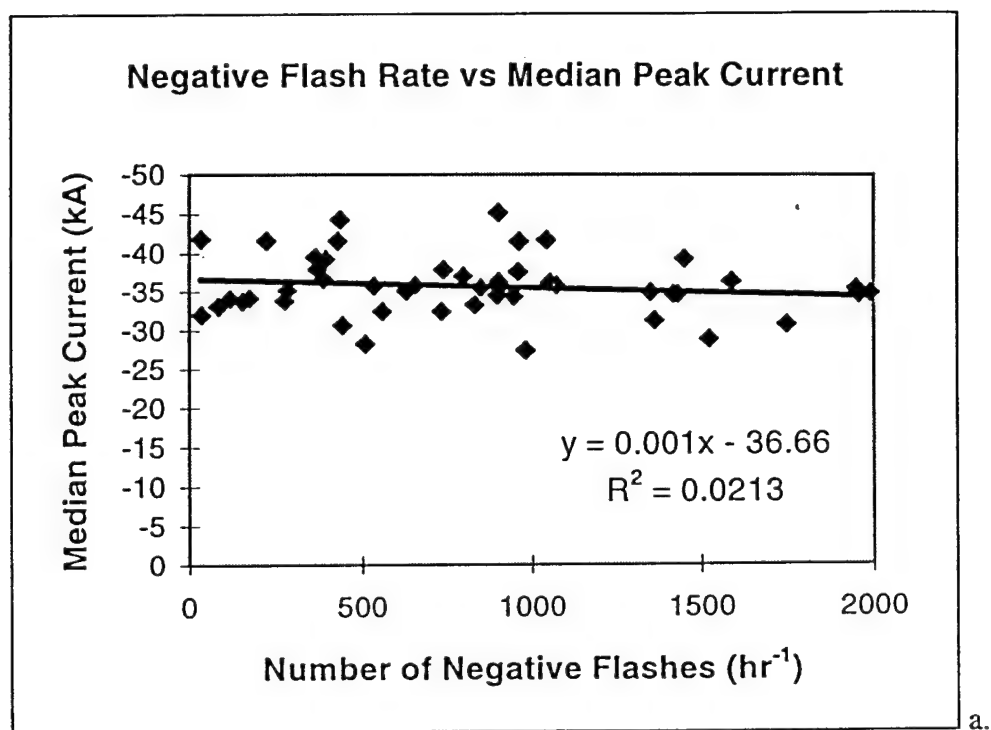
Fig. 4.1. Plots of (a) negative flash rate with respect to their median first stroke peak current, and (b) positive flash rate with respect to their median first stroke peak current. Trend line equation and R^2 value are superimposed on both graphs.

the breakdown potential in the electric field is reached, then the resulting CG flash may have a high first stroke peak current.

Figure 4.2a is a plot of the number of negative flashes per hour with respect to their mean multiplicities, while Fig. 4.2b is the same except for positive flashes. While Fig. 4.2a shows very little linear correlation (correlation coefficient of 0.35), an R^2 value of 0.45 exists for a fourth order polynomial equation describing the relationship between the two parameters (Fig 4.3). Holzer (1953) observed that the ratio between the multiplicity of both positive and negative discharges of flashes from frontally induced thunderstorms and air mass thunderstorms was 2.5. While the majority of the storms in this study are associated with frontal forcing, isolated convective complexes are also present. This may partially explain the results of Fig. 4.3.

Figure 4.4 shows the hourly CG flash rate superimposed with the percentage of positive lightning. The largest peak in the percentage of positive flashes (66.7%) occurs between 1300 UTC and 1700 UTC 21 November 1992. This is at the time of the minimum in the total CG flash rate. In general, peaks in the percentage of positive lightning coincide with decreases in the overall CG flash rate. Two main peaks in the CG flash rate are apparent at 0300 UTC and 2200 UTC 22 November 1992. The corresponding values of each peak in the overall CG flash rate are 2,158 min^{-1} and 1,863 min^{-1}, respectively. The first main peak corresponds mostly to intense convection ahead of the surface cold front over states bordering the Gulf of Mexico. The second large peak in the CG flash rate is attributed primarily to the development and existence of a squall line just east of the triple point. Secondary
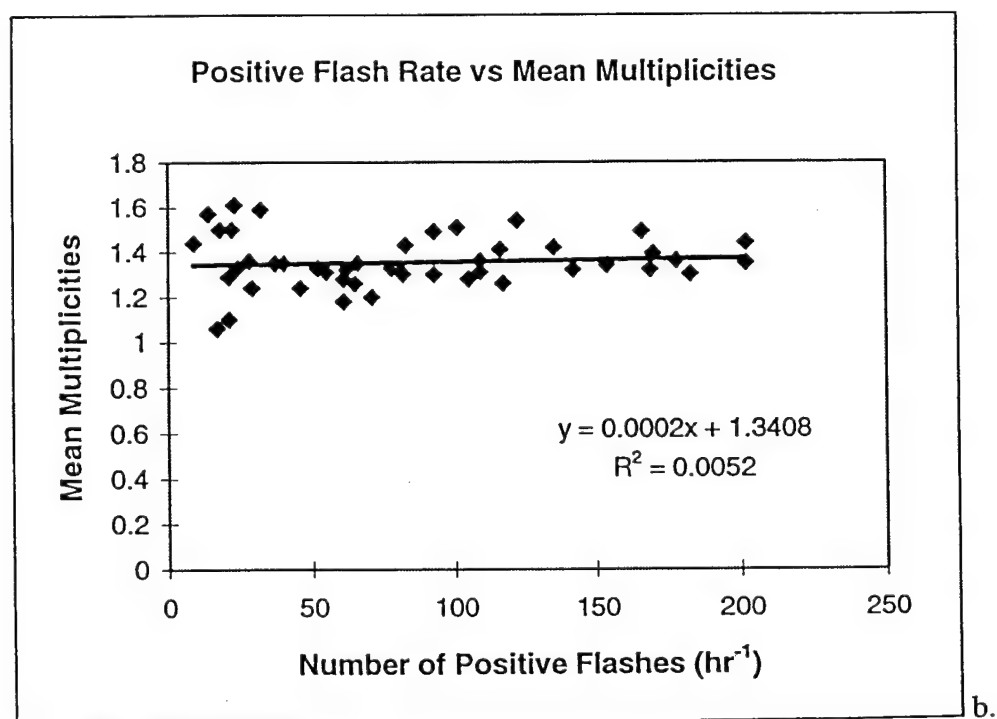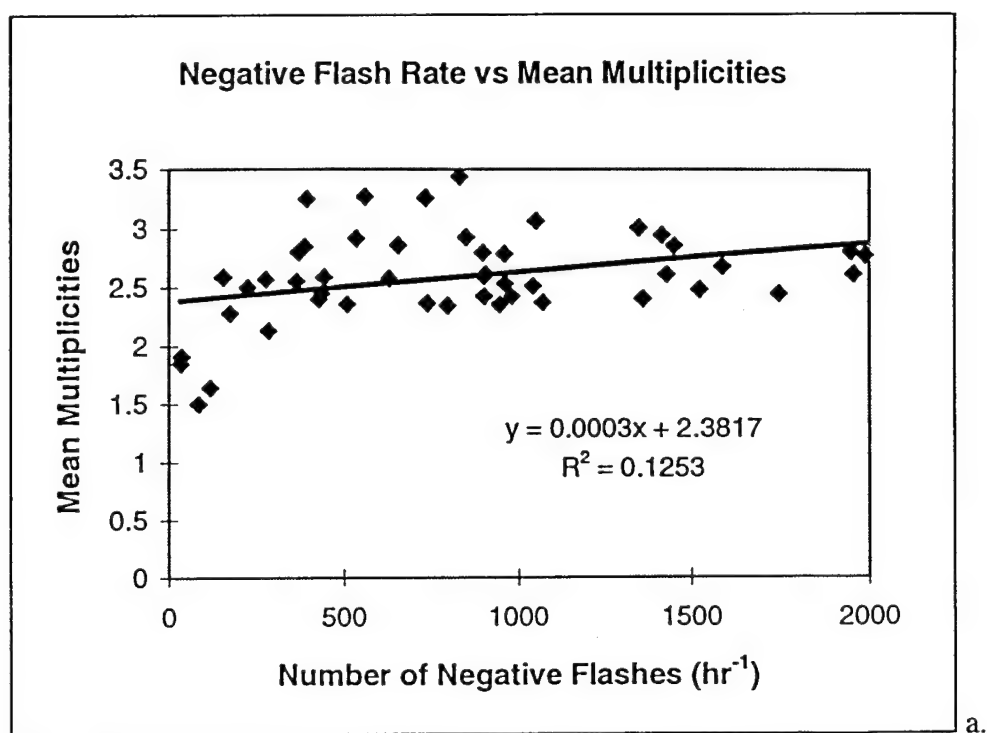
Fig. 4.2. Plots of (a) negative flashes per hour with respect to their mean multiplicities, and (b) positive flashes per hour with respect to their mean multiplicities. Trend line equation and R^2 value are superimposed on both graphs.
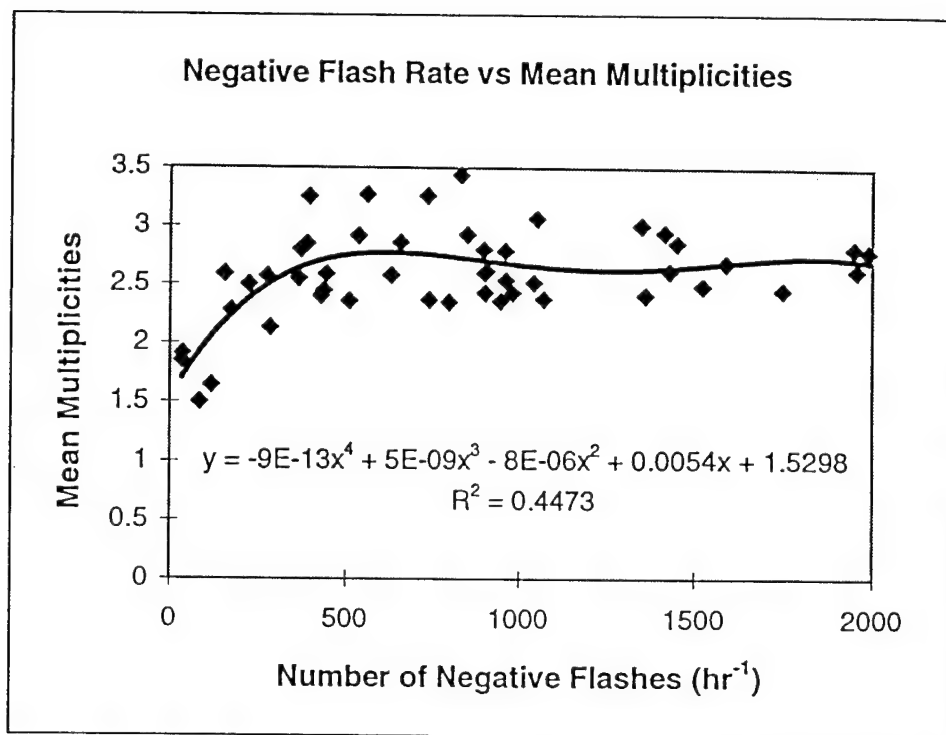
Fig. 4.3. Same as Fig. 4.2a except for a fourth order trendline and associated R^2 value.
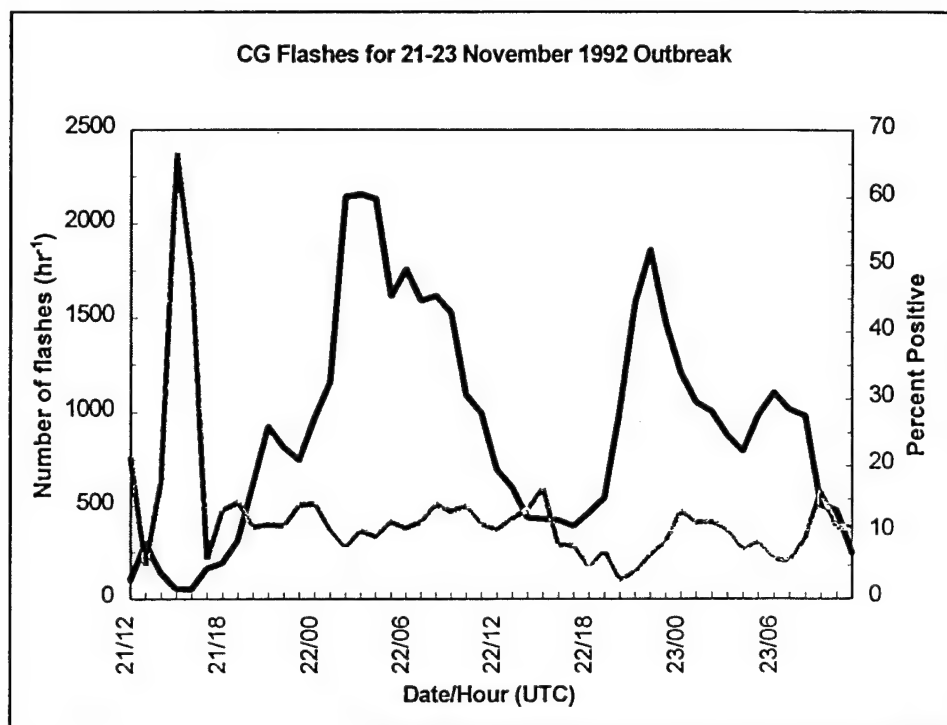
Fig 4.4. Hourly CG flash rate for 1200 UTC 21 November 1992 until 1200 UTC 23 November 1992. Solid line is number of flashes. Gray line is percent positive.
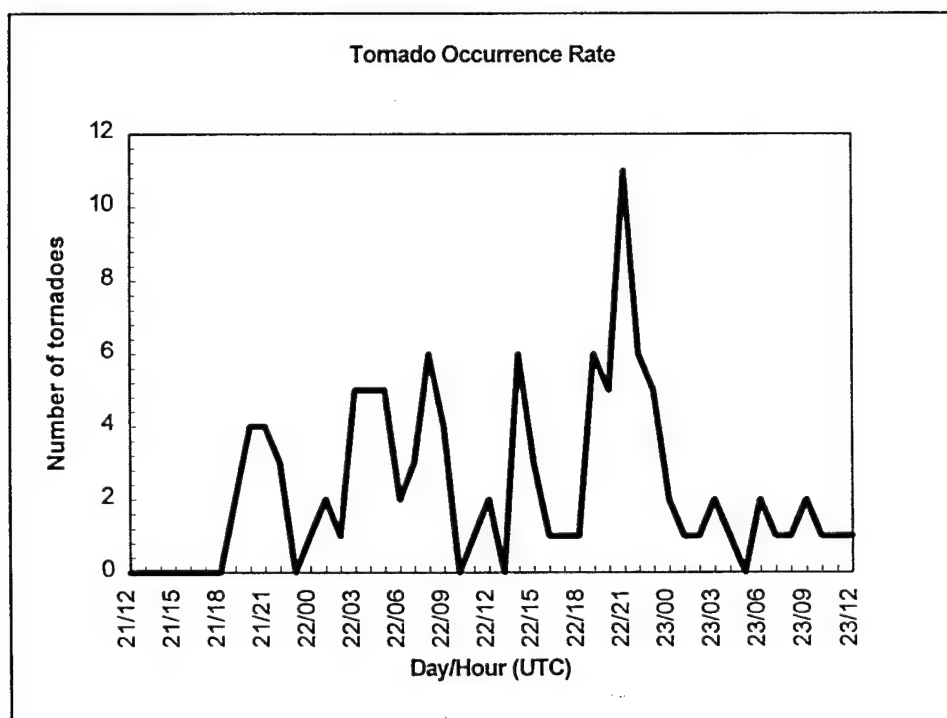
Fig. 4.5. The number of tornadoes that were active per hour is plotted from 1200 UTC 21 November 1992 through 1200 UTC 23 November 1992.

peaks in the CG flash rate are visible at 2100 UTC 21 November 1992 and at 0600 UTC 23 November 1992.

Figure 4.5 shows the number of reported tornadoes which were active during each 1-hr interval. A correlation coefficient of 0.53 exists between the CG flash rate and the number of tornadoes active for each hour. This finding is not entirely unexpected. A number of studies have suggested that lightning activity is greater in severe thunderstorms than in nonsevere storm (Taylor 1975; Turman and Tettelbach 1980).

Figures 4.6-4.9 depict contours of (a) positive ground flash density, (b) negative ground flash density, and (c) the percentage of positive lightning for each 12-hr interval. The single line represents the average surface frontal position. The CG lightning is plotted on a Mercator projection map, where the location of the triple point is at 40° N and 90° W. The latitude ranges between 23° N and 46° N, while the longitudinal variation is 40°; therefore, the spatial domain of each figure is roughly 2,600 km in the north-south direction, and between 3,100 km (top) and 4,100 km (bottom) in the horizontal direction. Table 4.1 provides a summary of the CG lightning characteristics for each 12-hr period. The characteristics provided are the number of total flashes, positive flashes, the maximum value of total, negative, and positive CG flash density, as well as the maximum value of percent positive lightning for each 12-hr interval. The maxima values for the aforementioned six categories all occurred during the second 12-hr interval (Table 4.1). In all cases the maximum in the positive ground flash density is less, by at least an order of magnitude, than the maximum in the negative ground flash density. While this does not always happen in
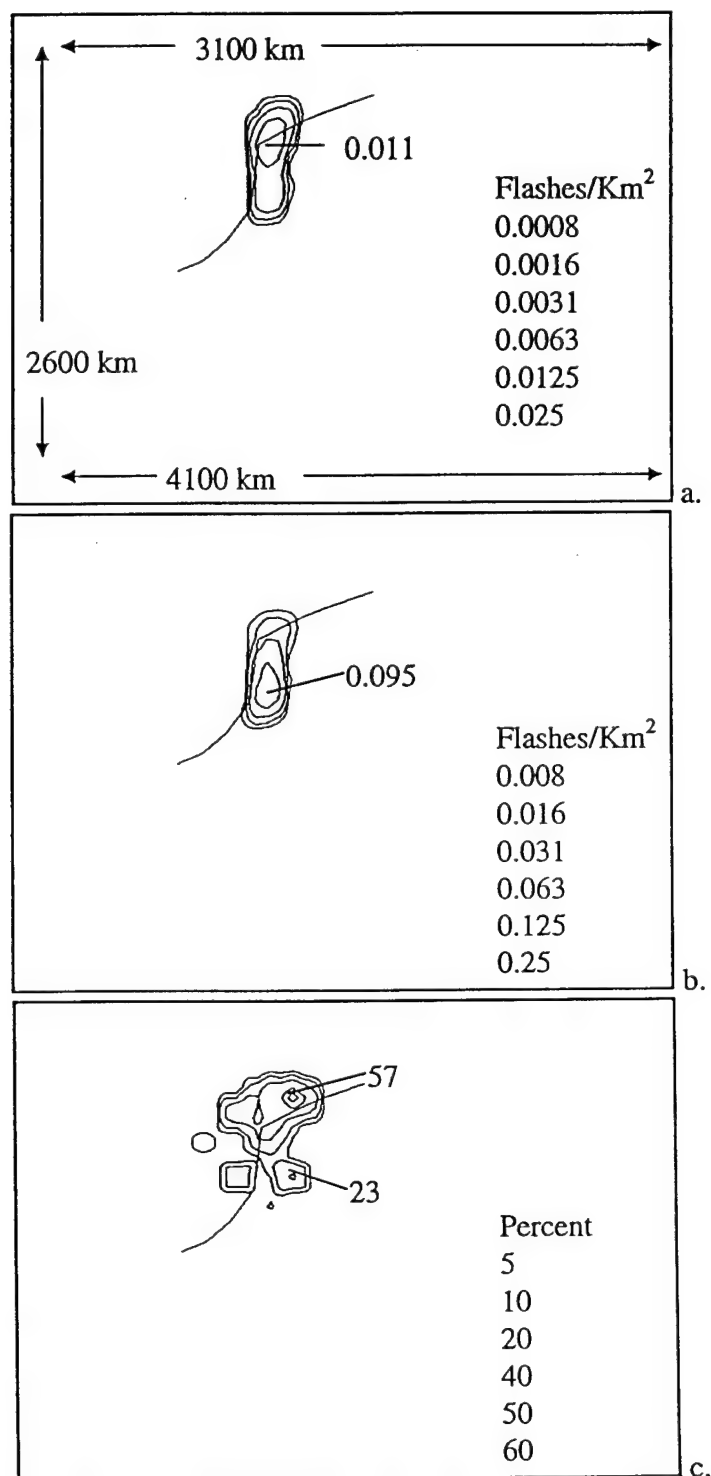
Fig. 4.6. 1200 UTC 21 Novmber 1992 - 0000 UTC 22 November 1992 ground flash densities for (a) positive and (b) negative lightning. Percent of positive lightning is plotted in (c). Contour intervals are displayed in the appropriate boxes. Maximum values are denoted on the figures. Spatial dimensions for b and c are the same as in a.
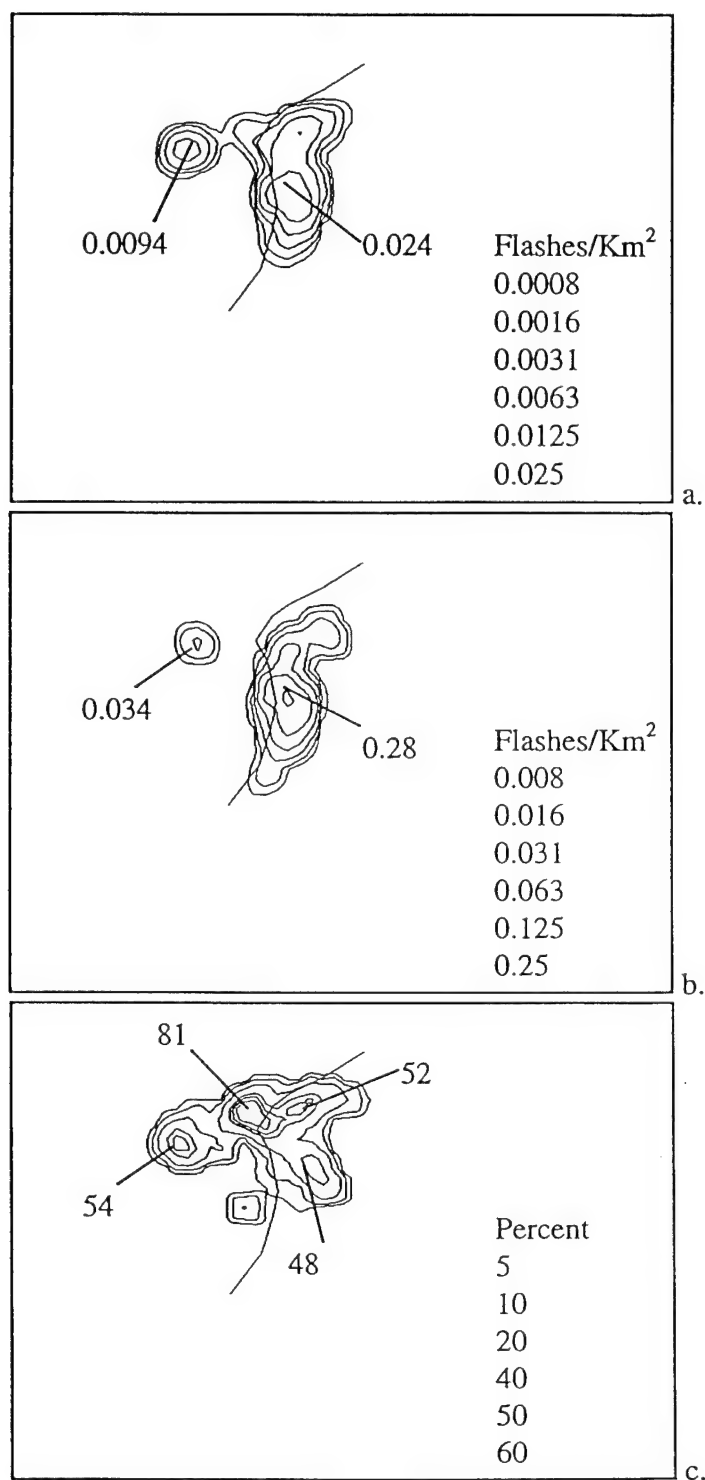
Fig. 4.7. 0000 UTC - 1200 UTC 22 November 1992 ground flash densities for (a) positive (b) negative lightning. Percent of positive lightning is plotted in (c). Contour intervals are displayed in the appropriate boxes. Maximum values are denoted on the figures. Spatial dimensions are the same as labeled on Fig. 4.6a.
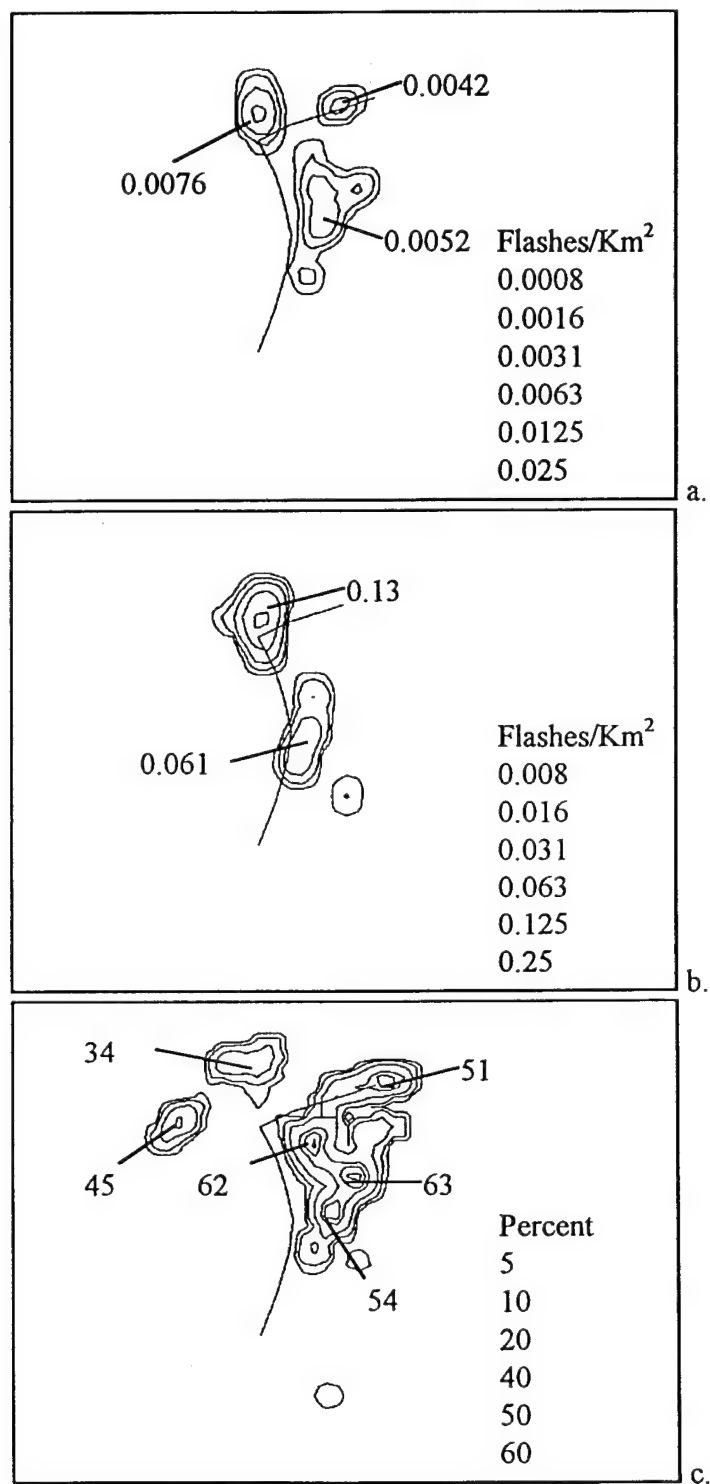
Fig. 4.8. 1200 UTC 22 November 1992 - 0000 UTC 23 November 1992 ground flash densities are plotted for (a) positive and (b) negative lightning. Percent of positive lightning is plotted in (c). Contour intervals are displayed in the appropriate boxes. Maximum values are denoted on the figures. Spatial dimensions are the same as labeled on Fig. 4.6a.
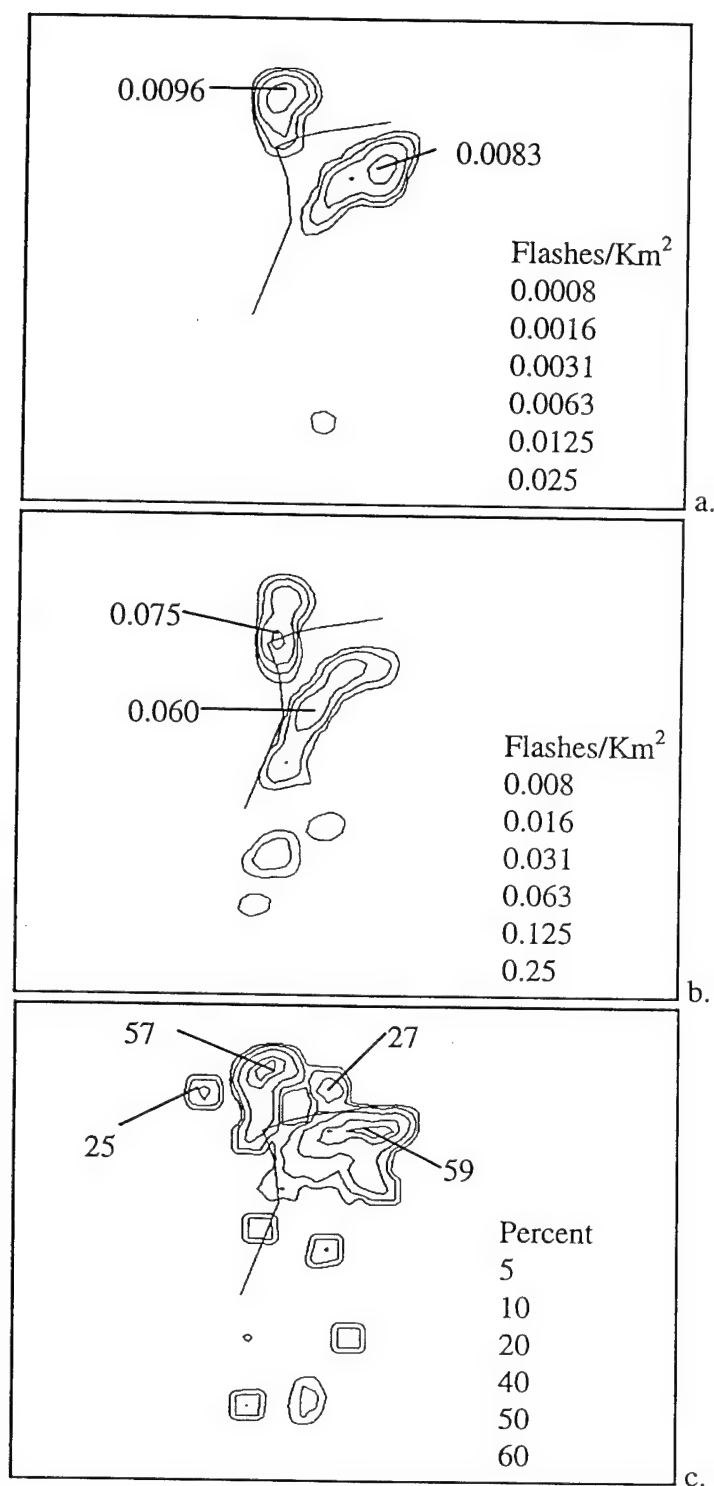
Fig. 4.9. 0000 UTC - 1200 UTC 23 November 1992 ground flash densities are plotted for (a) positive and (b) negative lightning. Percent of positive lightning is plotted in (c). Contour intervals are displayed in the appropriate boxes. Maximum values are denoted on the figures. Spatial dimensions are the same as the labeled on Fig.4.6a.

nature (Stolzenburg 1994), this effect is widely recognized as a common phenomenon (Fuquay 1982; Orville et al. 1988).

Table 4.1. Summary of CG lightning characteristics for 12-hr intervals between 1200 UTC 21 November 1992 and 1200 UTC 23 November 1992.

Time Interval Day/Hour (UTC)	Total Flashes	Positive Flashes	Max. in Total Ground Flash Density (flashes km^{-2})	Max. in Negative Ground Flash Density (flashes km^{-2})	Max. in Positive Ground Flash Density (flashes km^{-2})	Max. in Percent Positive (%)
21/12 - 22/00	4,425	492	0.10	0.095	0.011	57
22/00 - 22/12	18,777	1,891	0.30	0.28	0.024	81
22/12 - 23/00	9,930	686	0.14	0.13	0.0076	63
23/00 - 23/12	10,265	912	0.06	0.06	0.0096	59

During the first 12-hr period (Fig. 4.6), the maximum in the negative ground flash density is situated south of the triple point, while the maximum in the positive ground flash density is located farther north. A bipolar pattern is visible when both figures are overlaid. The length of the north-south oriented axis between the two ground flash density centers is approximately 300 km. This configuration is similar to that observed by Orville et al. (1988), Engholm et al. (1990), and Stolzenburg (1990), although on a much larger temporal scale. Spatially, the length of this bipolar pattern is larger than that found by Orville et al. (1988), but comparable to that found by Engholm et al. (1990) and Stolzenburg (1990). The maximum in the percentage of positive values is located to the northeast of the triple point, but mostly in the warm air sector of the storm.

In the subsequent period, between 0000 UTC 22 November 1992 and 1200 UTC 22 November 1992 (Fig. 4.7), two main ground flash density regions are evident for both positive and negative lightning. The aerial extent of both positive and negative flashes has increased since the last period. The configurations of the positive and negative ground flash density contours are also similar to each other. A notable exception is in the positive ground flash density contour pattern, which extends slightly farther north and west through the triple point. In the region to the west of the triple point, the local maximum in the positive ground flash density is displaced to the southwest of the negative ground flash density maximum. Contrary to this, is a collocation of both the positive and negative ground flash density centers in the region to the southeast of the triple point. In the northern portion of the large ground flash density region east of the triple point, another local maximum in the positive ground flash density is displaced from a localized center in the negative ground flash density contours. In this instance, the orientation from the negative to positive center is towards the northwest. Maxima in the contours of the percentage of positive lightning tend to regions where a localized maximum value in the positive ground flash density is displaced from a negative ground flash density center. During this 12-hr period the highest values in the percentage of positive lightning exist to the north of the triple point, with a secondary maximum located to the west of the triple point.

The next 12-hr period, between 1200 UTC 22 November 1992 and 0000 UTC 23 November 1992 (Fig. 4.8), shows that the maxima of positive ground flash density are once again located farther north than the maxima of negative ground flash density.

High percent positive values are still found to the northeast of the triple point. However, the highest percentage of positive lightning is found, for the first time, to the southeast of the triple point. Once again, maxima in the percentage of positive lightning highlight the spatial separation between localized positive and negative ground flash density centers. These high percent positive regions located to the southeast of the triple point are also associated with a decrease in the amount of convection ahead of the main surface cold front, as determined by examination of the radar summaries. Note the substantial decrease in the CG flash rate (Fig. 4.4) which extends into the first six hours of this period, and the existence of a localized minimum in the percentage of positive flashes during the last half of this period which increases to a peak by 0000 UTC 23 November 1992.

During the last 12-hr period, between 0000 UTC 23 November 1992 and 1200 UTC 23 November 1992 (Fig. 4.9), the locations of the maxima of positive ground flash density remain displaced to the north with respect to the locations of the maxima in the negative ground flash density. The two highest percent positive values (both greater than 50%) are located near the positions of the maxima of positive ground flash density. One is found to the north of the triple point, while the other is situated to the east. Scattered isolated pockets of low percent positive values are generally associated with low numbers of CG flashes.

It is interesting to note that the locations of the maxima of positive ground flash density were consistently displaced to the north or east of the locations of the maxima of negative ground flash density. The only major exceptions to this are during the

second 12-hr interval examined. Also noteworthy is the fact that high percent positive regions were located north of the location of most CG flashes. One major exception is during the third 12-hr interval when high percent positive values were observed southeast of the triple point in a region associated with the main surface cold front. These were noted to be coincident in time with a decrease in the convective activity associated with the cold front and a decrease in the total CG flash rate during this period. A number of studies (Brook et al. 1989; Kane 1991; and Williams and Boccippio 1994) have suggested that positive CG lightning activity tends to dominate during the downdraft phase of decaying thunderstorms.

A number of other studies have also shown a preference for negative CG flashes to occur in high equivalent potential temperature (theta-e) environments. Theta-e is defined as the maximum potential temperature a parcel of air would realize after condensing out all of its water vapor and releasing the maximum possible latent heat (Bluestein 1992). Engholm et al. (1990) noticed this effect for individual convective storms, where the negative flashes occurred within regions associated with high theta-e values. They also point out that high theta-e air tends to be located at lower latitudes for winter storms. Other studies, such as Branick and Doswell (1992) and MacGorman and Burgess (1994) have noticed a tendency for storms dominated by a particular flash polarity to be confined within a specific geographical region. Smith et al. (1995) extended this observation by noting that storms which developed west of the surface theta-e ridge produced mainly positive CG lightning and large hail. These storms were then noted to undergo a reversal in the dominant polarity of CG lightning

from positive to negative after crossing east of the theta-e ridge. In this study, a high percentage of positive lightning does appear to occur in the cold air region of the surface low pressure system, and consequently in a lower theta-e environment than those found in the warm sector of the surface cyclone.

Additionally, stratiform regions of squall lines are highly documented regions where positive lightning is the predominant polarity (Rutledge and MacGorman 1988; Rutledge et al. 1990; and, Rutledge et al. 1993). Also, the occurrence of positive flashes downshear of negative flashes, which create bipolar lightning patterns are also highly documented (Orville et al. 1988; Engholm et al. 1990; and, Stolzenburg 1990). Advection of positive charges as well as in situ charging mechanisms are the primary theories behind these occurrences. This may also explain the consistent separation of maxima of positive ground flash density from maxima of negative ground flash density. A more detailed examination of the effects of vertical windshear on bipolar lightning patterns follow in the next chapter.

CHAPTER V

THE EFFECTS OF SHEAR ON BIPOLAR LIGHTNING PATTERNS

In this chapter the effects of vertical windshear for the 300-500 mb, 300-700 mb, 500-700 mb, and 700 mb-surface layers on the 18 identified bipolar lightning patterns are given. For each bipolar case, Table 5.1 provides the time, duration, average length, and orientation. Direction is measured in the same manner as meteorological wind vectors, with the negative lightning ground flash density region located at the origin of the bipole vector.

Table 5.1. Summary of bipolar lightning cases.

Case	Day/Hour (UTC)	Duration (hr)	Average Length (km)	Average Orientation (°)
1	22/00 - 22/01	2	67	205
2	22/01 - 22/06	6	124	208
3	22/02	1	58	220
4	22/02 - 22/07	6	52	172
5	22/06 - 22/12	7	90	61
6	22/07 - 22/15	9	110	208
7	22/09 - 22/12	4	55	203
8	22/11 - 22/13	3	96	213
9	22/11 - 22/12	2	66	205
10	22/16 - 22/18	3	123	227
11	22/17	1	142	210
12	22/19	1	100	240
13	22/21	1	140	190
14	22/22 - 22/23	2	34	260
15	22/22 - 23/03	6	83	70
16	23/03 - 23/04	2	48	188
17	23/05 - 23/07	3	167	183
18	23/08 - 23/10	3	115	233
Mean		3	92	194
Std. Dev.		2	37	51

The average duration of the bipolar patterns in this study is relatively short. The average of all the cases is 3 hours. There are only five cases which last six hours, and the longest is 9 hours (Case 6). Some cases such as Cases 6 and 11 may actually be classified as the same case; however, there were not enough positive flashes during two 1-hr periods to meet the minimum criteria established in Chapter III. The result, therefore, is the classification of two bipolar patterns. The same holds true for Cases 8 and 10. The duration of the bipolar patterns defined in Stoltzenburg's (1990) study range between 2 and 15 hours. Orville et al.'s (1988) bipolar pattern was tracked for 11 hours.

The average length of the bipolar patterns is 92 km, with a range of values between 34 (Case 14) and 167 km (Case 17). The lengths of the bipolar patterns found in this study tend to reflect the lower range of values documented in published literature. The average monthly value of 91 bipolar patterns for 1988 is 180 km, with the average length for 10 patterns sampled during November 1988 is 270 km (Stolzenburg 1990). The average length of six wintertime cases in the Engholm et al. (1990) study is 167 km. The differences are most likely due to the identification techniques used in the aforementioned studies.

The orientations of the bipolar patterns are predominately from the south and southwest. Two cases (Case 5 and 15) are oriented from the northeast, and one case (Case 4) is oriented from the southeast. None of the cases in Table 5.1 have an average orientation from the northwest. The average value found in the Stolzenburg (1990) study is 240°. Stolzenburg reported that only 6 of 91 cases were not oriented

between 180° and 270°. Those documented by Engholm et al. (1990) are between 220° and 255°.

Variations in the length and orientation of the bipolar patterns in this study as compared to those previously mentioned studies may be due to the limited size of the original data set from which the bipolar patterns were identified. Also, the storms associated with the bipolar patterns are associated with the environments of a single synoptic storm system. Stolzenburg (1990) selected bipolar patterns from a source of one year's worth of lightning, while Engholm et al. (1990) selected cases from the two-month-long Genesis of Atlantic Lows Experiment (GALE). Variations may also be due to the intensity of the storm system responsible for the production of the bipolar patterns. The bipolar patterns in this study are believed to be representative of those which occurred during the 21-23 November 1992 widespread severe weather outbreak.

Figure 5.1 depicts Cases 5, 6, and 7, which occurred during the 60 minute period centered on 1000 UTC 22 November 1992. The variability in the characteristics of the bipolar patterns identified in this study are well represented during this one hour by these three cases. Case 5, which is in the cold air region of the surface cyclone, has an orientation of 40° and a measured length of approximately 98 km. Case 6 is associated with the main line of convection ahead of the surface cold front; its length and orientation are 131 km from 210°. Case 7 is associated with an isolated convective complex with a short bipolar pattern length and orientation of approximately 56 km
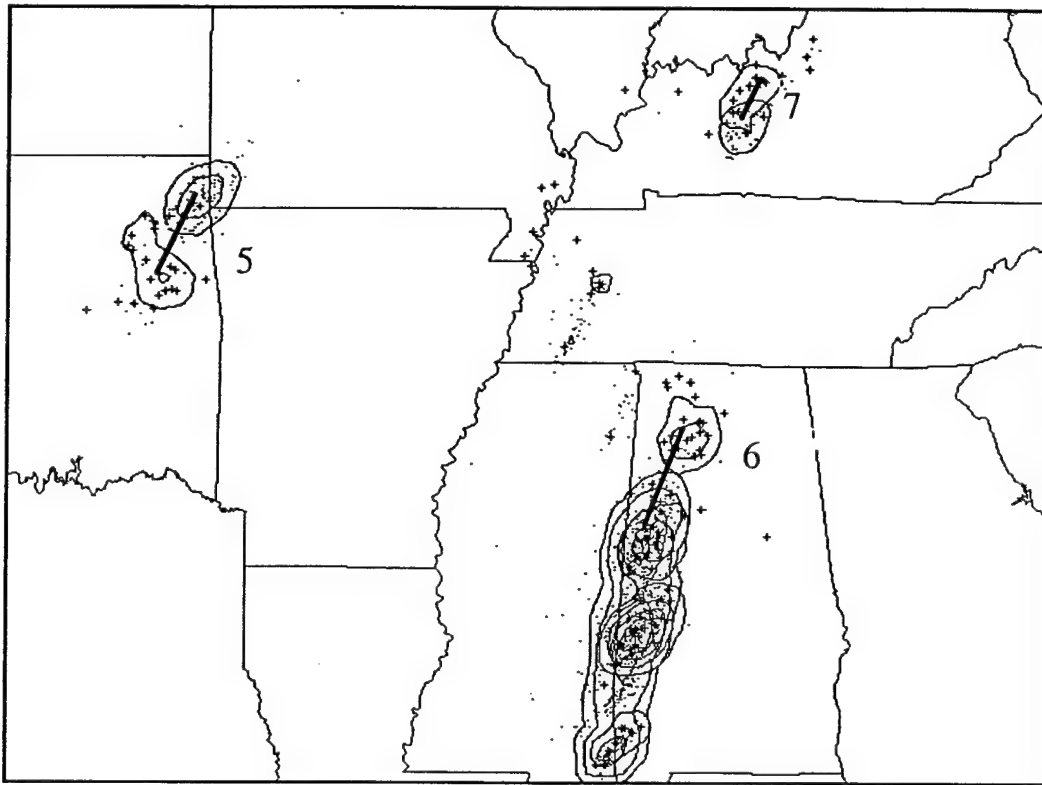
Fig. 5.1. Bipolar lightning patterns during the 60 minute period centered on
1000 UTC 22 November 1992. Numbers correspond to specific cases in Table 5.1.
Bar represents bipole. Pluses and dots represent positive and negative flashes,
respectively.

from 200°. The lightning characteristics of these three relatively persistent cases are reflected and easily identifiable in Fig. 4.7.

Table 5.2 provides the average magnitude and direction of the shear vector associated with each of the four layers. Bold values denote those shear vectors with the closest orientation to the respective bipolar patterns. The table also provides the maximum cloud top height from the NWS radar summaries. Surprisingly, the

Table 5.2. Summary of the shear vectors.
Bold values indicate vectors with the closest orientation to the bipolar pattern.

Case	300-500 mb shear vector (mag/dir) (km/°)	300-700 mb shear vector (mag/dir) (km/°)	500-700 mb shear vector (mag/dir) (km/°)	700 mb-sfc shear vector (mag/dir) (km/°)	Max cloud top height (1000 ft)
1	10/260	20/235	15/200	**15/205**	40
2	9/273	18/257	11/233	**16/202**	55
3	10/270	20/260	**10/230**	**15/210**	40
4	10/270	20/250	12/232	**17/197**	52
5	11/171	15/184	**9/220**	14/186	32
6	6/270	15/259	10/249	**21/208**	55
7	8/263	19/253	10/250	**24/200**	43
8	5/270	15/253	8/247	**20/210**	46
9	5/250	18/255	10/250	**25/195**	43
10	3/277	10/253	10/237	**20/220**	50
11	5/270	10/260	10/240	**25/210**	25
12	3/280	10/260	**5/250**	**20/230**	43
13	5/270	10/240	5/240	**20/230**	30
14	3/285	**5/265**	**5/255**	20/240	50
15	9/210	18/217	**10/240**	17/208	38
16	8/250	13/250	5/255	**20/240**	40
17	**17/207**	20/213	8/250	12/230	39
18	**10/223**	15/240	8/263	20/240	37
Total (bold values)	2	1	5	13	

bipolar patterns are most closely aligned with the low-level shear vectors. In 13 instances the bipolar patterns are aligned closest with shear vector associated with the 700 mb-surface layer. The average differences in the orientation of the bipolar patterns and the shear vectors for the 300-500 mb, 300-700 mb, 500-700 mb , and 700 mb-surface layers are 50°, 35°, 29°, and 19°, respectively. Another common occurrence among most of the cases was for the bipolar patterns to be rotated counterclockwise from the shear vectors. This occurred in almost every 1-hr interval associated with all of the cases and in all four shear layers.

The preference for the bipolar pattern to be more closely aligned with the shear vector associated with the lower levels is illustrated in Fig. 5.2. Figure 5.2 depicts the same three bipolar patterns as in Fig. 5.1 except that it superimposes the shear vector and contours of its magnitude (normalized for the thickness of the layer) for (a) the 500-700 mb layer and (b) the 700 mb-surface layer. Notice in Fig. 5.2a that the orientation of the shear vector associated with Case 5 is aligned with the bipolar pattern (as depicted in Fig. 5.1), but is also 180° out of phase. This is opposite of the majority of cases where the positive flash region is located downshear of the negative flash region, but is similar to the observations of Rutledge and MacGorman (1988). In their study positive flashes are located upshear in the trailing stratiform region of a squall line. While this convective feature does not appear to be a squall line, the NWS radar summary at 0935 UTC 22 November 1992 indicate that the propagation of the deepest convection is towards the northeast with a homogenous low reflectivity region to the southwest (not shown). Additionally, the NMC surface analyses at 0900 UTC
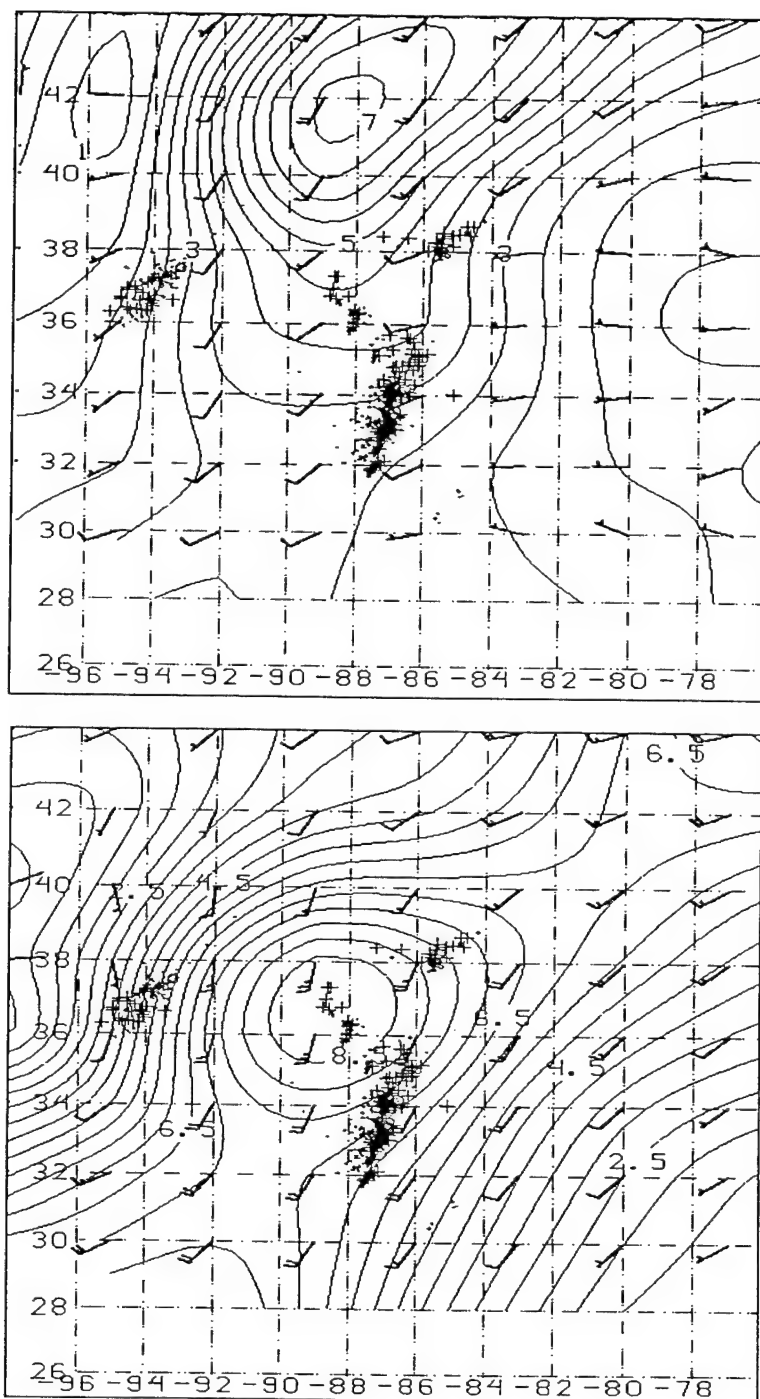
Fig. 5.2. Same as Fig. 5.1 except shear vectors and contours of its magnitude for (a) the 500-700 mb layer and (b) the 700 mb-surface layer are superimposed. Contours are every 0.5 m s^{-1} km^{-1}. Pluses and dots represent positive and negative lightning, respectively. CG lightning is in storm relative coordinates; therefore, latitude and longitude lines, which are plotted every two degrees, are for scale only. Refer to Fig. 5.1 for case labels and direction of the bipolar patterns.

and 1200 UTC 22 November 1992 (Fig. 2.2c) show that this bipolar pattern is west of the surface low center. Therefore, advection of positive charges as described by Rutledge and MacGorman (1988) may have occurred. As in the majority of the cases, Cases 6 and 7 are aligned more closely with the shear vectors associated with 700 mb-surface layer (Fig. 5.2b). The positive flash regions are located downshear of the negative flash regions.

The maximum cloud top height during the lifetime of each bipolar pattern was examined with respect to the magnitude and duration of all the cases. A weak correlation ($R^2 = 0.2$) between the maximum cloud top height and the duration of the bipolar pattern exists. Longer durations in the bipolar patterns are positively correlated with higher cloud top heights. While Engholm et al. (1990) found a positive correlation between the cloud top height and the length of the bipolar pattern, very little correlation between the two were found in this study.

No apparent correlation exists between the magnitude of the shear vectors and the length of the bipolar patterns for any of the four layers. As illustrated in Fig 5.2b, the magnitudes of the vertical windshear for Cases 6 and 7 are both approximately 7 m s^{-1} km^{-1}, but the lengths of the bipolar patterns range between 55 and 110 km. Engholm et al. (1990) also did not find any correlation between the length of the bipolar patterns and the speed of the geostrophic wind or the magnitude of the vertical speed shear.

CHAPTER VI

LARGE HAIL AND THE PERCENTAGE OF POSITIVE LIGHTNING

In this chapter a discussion of the results associated with the percentage of positive lightning and hail greater than or equal to 0.75 inches in diameter is provided. Table 6.1 lists the case number, day, time, location (county and state), and size of each hail event. Fig. 6.1 displays the corresponding position of each event as numbered in Table 6.1. The reported hail sizes range between 0.75 and 2.75 inches. The mean and median size of all the events are 1.2 and 1.0 inches, respectively. Most of the hail cases, 16 out of 31, including the largest event, occurred over the Midwest near the Ohio River Valley region and were associated with a line of thunderstorms just east of the triple point. One event (Case 25) appears to have occurred just north of the warm front.

Table 6.2 provides a summary of the CG lightning sampled for each hail event. Included in the table are the number of flashes and the percentage of positive lightning associated with each hail case for 10 and 15 minute periods before and after the hail report. These results belong to the hail CG category as labeled in the table. Additionally, the hail CG category is broken into two subcategories labeled as 10 min and 15 min. The sizes of the radius associated with the sample circles for these two hail CG subcategories range between 8.4 km and 15 km (10 min), and 12.6 km and 22.5 km (15 min). Also included in the table are the number of flashes and the percentage of positive lightning associated with all the storms active within a two hour

Table 6.1. Summary of hail cases.

Case	Date (1992)	Time (UTC)	Location (County, State)	Size (Inches)
1	22 Nov	0020	Sabine Parish, LA	1.00
2	22 Nov	0130	Calcasieu Parish, LA	0.75
3	22 Nov	0215	Morehouse Parish, LA	0.88
4	22 Nov	0230	West Carroll Parish, LA	1.75
5	22 Nov	0330	Tensas Parish, LA	1.75
6	22 Nov	0340	Franklin Parish, LA	1.75
7	22 Nov	0648	Jefferson Parish, LA	0.88
8	22 Nov	0705	Newton, MS	0.75
9	22 Nov	1445	Tallapoosa, AL	1.00
10	22 Nov	1505	Trenton Cloudland State Park, GA	0.88
11	22 Nov	1510	Hamilton, TN	1.75
12	22 Nov	1915	Greene, IN	1.25
13	22 Nov	1945	Owen, IN	1.75
14	22 Nov	1956	Putnam, IN	1.00
15	22 Nov	2030	Marion, IN	1.00
16	22 Nov	2110	Bartholomew, IN	0.88
17	22 Nov	2220	Fayette, IN	1.75
18	22 Nov	2315	Franklin, IN	0.75
19	22 Nov	2330	Pendleton, KY	0.75
20	22 Nov	2352	Shelby, OH	1.00
21	23 Nov	0006	Miami, OH	1.75
22	23 Nov	0040	Highland, OH	2.75
23	23 Nov	0100	Fayette, OH	0.75
24	23 Nov	0125	Ross, OH	1.75
25	23 Nov	0200	Sandusky, OH	0.75
26	23 Nov	0240	Spartanburg, SC	0.75
27	23 Nov	0240	Kershaw, SC	1.00
28	23 Nov	0240	Richland, OH	0.75
29	23 Nov	0245	Knox, OH	0.75
30	23 Nov	0512	Chatham, NC	0.75
31	23 Nov	0521	Nelson, VA	1.75
Mean				1.20
Std. Dev.				0.5
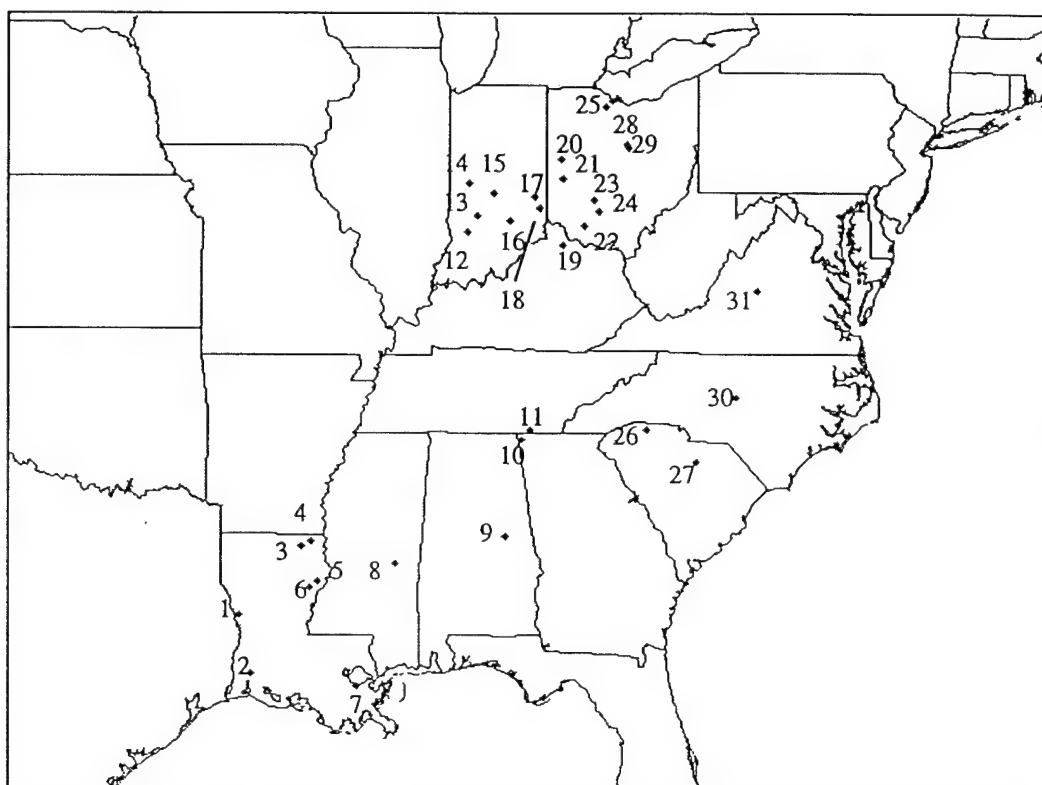
Fig. 6.1. Location of large hail (≥ 0.75 inches in diameter) occurrences. Numbers correspond to the cases listed in Table 6.1.

Table 6.2. Summary of hail and associated CG lightning. Bold values indicate the highest percent positive value for the given case.

Case	Hail CG				Environmental CG	
	10 min		15 min		60 min	
	Total	% Positive	Total	% Positive	Total	% Positive
1	0	0	2	0	1793	**12.4**
2	12	0	26	3.8	2104	**6.2**
3	1	**100**	6	50	2662	9.2
4	8	0	44	6.8	2921	**9.0**
5	4	0	13	0	3388	**9.5**
6	103	3.9	199	7.5	3288	**9.1**
7	23	**4.3**	44	2.3	1363	3.4
8	49	**8.2**	86	8.1	2292	6.6
9	3	0	8	0	722	**6.2**
10	1	0	3	0	534	**12.9**
11	4	25	11	9.1	480	15.0
12	4	0	14	0	779	**2.6**
13	6	0	25	0	1104	**2.3**
14	8	0	20	0	1281	**2.6**
15	17	0	84	0	1700	**2.0**
16	9	0	24	**4.2**	2066	1.6
17	11	0	16	0	2186	**3.1**
18	5	0	18	0	1197	**6.0**
19	0	0	4	0	650	**2.5**
20	1	0	4	0	1592	**6.4**
21	6	0	25	0	1119	**6.6**
22	6	0	13	0	749	**3.1**
23	0	0	1	0	836	**3.2**
24	3	0	11	0	796	**2.6**
25	9	0	32	3.1	1184	**8.2**
26	8	0	15	0	280	**2.1**
27	1	0	4	0	293	**2.0**
28	1	0	20	0	854	**5.2**
29	5	0	14	0	815	**5.0**
30	0	0	1	0	380	**1.6**
31	11	**9.1**	42	2.4	854	**3.3**
Mean	10.3	4.9	26.7	3.1	1363.3	5.5
Std. Dev.	19.6	18.3	38.2	9.1	872.8	3.6

period centered at the time of the hail report and within a 250 km radius circle. This category is labeled as environment CG. Bold-typed values indicate the highest percentage of positive lightning for a given case. The flash rate densities for the 10 min and 15 min subcategories are equivalent to flash rate densities of 1,700-5,300 and 500-1,600, respectively, for the environment CG category. Except for those cases where zero CG flashes were detected, the flash rate densities are greater for the 10 min and 15 min subcategories than for the environment CG category.

The percentage of positive lightning values associated with the environment CG category range between 1.6% and 15%, while the range of values associated with the hail CG category are between 0% and 100% (10 min) and 0% and 50% (15 min). The number of CG flashes sampled for the environment CG category are relatively high, with an average of 1,363 flashes, while the number of flashes associated with each subcategory varies between 0 and 103 flashes (10 min) and 1 and 199 (15 min). The average percentage of positive lightning is greater for the environment CG category than for each hail CG subcategory.

The results indicate that in 84% of the cases the highest percentage of positive lightning is associated with all the storms within 250 km of the hail report. As might be expected some variability in the results exists in the percentage of positive lightning values for each hail CG subcategory. Only the results of Case 3 and 8 show that a greater percentage of positive lightning exists for the specific hail cases, rather than for the 250 km radius environment. Therefore, dismissing those cases where the bold values do not belong to the environment CG category, and the values associated with

the hail CG subcategories are not analogous because they are not either greater than or less than the environment CG category (Cases 7,11,16, and 31), indicate that 93% (25 of 27 cases) are associated with the environment CG category. Incidentally, only one (10 min) and six (15 min) flashes were sampled during Case 3, which had the highest percentage of positive lightning.

The results of the percentage of positive lightning associated with 31 cases of large hail appear to better fit the results of Changnon (1994), who did not find a single positive lightning flash for 44 hailstreaks. The results found here differ with those studies which found an apparent link between large hail and positive lightning (Curran and Rust 1992; Seimon 1993; MacGorman and Burgess 1994; and Stolzenburg 1994). A number of these studies suggest that it is the storm structure which creates this phenomenon. Curran and Rust (1992) specifically associate positive lightning to LP supercell storms. While storm classification was not attempted in this study, it is reasonable to assume that the majority of the storms were either classic or HP supercell storms, because LP storms normally occur near the surface dry line, while HP storms are the most common and can occur in the humid Southeast as well as the Great Plains (Doswell and Burgess 1993). Additionally, most of the hail cases which occurred in the Midwest appear to be associated with a squall line ahead of the triple point. A number of studies have shown that negative lightning preferentially occurs from the convective region of squall lines (Rutledge and MacGorman 1988; and Rutledge et al. 1990).

CHAPTER VII

LIGHTNING AND TORNADIC ACTIVITY

1. Results

a. Overview of the tornado and CG lightning characteristics

This section provides information concerning the tornado and CG lightning

characteristics for all 21 cases, as sampled by a boxed region around the tornado path.

Table 7.1 lists all tornado cases including the date, time, location, the total number of

CG flashes (flashes 30 minutes prior to touchdown to 30 minutes after retraction), the

percentage of positive lightning, total storm flash rate, and the tornado path length in

miles. The total storm flash rate is the total number of flashes divided by the duration

of each case. Also, this table includes the mean and standard deviations for the total

number of flashes, percent positive, total storm flash rate, and path lengths for the F3

cases, F4 cases, and both types combined. Figure 7.1 shows the distribution of the

tornado locations. The numbers correspond to the cases listed in Table 7.1.

Generally, the tornadoes in this study are concentrated in two main regions. Seven

tornadoes occur in the Midwest near the Ohio River Valley region, while the rest

occur mainly in states adjacent to the Gulf of Mexico or the Atlantic Ocean. With the

exception of Case F4-6, which occurs in Kentucky, all the other F4 cases occur in the

Southeast.

The duration and path lengths of the tornadoes sampled vary considerably. These

path lengths range from 3 miles (F3-2) to 160 miles (F3-15). Case F3-15, which has

Table 7.1. Summary of tornado cases. Time reflects touchdown and retraction times of tornadoes. The total number of flashes includes the periods 30 minutes prior and after tornado touchdown and retraction, respectively.

Case	Date (Nov 1992)	Time (UTC)	State	Total Flashes	Percent Positive (%)	Total Storm Flash Rate (min $^{-1}$)	Path Length (miles)
F3-1	21	2120-2223	TX	1105	5.3	8.9	32
F3-2	22	0130-0208	LA	840	6.2	8.5	6
F3-3	22	0345-0351	LA	1178	11.0	17.6	3
F3-4	22	0355-0455	LA	1787	9.7	14.8	38
F3-5	22	0523-0605	MS	1317	5.4	12.8	27
F3-6	22	1810-1825	GA	82	17.1	1.1	10
F3-7	22	1935-1944	IN	456	1.5	6.5	5.3
F3-8	22	1950-2015	IN	742	2.4	8.6	12
F3-9	22	1955-2020	IN	694	1.0	8.1	15
F3-10	22	2045-2104	IN	907	1.7	11.3	9
F3-11	22	2105-2127	IN	800	0.4	9.6	10
F3-12	22	2300-2329	OH	402	2.5	4.5	20
F3-13	22-23	2300-0100	GA/SC	219	8.2	1.2	67
F3-14	23	0720-0730	NC	30	3.3	0.4	5.5
F3-15	23	0910-1225	NC	410	4.6	1.6	160
F3 Mean				731.3	5.4	7.7	28.0
F3 Std. Dev.				486.2	4.6	5.2	40.3
F4-1	21	2127-2206	TX	842	4.9	8.4	30
F4-2	22	0527-0801	MS	3486	7.7	16.2	128
F4-3	22	0614-0714	MS	1926	5.6	15.9	40
F4-4	22	1644-1734	GA	202	10.9	1.8	20
F4-5	22	2145-2220	GA	140	13.6	1.5	32
F4-6	22	2152-2227	KY	351	0.6	3.7	16
F4 Mean				1157.8	7.2	7.9	44.3
F4 Std. Dev.				1319.9	4.6	6.8	41.9
Total Mean				853.1	5.9	7.8	32.7
Total Std. Dev.				800.0	4.5	5.5	40.4
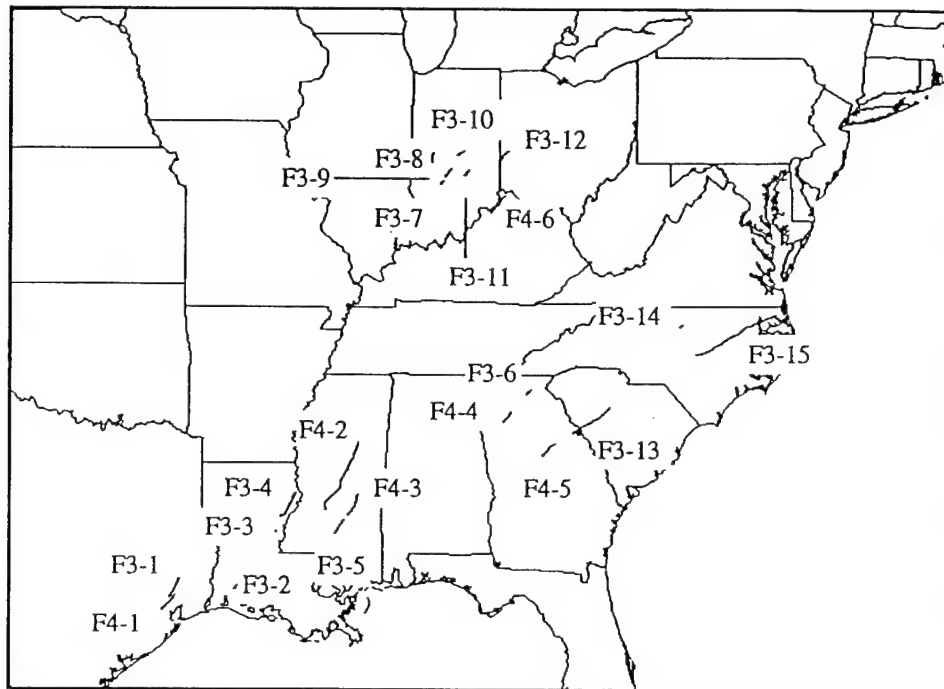
Fig. 7.1. Twenty-one tornado paths for F3 and F4 cases. Case numbers correspond to Table 7.1.

the longest tornado path, occurs in North Carolina towards the end of the severe weather outbreak. Incidentally, the second longest path belongs to case F4-2 which occurs in Mississippi. This tornado has the longest path of any known F4 or F5 tornado which occurred between 1989 and 1992 (Perez et al. 1995). There are nine cases, all of which are F3 in intensity, with tornado paths 15 miles or less. The average path lengths for the F3 and F4 cases are 28 miles and 44.3 miles, respectively. The average path length for all the tornadoes sampled is 32.7 miles.

Besides the existence of a large variation in the tornado path lengths, significant variation also exists for the percentage of positive lightning and the total storm flash rate. Values of percent positive range between 17.1% (F3-6) and 0.6% (F4-6). High percent positive cases occur predominantly in Georgia and Louisiana. Interestingly, the cases with the lowest percent positive values (less than 3%) are confined to the Midwest. Only five cases have percent positive values greater than, or within, 1% of the average value of the synoptic storm system (9.2%). The values of the total storm flash rate range from 17.6 min^{-1} (F3-3) to 0.4 min^{-1} (F3-13). The cases with the highest total storm flash rates occur in Louisiana and Mississippi, while those cases with the lowest flash rates occur in Georgia and the Carolinas. In general, mean values of percent positive and total storm flash rate are slightly greater for F4 cases than for F3 cases. The average percentages of positive lightning for F3 and F4 cases are 5.4 percent and 7.2 percent, respectively, while the average total storm flash rates for F3 and F4 cases are 7.7 min^{-1} and 7.9 min^{-1}, respectively.

The results between the tornado path lengths and the total storm flash rates reveal no apparent correlation. While case F4-1 (path length of 128 miles) has a total storm flash rate of 16.2 min^{-1}, case F3-15 (path length of 160 miles) only has a total storm flash rate of 1.6 min^{-1}. Initially, a relationship does not appear to exist between the percentage of positive lightning and the total storm flash rate (Fig. 7.2a). However, filtering the six cases with a total storm flash rate less than 1.8 min^{-1} (F3-6, 13, 14, 15, and F4-4, 5) reveals a linear correlation with a correlation coefficient of 0.77 (Fig. 7.2b).

b. *Flash rate tendencies*

In this section the results of the 5-min flash rates associated with the total (positive and negative), negative, and positive CG flashes are provided. Table 7.2 lists the lag time between the peak in the 5-min flash rate and the tornado touchdown, and whether the largest peak in the flash rate occurred before, during, or after the time the tornado was on the ground. Values of zero minutes with an asterisk denote cases where the peak in the CG flash rate during the 30 minutes prior to tornado touchdown occurred at the 5-min interval associated with the tornado touchdown. Therefore, no discernible peaks prior to the tornado touchdown are visible. This is true for the total and negative 5-min flash rates for four F3 cases (F3-3, 5, 7, and 8), as well as for Case F3-3 and 8 for the positive 5-min flash rate. Values of zero minutes without an asterisk signify that the peak in the 5-min flash rate occurred just prior to the interval of the tornado occurrence. Double asterisks denote zero CG flashes were detected for
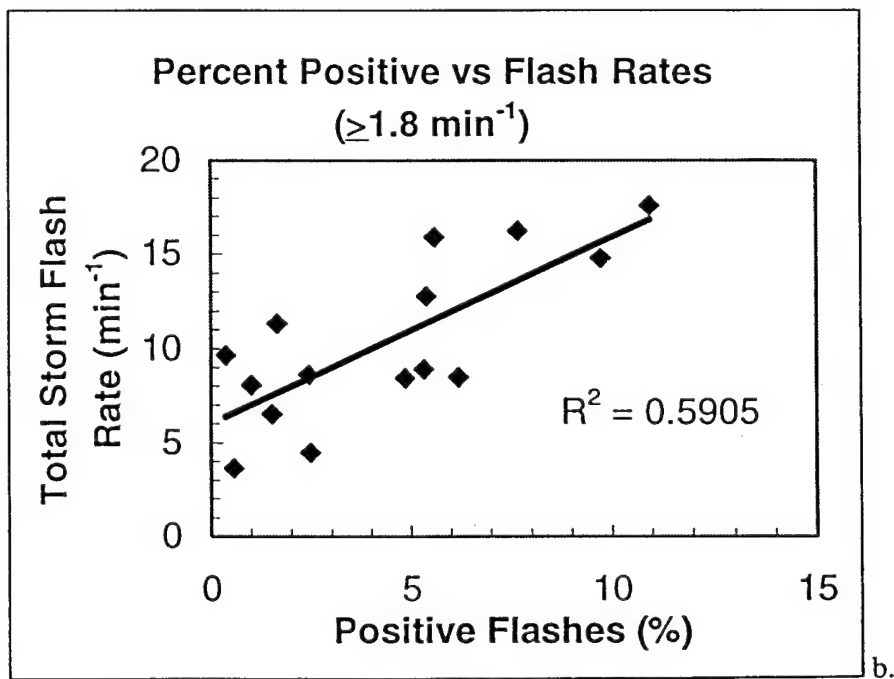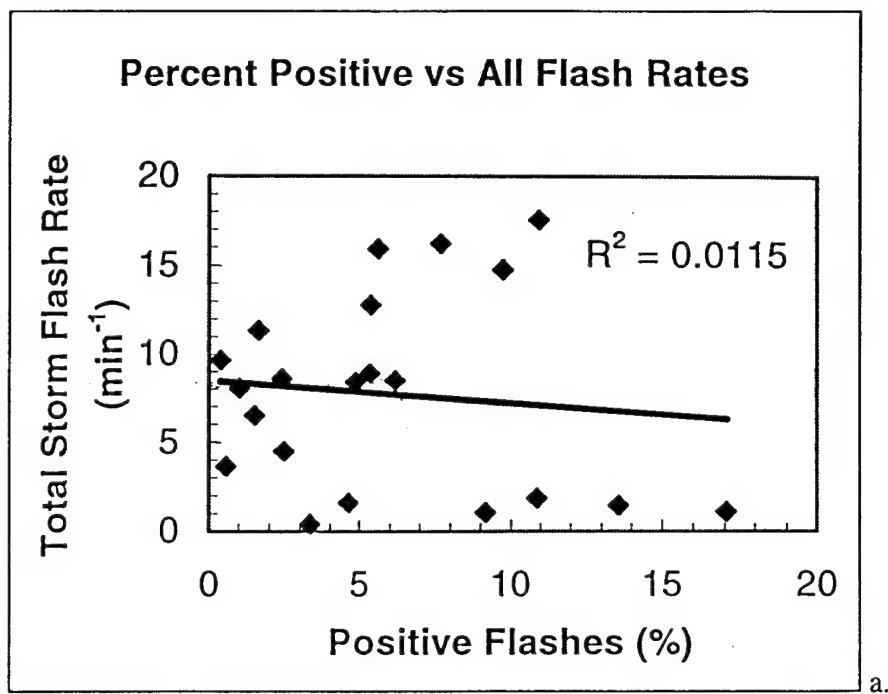
Fig. 7.2. Graph of percentage of positive flashes versus total storm flash rate for (a) all 21 cases, (b) only those cases with a total storm flash rate at least 1.8 min^{-1}.

Table 7.2. Tornado lag times. Time of the maximum peak in the CG flash rate with respect to the time of the tornado is plotted as an "x".

Case	Total Flash Rate Lag Time (min)	Positive Flash Rate Lag Time (min)	Negative Flash Rate Lag Time (min)	Pre	Dur	Post
F3-1	10	5	10	x		
F3-2	5	15	5	x		
F3-3	0*	0*	0*		x	
F3-4	5	10	5	x		
F3-5	0*	5	0*		x	
F3-6	10	25	10	x		
F3-7	0*	20	0*			x
F3-8	0*	0*	0*			x
F3-9	0	0	0			x
F3-10	0	10	0			x
F3-11	0	0	0	x		
F3-12	15	**	15		x	
F3-13	0	25	0	x		
F3-14	5	**	5	x		
F3-15	10	5	10		x	
F3 Mean	4.0	8.0	4.0			
F3 Std Dev.	4.5	9.2	4.5			
F4-1	20	15	20	x		
F4-2	25	5	25		x	
F4-3	15	5	15	x		
F4-4	5	10	5			x
F4-5	15	0	15		x	
F4-6	5	**	5	x		
F4 Mean	14.2	5.8	14.2			
F4 Std Dev.	8.0	5.6	8.0			
Total Mean	6.9	7.4	6.9			
Total Std Dev.	7.5	8.3	7.5			

* Denotes the peak in the 5-min flash rate occurred during the 5-min interval of the tornado touchdown.

** Denotes zero CG flashes of a specific type occurred prior to tornado touchdown.

the 30 minutes prior to the tornado touchdown and the 5-min interval associated with the tornado touchdown. This occurred in Case F3-12, Case F3-14, and Case F4-6 for the positive flash rate.

Average lag times, in minutes, between the peak in the total, positive, and negative flash rates to the time of the tornado touchdown for all 21 cases are 6.9, 7.4, and 6.9, respectively. When the asterisked values are ignored, the average lag times for F3 and F4 cases combined increase to approximately 8.5 minutes for the total and negative flash rates, and 8.2 minutes for the positive flash rate. The flash rates increase further when those cases where the peak in the flash rate occurred just prior to the 5-min interval of the tornado are also excluded to approximately 11 minutes for the total and negative flash rates, and 12 minutes for the positive flash rate.

Further analyses reveal nine F3 cases (1, 6, 7, 9, 10, 11, 12, 14, and 15) and one F4 (Case 6) which do not show any positive CG lightning at the 5-min interval associated with the time of the tornado touchdown. Additionally, Cases F3-12 and 14 and Case F4-6 show no positive flashes during the 30 minutes prior to tornado touchdown. Interestingly, while Case F4-6 and Case F3-14 do not show any positive lightning before touchdown, they both show a 5-min interval dominated exclusively by positive flashes after the tornadoes' demise. Also noteworthy is that Case F3-15 shows two consecutive 5-min intervals where no CG lightning was detected during the tornado. Case F3-14 shows a 5-min interval without any CG lightning prior to the tornado.

While a number of studies (MacGorman and Nielsen 1994; Seimon 1993; Curran and Rust 1992) reveal the occurrence of tornadoes to coincide with a sharp decrease

in the CG flash rate and a reversal in the dominant polarity in CG flashes, no clear polarity reversals are found. Two cases, however, do reveal a tendency for positive lightning to occur primarily during or close to the time of the tornado (F3-8 and 9), while one case (F3-10) exhibits most of the positive flashes prior and after the tornado. Nevertheless, only one 5-min interval contains exclusively positive flashes (Case F-14), and only two other 5-min intervals (Cases F3-6 and F4-4) contain percent positive flashes greater than 60%.

Contrary to Kane's (1991) findings, only seven cases show a minimum in the total lightning flash rate with respect to the 5-min interval prior to the tornado touchdown. There are no cases which show an absolute minimum in the total flash rate with respect to the 30 minutes prior to the tornado touchdown time. In 10 cases the maximum in the total CG flash rates for their study period occur prior to the tornado touchdown. The maximum peak occurs during the tornadic period for six cases, and occurs after the tornado retraction for five cases. Fifteen of the 21 cases reveal a localized maximum in the total CG flash rate to occur during the last half of the tornadic period of the storm.

The white noise test was conducted in an attempt to identify whether the peak chosen to calculate the lag time was meaningful and not an artifact of a possible periodicity in the data set. A larger periodicity is favorable to a smaller one, because there is less chance for the tornado touchdown time to coincide with a greater number of peaks given that the tornado touchdown data is $\pm$ 15 minutes. The results indicate that five of the 21 cases are white noise; therefore, no meaningful peak

determination can be made using this method. The results of the white noise test on the remaining cases show possible periodicities ranging from 6.7 to 50 minutes (Table 7.3). Thus, a single representative periodicity does not exist for all the cases. Of the cases which are white noise, 12 have periodicities greater than 15 minutes. Of these, five are associated with cases that either do not have discernable peaks or do not a have a lag time. Four of the five cases with lag times greater than or equal to 15 minutes are classified as F4 and have periodicites greater than 20 minutes. The white noise test was only able to identify seven cases where the peak in the CG flash rate may be meaningful.

c. Case study isolating the CG lightning of two Houston tornadic storms

It is fully recognized that varying degrees of contamination exists in the CG lightning signal due to the box-type sampling technique previously used. Therefore, in order to further investigate the possible relationship between tornadoes and lightning, CG flashes are isolated for two tornadic storms. The tornadic characteristics of these two storms are the same as case F3-1 and F4-1 (Table 7.1).

Figures 7.3 and 7.4 are the skew-T, log-P diagrams for Corpus Christi, Texas 1200 UTC 21 November 1992, and Lake Charles, Louisiana 0000 UTC 22 November 1992, respectively. Figure 7.3 indicates modest levels of instability with a convective available potential energy (CAPE) of 679 J kg^{-1} and strong low-level wind shear exists in the pre-storm environment. Note that the surface parcel was used to calculate the CAPE value. The range of CAPE values for moderately unstable convective days is between 1500 J kg^{-1} and 2500 J kg^{-1} (Weisman and Klemp 1986). Figure 7.4 indicates

Table 7.3. Results of white noise test.

Case	Period (min)
F3-1	10
F3-2	15.4
F3-3	28.6
F3-4	50
F3-5	16.7
F3-6	7.7
F3-7	6.7
F3-8	25
F3-9	28.6
F3-10	25
F3-11	14.3
F3-12	WN
F3-13	WN
F3-14	40
F3-15	WN
F3 Mean	22.3
F3 Std. Dev.	13.2
F4-1	40
F4-2	40
F4-3	20
F4-4	WN
F4-5	20
F4-6	WN
F4 Mean	30
F4 Std. Dev.	11.5
Total Mean	24.3
Total Std. Dev.	12.9

WN denote cases which are white noise. White noise cases are not used in the mean and standard deviation calculations.

```
921121/1200  72251    CRP        CAPE:     679
                                 BRCH:       6
                                 SHOW:       7
```
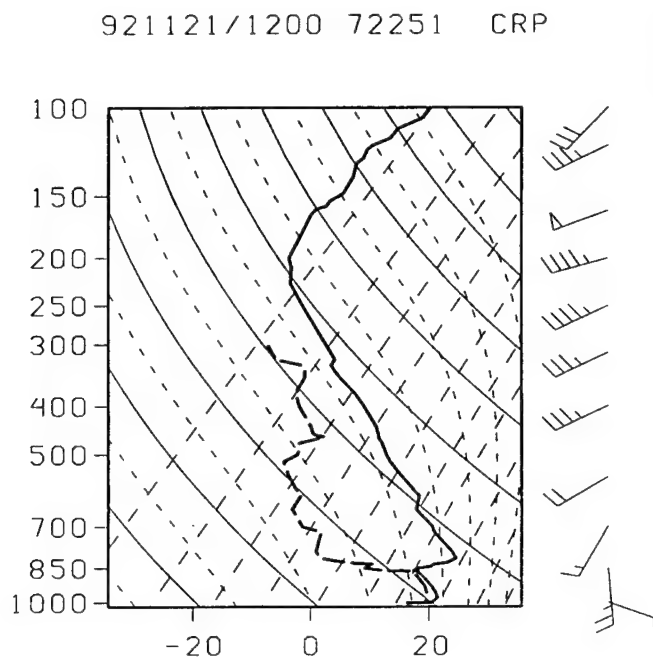
Fig. 7.3. Corpus Christi, Texas (CRP) 1200 UTC 21 November 1992 skew T-log p profile of temperature (solid line), dewpoint temperature (dashed line), and windspeed (knots). Pressure is indicated in mb, temperature in °C.


```
921122/0000  72240    LCH        CAPE:    2228
                                 BRCH:      21
                                 SHOW:      -2
```

Fig. 7.4. Same as Fig. 7.3 except for Lake Charles, Louisiana (LCH) at 0000 UTC 22 November 1992.

a highly unstable environment with a measured CAPE value of 2228 J kg^{-1} and strong low-level shear. Observed storm relative helicity values during the Houston outbreak range from 400 m^2 s^2 to over 700 m^2 s^2 (Guerrero and Read 1993). Davies-Jones et al. (1992) classify values of helicity for weak (F0-F1), strong (F2-F3), and violent (F4-F5) tornadoes as 150-299 m^2 s^2, 300-449 m^2 s^2, and $\geq$ 450 m^2 s^2, respectively.

The period when the supercell storms are first examined begins at 1942 UTC 21 November 1992. This is over 90 minutes prior to either of the tornadic events. At this time both of the storm cells are part of a linear formation of storms which is located about 90 km ahead of two other lines of convection. The strongest line of convection is located to the far left (Fig. 7.5). Over the course of the next 50 minutes the storms develop some of the characteristics indicative of supercells, such as a hook echo. Cyclonic shear at 2023 UTC is visible for the F3 storm from the 0.5° storm-relative velocity field (not shown). Fig. 7.6a is the 0.5° base reflectivity field at 2046 UTC. The locations of the F3 and F4 producing supercell storms are denoted accordingly. The F4 storm, which is located to the south of the F3 storm, has been splitting into two separate storms since approximately 2040 UTC. The left-moving supercell eventually merges into the line of convection 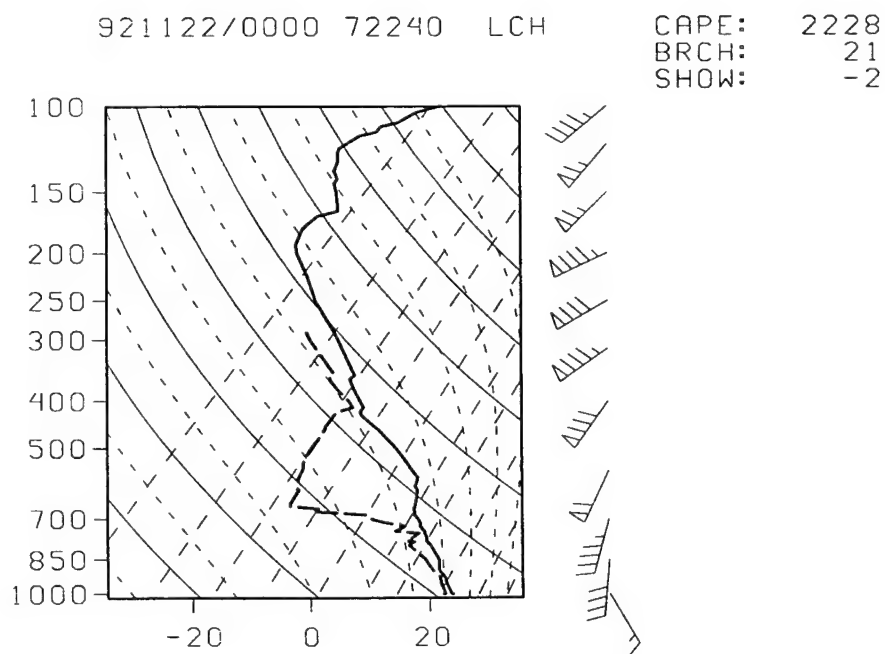to the west, while the right-moving storm intensifies. The center band of convection begins to merge with the convective line to the west. A bow in this line of convection is visible to the west of the F4 producing supercell. At 2110 UTC the F4 producing supercell spawns a short-lived F1 tornado. At 2127 UTC the F4 tornado has just touched down in Harris County, while the F3 tornado has been active for nearly seven minutes in Liberty
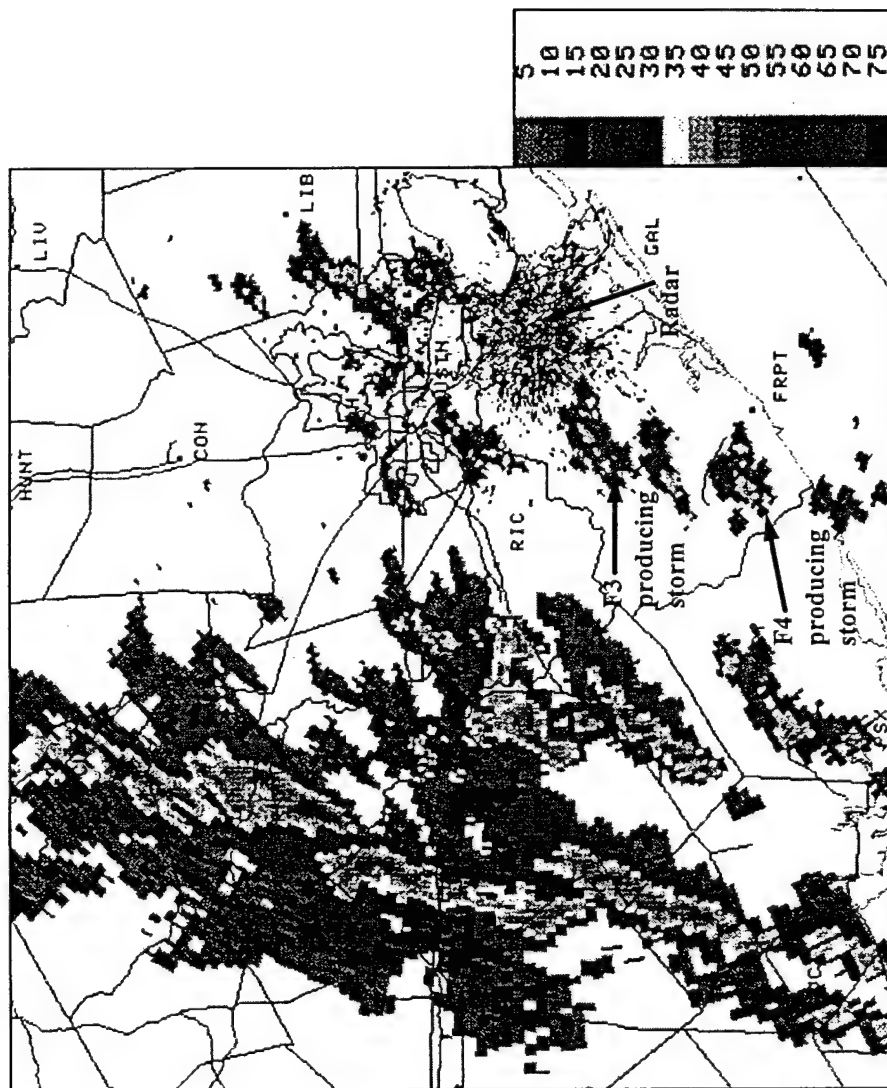
Fig. 7.5. Houston WSR-88D Doppler radar base reflectivity at 0.5° elevation angle at 1942 UTC 21 November 1992. F3 and F4 producing storms and radar location are appropriately denoted. North to south distance is approximately 250 km, and west to east distance is approximately 290 km. Reflectivity scale ranges from 5 dBZ to 75 dBZ.
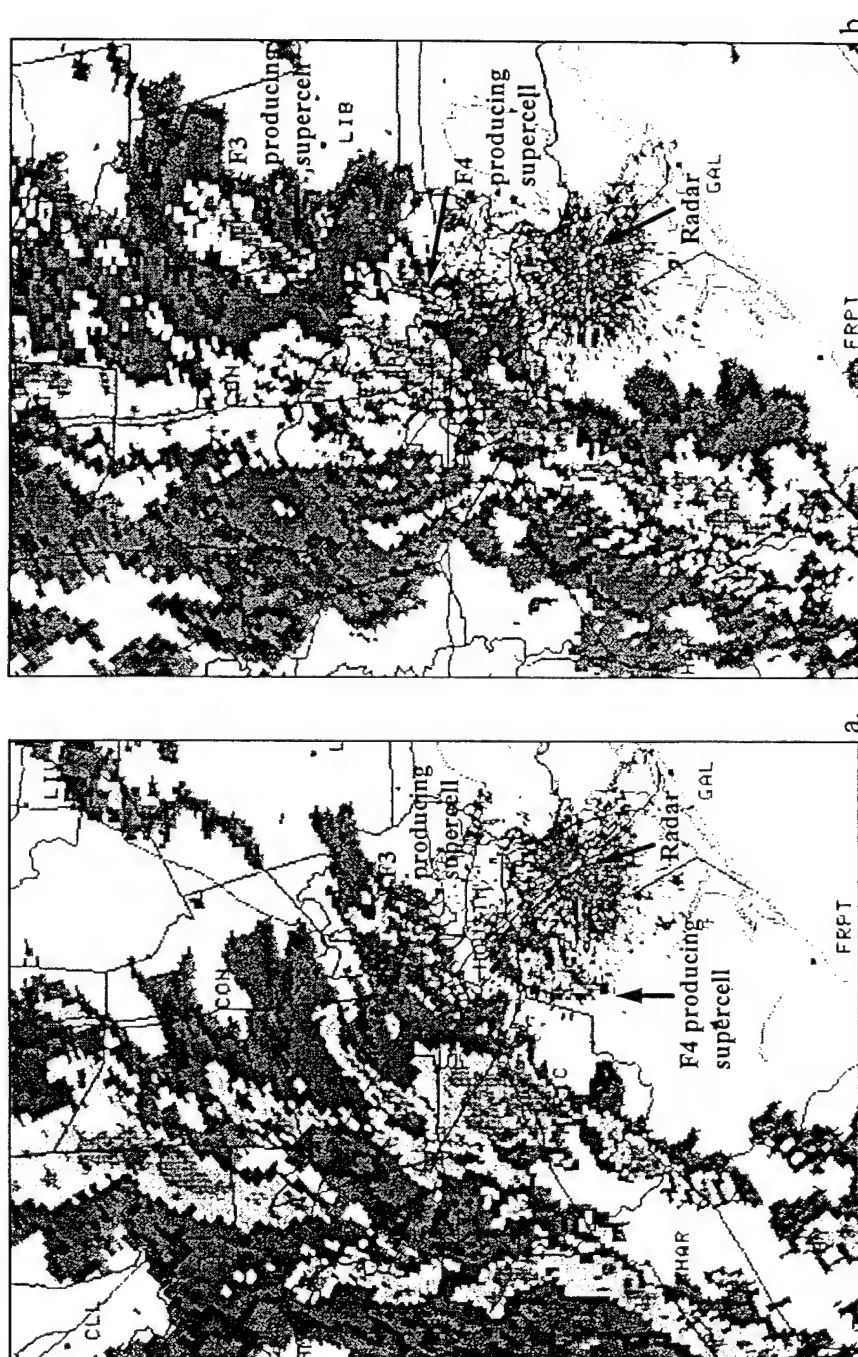
Fig. 7.6. Same as Fig. 7.5 except for (a) at 2046 UTC 21 November 1992, and (b) at 2127 UTC 21 November 1992. North to south distance is approximately 200 km, and west to east distance is approximately 150 km.

County (Fig 7.6b). Additionally, the 0.5° radar reflectivity field at this time indicates that the F4 supercell is already beginning to merge into the main line of convection. Cyclonic shear is visible ahead of the bow in the line of convection and is associated with a weaker F2 tornado which is also presently on the ground. By 2133 UTC the 0.5° radar reflectivities associated with the F4 producing supercell have fully merged with the main squall line. By 2208 UTC the F3 producing supercell storm has merged with the main squall line as depicted by the 0.5° radar reflectivity field (not shown).

The first CG flashes detected for the F3 and F4 storms occur at 2054 UTC and 2044 UTC, respectively. This is over 80 minutes prior to the touchdown of either of the tornadoes. CG lightning was only isolated until the storms' identities were no longer discernible, which is after the time they merge into the main line of convection. This was 11 minutes after the retraction time for the F3 case and six minutes for the F4 case. The CG lightning samples for both of the isolated cases are almost 90% less than their boxed-case counterparts. There are 74 and 54 total flashes associated with the F3 and F4 tornadic storms, respectively. Only two and four positive flashes were detected for each respective case. Interestingly, 3 of the 4 positive flashes detected for the F4 case are located in the downshear, low reflectivity region of the storm. This is true for one of the two positive flashes for the F3 case.

Figure 7.7a shows the 5-min running average in the CG flash rate for every minute associated with the F3 (Liberty County) tornado case. Note the flash rate begins at the time of the first detected flash. Additionally, the flash rates are multiplied by 60 to get an extrapolated hourly flash rate in order to better discern flash rate patterns. The
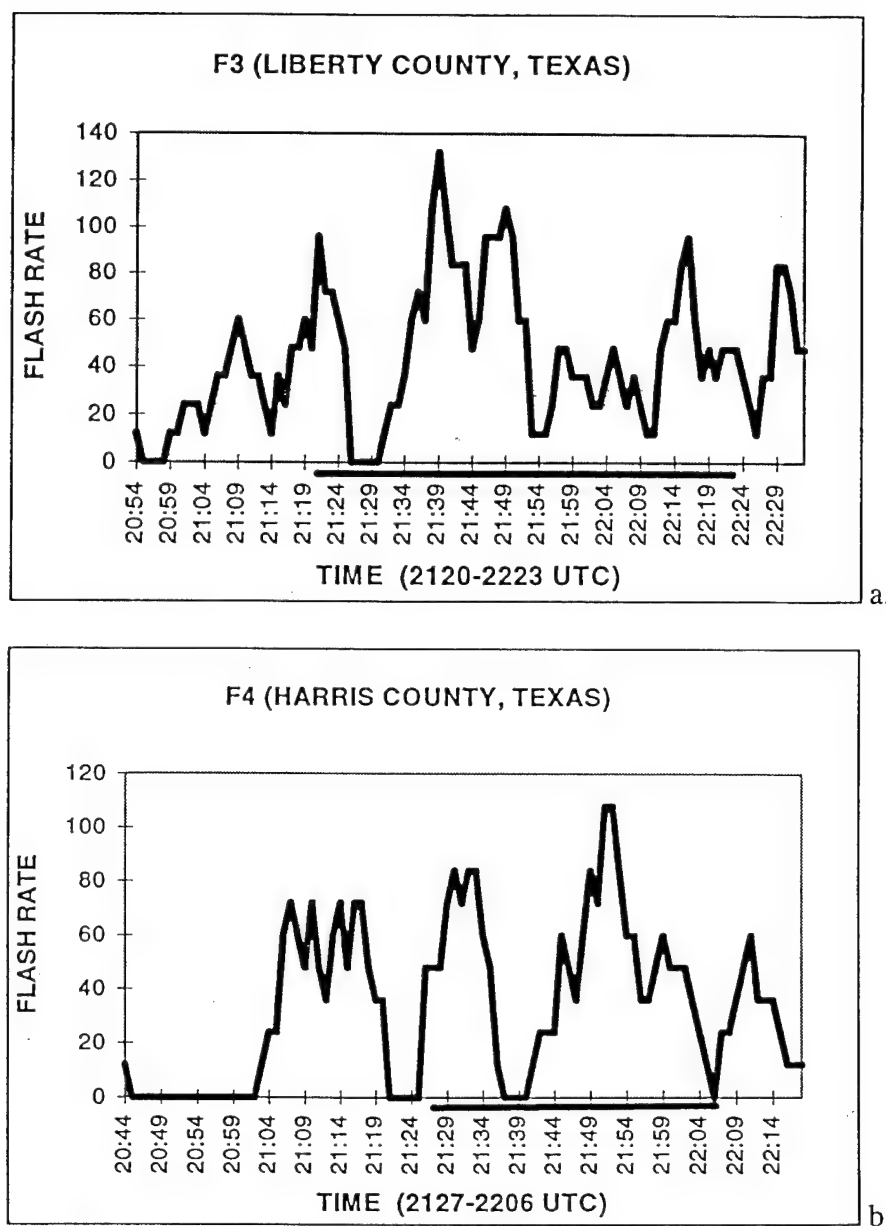
Fig. 7.7. 5-min average CG flash rate for (a) Liberty County, Texas F3 tornado, (b) Harris County, Texas F4 tornado. Thick bar represents period of the tornado. Times in parenthesis are the touchdown and retraction times for the tornadoes.

CG flash rate is seen to increase to a peak at 2109 UTC and decrease to a localized minimum at 2114 UTC. The recorded tornado touchdown occurs at 2120 UTC during an increase in the CG flash rate. Within three minutes of the peak at 2121 UTC (seven minutes after reported tornado touchdown), the average CG flash rate drops to zero for five minutes. While the flash rate does not return to zero again, other localized minima in the CG flash rate are also visible during the tornado's lifetime. These appear to occur every 10-15 minutes. The greatest peak in the flash rate occurs at 2139 UTC during the first half of the tornado's lifetime. If the peak in the CG flash rate at 2110 UTC is used to calculate a lag time similar to the previous section, then a lag time of 10 minutes is the result. This value is equivalent to the lag time found for the boxed-case counterpart.

The CG flash rate for the F4 case (Harris County) is illustrated in Fig. 7.7b. Similar to the F3 case, a series of peaks and minima are also visible. A plateau in the CG flash rate manifests itself as a series of high frequency peaks after an 18 minute void of flashes. Following this feature in the CG flash rate is a five minute period where the CG flash rate is zero. One minute after this lull in the flash rate, the tornado reportedly touches down at 2127 UTC. During the period when the tornado is on the ground, two large peaks, as well as other higher frequency peaks are visible. The largest overall peak occurs during the last half of the tornado's lifetime. Two other minima in the flash rate having zero value also occur while the tornado is on the ground, the first of which lasts for four minutes, while the other is coincidental with

the tornado retraction. The calculated lag time associated with this case is 9 minutes. This is 55% less than the 20 minute lag time found for the respective boxed case.

The results of the white noise test indicate that no serial correlation exists for either the F3 or F4 case. This is not true for their boxed-case counterparts, nor is it true for the majority of the boxed cases in general. The white noise test was also applied to the individual periods before, during, and after the tornado was on the ground. The results for both cases indicate each of these three periods was also white noise.

2. Tornado Study Discussion

The results show significant variation in the percentage of positive lightning and the total storm flash rate associated with each case. While Case F4-1 (path length of 128 miles) has a total storm flash rate of 16.2 min^{-1}, Case F3-15 (path length of 160 miles) has a total storm flash rate of only 1.6 min^{-1}. Therefore, the results between the tornado path length and the total storm flash rate reveal no correlation. This is consistent with the findings of Perez et al. (1995) who also found no correlation between the number of flashes and the duration of the tornado. Interestingly, a linear correlation with a correlation coefficient of 0.77 exists between the percentage of positive lightning and total storm flash rate for cases with flash rates greater than 1.8 min^{-1}. The five cases with flash rates less than or equal to 1.8 min^{-1} occur in either Georgia or the Carolinas, while the cases with the strongest flash rates occur in Louisiana and Mississippi. This indicates a possible regional dependence on the CG lightning characteristics.

Other instances where the CG lightning characteristics appear to have a regional

dependence also exist. A direct comparison of the F4 cases versus the F3 cases show

a slightly higher percentage of positive lightning. Additionally, five of the six F4

tornado cases occur within states along or near the Gulf of Mexico, which is the

primary source of low-level moisture for this synoptic storm system. The one F4

exception (Case 6) is found to occur in Kentucky. This is the only F4 case that did not

show any positive lightning prior to its occurrence and had the lowest percentage of

positive lightning. Additionally, all the cases with the lowest percentage of positive

lightning occur well inland (Kentucky, Indiana, and Ohio) and north of the surface

occluded front. All of these cases show at least three 5-min intervals with zero

positive flashes.

The severity and storm type are largely influenced by the environmental conditions

in which they develop (Weisman and Klemp 1984). Therefore, the CG lightning

characteristics appear to have a regional dependence, because the environment in

which the tornadic storms develop is tied to the evolution of the synoptic storm

system. The cases with the lowest percentage of positive lightning not only occur in

the Midwest, but are located just east of the triple point. All the other cases occurred

ahead of the surface cold front in the warm air sector of the surface cyclone. Based on

charge reversal microphysics, MacGorman and Nielsen (1991) hypothesize that a

lower positive region below the main negative charge region may develop if enough

collisions occur between the riming graupel and ice crystals at temperatures warmer

than the reversal temperature and colder than the freezing level. While others suggest

that the role of this smaller positive charge region is to initiate negative CG discharges and air discharges (Williams 1989), this positive charge region may also initiate positive lightning. Therefore, it is possible that there were not enough collisions between ice particles occurring below the charge reversal temperature for cases with low percentages of positive lightning.

Furthermore, the percentage of positive lightning may also be a function of the amount of liquid water content. Researchers have already made a strong case that microphysical charging due to noninductive mechanisms is a function of supercooled liquid water (Takahashi 1978; Jayaratne et al. 1983; Saunders et al. 1991; Williams et al. 1991). The charge reversal temperature is located at warmer (colder) temperatures when the liquid water content is decreased (increased) from an effective value of 1-2 g m^{-3} (Jayaratne et al. 1983). Added to this, Price and Rind (1993) found that the ratio between IC and CG lightning is dependent on the thickness of the cold cloud region in thunderstorms (0° to cloud top). From the radar summaries, the heights of the precipitation cores of the line of convection over the Midwest at the time of the associated tornadoes are generally lower by approximately 5,000 to 15,000 feet than are the storms near the Gulf of Mexico between 2235 UTC 21 November 1992 and 0735 UTC 22 November 1992.

Other studies such as MacGorman and Burgess (1994) have shown that supercell storm type appears to play an important role in the CG lightning characteristics of a storm. They found the occurrence of a tornado to coincide with the change in dominant polarity of the CG lightning, which was also tied to a change in supercell

type. While studies have shown LP supercells to be dominated by positive CG flashes and HP supercells to be dominated by negative CG flashes, none of the 21 cases reveal a substantial period when positive CG flashes were dominant. LP supercell storms normally occur near the surface dry line, while HP supercells are the most common and can occur in the humid Southeast as well as the in Great Plains (Doswell and Burgess 1993). Storms in this study were most likely HP and classical supercells. Doswell and Burgess (1993) point out that classic supercells tend to account for the majority of F4 and F5 tornadoes and tend to be associated with major outbreaks east of the Mississippi.

Examination of the total, positive, and negative lightning flash rate tendencies and the onset of tornadoes does yield lag time values which are reasonably close to Kane's (1991) findings of 10 to 15 minutes when zero lead time cases are excluded. Additionally, Kane (1991) found in two of his cases that the total flash rate at the time of the tornado touchdown was less than the prior 5-min interval. In this study, there are only 10 cases which did. There are also four cases where the total flash rate tendency increased to an absolute maximum at the time of occurrence. It should be pointed out that differing results here are most likely due to the larger area sampled and possible contamination of the lightning flash rate.

Another interesting observation is the occurrence of a pronounced peak in the total flash rate during the last half of the tornado's lifetime. This finding occurred in 12 of the 20 cases. After an examination of the histograms for Case F3-15 and Case F4-2, two events which reportedly lasted over 2.5 hours, a definite oscillation in the peaks

seems to be occurring during the tornadoes' lifetimes. Perhaps both cases were actually a series of tornadoes rather than one long-lived event. This would fit the tornado family model (Burgess et al. 1982). Added to this, it is often difficult to distinguish between single long path tornadoes and successive short path tornadoes from damage surveys (Doswell and Burgess 1988).

The results of the white noise test indicate significant variability in the periodicities and do not correlate well with the lag times. This may be expected because the amount of lightning data varied considerably from case to case; additionally, contamination of the lightning signal may have also been a problem.

The results of restricting the CG lightning to the two storms which occurred in Houston do not have the aforementioned problem of contamination of the CG lightning signal. Common to both cases is the relatively low number of total flashes and positive flashes despite the fact that one supercell produced an F4 and another an F3. Incidentally, the F4 supercell storm is smaller than the F3 storm. The dimensions of the F4 storm are only 7 km by 15 km (Guerrero and Read 1993), and may be classified in a special group of small supercells (Foster et al. 1995).

The most interesting result for the two isolated cases are that they both show a lull in the CG flash rate just prior (F4 case) or within 10 minutes of the reported tornado touchdown (F3 case). Given that the accuracy of the tornado touchdown data for these two cases are ± 6 minutes (based on the WSR-88D radial velocity fields and tornado tracks), it is conceivable that the minimum in the CG flash rate to zero for the F3 case also coincides with the tornado formation. MacGorman and Nielsen (1991)

hypothesize that flash rates for supercell storms will vary due to the strength of the mesocyclone. Stronger updrafts will tend to suspend the larger negatively charged particles. Consequently, the height of the main negative charge region will be located nearer to the main positive charge region. This favors IC flashes over CG flashes, because the breakdown potential needed for a CG flash to occur is increased. This was used to explain why the peak in the negative CG flash rate occurred 15-20 minutes after the peak in the IC flash rate during the time the storm's intensity was the greatest. Kinematic numerical cloud model simulations have added support to this theory (Ziegler and MacGorman 1994). Additionally, the results of another modeling study indicate that the development of tornado cyclones occur 5-7 minutes after an intensification of the 3-4 km updraft (Wicker and Wilhelmson 1993). The flash rates associated with the F3 and F4 cases show oscillations between the largest peaks and troughs to occur on the order of 10-15 minutes. Therefore, this may imply that the periods of low CG flash rates are associated with periods dominated by IC flashes. Rust (1989) observed that many storms, especially if they are severe, have a predominance of IC lightning and IC flash rates.

Rotational velocities for the F4 case studied here, as calculated by Livingston and Kallas (1995), indicate that by approximately 2120 UTC the strongest rotational velocities associated with the mesocyclone was located through the greatest depth of the supercell -- from the low-level to upperlevel. It follows that increased low-level convergence, which enhances the low-level mesocyclone, is indicative of strengthening updrafts. Based on the hypothesis by MacGorman et al. (1989), the CG flash rate

should be weak as the IC flash rate dominates. While IC lightning data are not available for this study, their hypothesis appears to correlate well, because the associated flash rate for the F4 case drops to zero after 2122 UTC for five minutes. However, low-level rotational velocities are missing at the time when the CG flash rate returns to zero at approximately 2139 UTC; therefore, it is impossible to assess whether the same relationship occurs. Furthermore, the rotational velocities calculated for the F3 case by Livingston and Kallas (1995) indicate that the strongest low-level rotational velocities occur at 2149 UTC, which is not coincident with the zero CG flash rate. Instead, the strongest low-level rotational velocities occur when the tornado is on the ground, and concomitant to the second largest peak in the CG flash rate. This variability may be explained by the difference in the storm structure and possibly the associated updraft intensities between the two storms. MacGorman and Nielsen (1991) noticed that in one storm case (Edmond, OK) the CG lightning flash rate was positively correlated with the low-level cyclonic shear, while another case (Binger, OK) was also negatively correlated.

While a 10-15 minute period between the largest peaks and troughs are roughly apparent, the results of the white noise test show that no serial correlation exists for any of these individual periods for either case the F3 or the F4 case. Additionally, the CG flash rate associated with the time periods before, during, and after the tornadoes were all white noise. Updraft strengths in supercells storms can vary in intensity and height (Wicker and Wilhelmson 1993); therefore, the CG flash rates may still be affected and vary accordingly, and not show a regular pattern.

CHAPTER VIII

CONCLUSIONS AND RECOMMENDATIONS

1. Conclusions

An attempt was made to study a number of CG lightning phenomena from a single

synoptic storm system with the primary goal of increasing the understanding of

lightning characteristics in severe weather systems by: 1) examining the CG lightning

characteristics of the 21-23 November 1992 widespread severe weather outbreak

relative to the position of the synoptic low pressure system; 2) correlating vertical

windshear to bipolar lightning patterns; 3) studying the percentage of positive lightning

associated with hail greater than or equal to 0.75 inches in diameter; and 4) examining

the temporal and spatial CG lightning patterns of all 21 F3 and F4 tornado occurrences

during this outbreak.

a. CG lightning with respect to the storm system

A moderate negative correlation exists between the positive flash rate and the

median first stroke peak current. This is most likely attributed to a difference in the

convective structure of the cloud which is generating the positive charge region. A

higher order negative correlation appears to exist between the negative flash rate and

the mean multiplicities. The CG lightning predominantly occur ahead of the surface

cold front during the 48 hour period. The largest maximum in the storm system CG

flash rate occurs at 0300 UTC 22 November 1992 when the low pressure is located

over northeastern Texas. High percentages of positive lightning occur north of the

lightning density centers and north of the triple point. One major exception occurred between 1200 UTC 22 November 1992 and 0000 UTC 23 November 1992 when a number of percentage of positive lightning maxima associated with a decrease in the amount of convection were located southeast of the triple point. A stronger preference for the occurrence of positive lightning appears to be associated with the cold air region of the synoptic storm system. This may be attributed to lower theta-e values and thus lower convective instability. Locations in the maxima of positive flash density were consistently displaced to the north or east of the negative ground flash density maxima locations.

b. *The effects of shear on bipolar lightning patterns*

The average bipole lengths were 50% shorter than previous studies of wintertime bipoles. Average bipole durations were also shorter. The bipolar patterns in this study were more closely aligned with the shear vector associated with the lower layers of this intense storm system. In 13 of the 18 cases the bipole was aligned with the shear vector associated with the 700 mb-surface layer. The average orientation of the bipolar patterns were from 194°, with the positive flash region located downshear of the negative flash region. One of the bipole patterns, which was aligned but oriented 180° out of phase with the shear vector, was located to the west of the surface low center. In this case the positive flashes were located upshear of the negative flash region, similar to the observations of a number of studies which have found positive and negative lightning to be associated with the stratiform and convective regions of squall lines. Therefore, local advection of positive charges or a separate in situ

charging mechanism associated with positive lightning may be responsible. No correlation between the magnitude of the shear vector and the length of the bipolar pattern was found.

c. Large hail and the percentage of positive lightning

A relationship between high percentages of positive lightning and hail does not exist for this study. This is attributed to the fact that storms producing high percentages of positive lightning can be associated with LP supercell storms. Due to the location of the outbreak near the Gulf of Mexico, it is most likely that many of the supercell storms were either classic or of the more common HP supercell variety. Added to this, negative flashes are generally associated with the convective region of storms which produce hail. The highest concentration of hail events occurred in the Midwest. These cases showed relatively low numbers of positive lightning; only two positive flashes were detected for the sample regions associated with the large hail-producing storms.

d. Lightning and tornadic activity

A relationship between the total number of flashes and the duration of the tornado does not exist. Cases with the highest percentage of positive lightning occurred in Louisiana and Georgia. Those storms with the lowest percentage of positive lightning occurred in the Midwest. A reversal in the dominant polarity of CG lightning coincident to the touchdown of a tornado was not found. This was attributed to the likelihood that most of the tornadic supercells were of the more common HP type. An average lag time of approximately 10 minutes was found between the peak in the 5-

min flash rate and the 5-min interval associated with the tornado touchdown. Since

varying degrees of contamination exists for the tornado cases as sampled by a box

region, two Houston tornadic cases for which CG flashes could be isolated to were

studied. The most interesting result of these two cases is the existence of a zero CG

flash rate just prior (F4 case) or within 10 minutes (F3 case)of the reported

touchdown. Strong rotational velocities extending down to the low levels of the

supercell storm during the F4 case lend some support to the hypothesis that IC flashes

dominant while CG flashes are suppressed during strong updrafts. However, the

existence of strong rotational velocities throughout the depth of the supercell storm

did not coincide with two other occurrences where the CG flash rate decreased to

zero.

2. Recommendations

a. CG lightning with respect to the storm system

Investigate the lightning characteristics associated with a number of synoptic storm

systems. These should be categorized by surface low pressure origination and season.

Not only investigate the lightning characteristics in a similar manner to this study, but

separate the CG lightning into warm and cold air origination. Use an appropriate

1,000-500 mb thickness line to demarcate the thermal boundary between the cold air

region of the warm air sector of the surface cyclone. Additionally, analysis of the

relationship between positive lightning and its median peak current as well as the

relationship between negative lightning and its median peak current should be carried

out with a larger data set, such as on a yearly time scale.

b. The effects of shear on bipolar lightning patterns

Further studies concerning the shear vector and bipolar patterns are needed in conjunction with Doppler radar data and microphysical data to test the advection theory of positive charge, and if an in situ charging mechanism within the stratiform cloud region is partially responsible for the production of positive lightning.

c. Large hail and the percentage of positive lightning

Evaluate the percentage of positive lightning and large hail on a larger time scale (monthly, yearly, etc.). Use Doppler radar data to isolate CG lightning to the hail producing storm, then examine the flash rate tendencies associated with it.

d. Lightning and tornadic activity

Only examine the lightning directly associated with the tornadic storm. Use Doppler radar data to isolate the appropriate CG lightning. Compare the flash rate tendencies of tornadic storms to non-tornadic storms which occur in similar environments. Determine if a lull in the CG flash rate systematically occurs in tornadic storms and at what point in the storm's lifetime it is useful to examine the CG flash rate. Additionally, the study should use dual Doppler analysis to calculate vertical velocities in order to test MacGorman et al.'s (1989) hypothesis that strong updrafts may inhibit the production of CG flashes, while favoring the production of IC flashes.

e. *Miscellaneous*

Use caution when using the NSSFC data base. If available, incorporate IC lightning data and microphysical data to test the ice-ice noninductive process of charge separation.

REFERENCES

Bluestein, H. B., 1992: *Synoptic-Dynamic Meteorology in Midlatitudes.* Vol. 1. *Principles of Kinematics and Dynamics.* Oxford University Press, 431 pp.

Branick, M. L., and C. A. Doswell III, 1992: An observation of the relationship between supercell structure and lightning ground strike polarity. *Wea. Forecasting,* 7, 143-149.

Brook, M., M. Nakano, and P. Krehbiel, T. Takeuti, 1982: The electrical structure of the Hokuriku winter thunderstorms. *J. Geophys. Res.,* 87, 1207-1215.

_____, R. W. Henderson, and R. B. Pyle, 1989: Positive lightning strokes to ground. *J. Geophys. Res.,* 94, 13 295-13 303.

Burgess, D. W., V. T. Wood, and R. A. Brown, 1982: Mesocyclone evolution statistics. Preprints, *12th Conference on Severe Local Storms,* San Antonio, TX, Amer. Meteor. Soc., 422-424.

Changnon, S. A., 1992: Temporal and spatial relations between hail and lightning. *J. Appl. Meteor.,* 31, 587-604.

Curran, E. B., and W. D. Rust, 1992: Positive ground flashes produced by low-precipitation thunderstorms in Oklahoma on 26 April 1984. *Mon. Wea. Rev.,* 120, 544-553.

Davies-Jones, R. P., D. W. Burgess, and M. P. Foster, 1990: Test of helicity as a tornado forecast parameter. Preprints, *16th Conference on Severe Local Storms,* Kananaski Park, Alberta, Canada, Amer. Meteor. Soc., 588-592.

Doswell, C. A., III, and D. W. Burgess, 1988: On some issues of United States tornado climatology. *Mon. Wea. Rev.,* 116, 495-501.

_____, and _____, 1993: Tornadoes and tornadic storms: A review of conceptionual models. *The tornado: Its structure, dynamics, prediction, and hazards, AGU Monogr.,* No. 79, Amer. Geophys. Union, 161-172.

_____, and H. E. Brooks, 1993: Comments on "Anomalous cloud-to-ground lightning in an F5 tornado producing supercell thunderstorm on 28 August 1990." *Bull. Amer. Meteor. Soc.,* 74, 2213-2218.

Engholm, C. D., E. R. Williams, and R. M. Dole, 1990: Meteorological and electrical conditions associated with positive cloud-to-ground lightning. *Mon. Wea. Rev.*, **118**, 470-487.

Foster, M. P., A. R. Moller, L. J. Wicker, and L. Cantrell, 1995: The rapid evolution of a tornadic small supercell, observations and simulation. Preprints, *14th Conference on Weather Analysis and Forecasting*, Dallas, TX, Amer. Meteor. Soc., 323-328.

Fujita, T. T., 1981: Tornadoes and downbursts in the context of generalized planetary scales. *J. Atmos. Sci.*, **38**, 1511-1534.

Fuquay, D. M., 1982: Positive cloud-to-ground lightning in summer thunderstorms. *J. Geophys. Res.*, **87**, 7131-7140.

Goodge, G. W., Ed., 1993: *Storm Data*. NOAA, U.S. Dept. of Commerce, 99 pp.

Grazulis, T. P., 1991: *Significant Tornadoes, 1880-1989,* Vol. 1. *Discussion and Analysis.* Environmental Films, 526 pp.

Guerrero, H., and W. Read, 1993: Operational use of the WSR-88D during the November 21 1992 Southeast Texas tornado outbreak. Preprints, *17th Conference on Severe Local Storms/Conference on Atmospheric Electricity,* St. Louis, MO, Amer. Meteor. Soc., 399-402.

Hart, J. A., 1993: A new method of assessing and manipulating the NSSFC severe weather database. Preprints, *17th Conference on Severe Local Storms/Conference on Atmospheric Electricity,* St. Louis, MO, Amer. Meteor. Soc., 40-41.

Holzer, R. E., 1953: Simultaneous measurement of sferics signals and thunderstorm activity. *Thunderstorm Electricity*, H. R. Byers, Ed., University of Chicago Press, 267-275.

Illingworth, A. J., 1985: Charge separation in thunderstorms: Small scale processes. *J. Geophys. Res.*, **90**, 6026-6032.

Jayaratne, E. R., C. P. R. Saunders, and J. Hallet, 1983: Laboratory studies of the charging of soft-hail during ice crystal interactions. *Quart. J. Roy. Meteor. Soc.*, **109**, 609-630.

Kane, R. J., 1991: Correlating lightning to severe storms in the Northeastern United States. *Wea. Forecasting*, **6**, 3-12.

Koch, S. E., M. desJardins, and P. J. Kocin, 1983: An interactive Barnes objective map analysis scheme for use with satellite and conventional data. *J. Climate Appl. Meteor.*, **22**, 1487-1503.

Livingston J., and T. Kallas: 1994: Tornadic mesocyclones observed by the Houston WSR-88D. Southern Region Scientific Services Division TA 94-58, NOAA, U.S. Dept. of Commerce, 7 pp.

MacGorman, D. R., D. W. Burgess, V. Mazur, W. D. Rust, W. L. Taylor, and B. C. Johnson, 1989: Lightning rates relative to tornadic storm evolution on 22 May 1981. *J. Atmos. Sci.*, **46**, 221-250.

_____, and K. E. Nielsen, 1991: Cloud-to-ground lightning in a tornadic storm on 8 May 1986. *Mon. Wea. Rev.*, **119**, 1557-1574.

_____, 1993: Lightning in tornadic storms: A review. *The tornado: Its structure, dynamics, prediction, and hazards, AGU Monogr.*, No. 79, Amer. Geophys. Union, 173-182.

_____, and D. W. Burgess, 1994: Positive cloud-to-ground lightning in tornadic storms and hailstorms. *Mon. Wea. Rev.*, **122**, 1671-1697.

Natural Disaster Survey Report, 1993: The widespread November 21-23, 1992, tornado outbreak: Houston to Raleigh and Gulf Coast to Ohio Valley. NOAA, U.S. Dept. of Commerce, 119 pp.

Newton, H. J., 1988: *TIMESLAB: A Time Series Analysis Laboratory.* Wadsworth & Brooks/Cole Publishing Company, 92 pp.

Nielsen, K. E., 1994: The evolution of cloud-to-ground lightning within a portion of the 10-11 June 1985 squall line. *Mon. Wea. Rev.*, **122**, 1809-1817.

Orville, R. E., R. A., Wiesman, R. B. Pyle, R. W. Henderson, and R. E. Orville, Jr., 1987: Cloud-to-ground lightning flash characteristics from June 1984 through May 1985. *J. Geophys. Sci.*, **92**, 5640-5644.

_____, R. W. Henderson, and L. F. Bosart, 1988: Bipole patterns revealed by lightning locations in mesoscale storm systems. *Geophys. Res. Lett.*, **15**, 129-132.

_____, 1994: Cloud-to-ground lightning characteristics in the contiguous United States: 1989-1991. *J. Geophys. Res.*, **99**, 10 833-10 841.

Perez, A. H., R. E. Orville, and L. J. Wicker, 1995: Characteristics of cloud-to-ground lightning associated with violent-tornado producing supercells. Preprints, *14th Conference on Weather Analysis and Forecasting*, Dallas, TX, Amer. Meteor. Soc., 409-413.

Prentice, S. A., and D. Mackerras, 1977: The ratio of cloud to cloud-ground lightning flashes in thunderstorms. *J. Appl. Meteor.*, **16**, 545-550.

Price, P., and D. Rind, 1993: What determines the cloud-to-ground lightning fraction in thunderstorms. *Geophys. Res. Lett.*, **20**, 463-466.

Reap, R. M., and D. R. MacGorman, 1989: Cloud-to-ground lightning: Climatological characteristics and relationships to model fields, radar observations, and severe local storms. *Mon. Wea. Rev.*, **117**, 518-535.

Riordan, A. J., M. D. Vescio, and K. K. Keeter, 1993: An overview of the severe weather outbreak of 21-23 November 1992. Preprints, *17th Conference on Severe Local Storms/Conference on Atmospheric Electricity*, St. Louis, MO, Amer. Meteor. Soc., 613-617.

Rotunno, R., and J. B. Klemp, 1985: On the rotation and propagation of simulated supercell thunderstorms. *J. Atmos. Sci.*, **42**, 271-292.

Rust, W. D., W. L. Taylor, D. R. MacGorman, and R. T. Arnold, 1981: Research on electrical properties of severe thunderstorms in the Great Plains. *Bull. Amer. Meteor. Soc.*, **62**, 1286-1293.

_____, D. R. MacGorman, and S. J. Goodman, 1985: Unusual positive cloud-to-ground lightning in Oklahoma storms on 13 May 1983. Preprints, *14th Conference on Severe Local Storms*, Indianapolis, IN, Amer. Meteor. Soc., 372-375.

_____, 1989: Utilization of a mobile laboratory for storm electricity measurements. *J. Geophys. Res.*, **94**, 13 305-13 311.

Rutledge, S. A., and D. R. MacGorman, 1988: Cloud-to-ground lightning activity in the 10-11 June 1985 mesoscale convective system observed during the Oklahoma-Kansas PRE-STORM project. *Mon. Wea. Rev.*, **116**, 1393-1407.

_____, C. Lu, and D. R. MacGorman, 1990: Positive cloud-to-ground lightning in mesoscale convective systems. *J. Atmos. Sci.*, **47**, 2085-2100.

_____, E. R. Williams, and W. A. Petersen, 1993: Lightning and electrical structure of mesoscale convective systems. *Atmos. Res.*, **29**, 27-53.

Saunders, C. P. R., 1988: Thunderstorm electrification. *Weather,* **43**, 318-324.

_____, W. D. Keith, and R. P. Mitzeva, 1991: The effect of liquid water on thunderstorm charging. *J. Geophys. Res.,* **96**, 11 007-11 017.

Seimon, A., 1993: Anomalous cloud-to-ground lightning in an F5-tornado producing supercell thunderstorm on 28 August 1990: *Bull. Amer. Meteor. Soc.,* **74**, 189-203.

Silver, A., and R. E. Orville, 1995: A climatology of cloud-to-ground lightning for the contiguous United States: 1992-1993. Preprints, *9th Conference of Applied Climatology*, Dallas, TX, Amer. Meteor. Soc., 325-330.

Smith, S. B., J. G. LaDue, and D. R. MacGorman, 1995: Integrated data sets in the study of and forecasting of thunderstorms. Preprints, *14th Conference on Weather Analysis and Forecasting*, Dallas, TX, Amer. Meteor. Soc., 347-351.

Stolzenburg, M., 1990: Characteristics of the bipolar pattern of lightning locations observed in 1988 thunderstorms. *Bull. Amer. Meteor. Soc.,* **71**, 1331-1338.

_____, 1994: Observations of high ground flash densities of positive lightning in summertime thunderstorms. *Mon. Wea. Rev.,* **122**, 1740-1750.

Takahashi, T., 1978: Riming electrification as a charge generation mechanism in thunderstorms. *J. Atmos. Sci.,* **35**, 1536-1548.

Taylor, W. L., 1973: Electrical radiation from severe storms in Oklahoma during April 29-30 1970. *J. Geophys. Res.,* **78**, 8761-8777.

Turman, B. N., and R. J. Tettlebach, 1980: Synoptic-scale satellite lightning observations in conjuction with tornadoes. *Mon. Wea. Rev.,* **180**, 1878-1882.

Uman, M. A., 1987: *The Lightning Discharge*. Academic Press, Inc., 190 pp.

Wallace, J. M., and P. V. Hobbs, 1977: *Atmospheric Science*. Academic Press, Inc., 467 pp.

Weisman, M. L., and J. B. Klemp, 1986: Characteristics of isolated convective storms. *Mesoscale Meteorology and Forecasting*, P. S. Ray, Ed., Amer. Meteor. Soc., 331-358.

Wicker, L. J., and R. B. Wilhelmson, 1993: Numerical simulation of tornadogenesis within a supercell thunderstorm. *The tornado: Its structure, dynamics, prediction, and hazards, AGU Monogr.*, No. 79, Amer. Geophys. Union, 75-87.

Williams, E. R., 1989: The tripole nature of thunderstorms. *J. Geophys. Res.*, **94**, 13 151-13 167.

_____, R. Zhang, and J. Rydock, 1991: Mixed-phase microphysics and cloud electrification. *J. Atmos Sci.*, **48**, 2195-2203.

_____, and D. Boccippio, 1993: Dependence of cloud microphysics and electrification on mesoscale vertical air motions in stratiform precipitation. Preprints, *17th Conference on Severe Local Storms/Conference on Atmospheric Electricity*, St. Louis, MO, Amer. Meteor. Soc., 399-402.

Ziegler C. L., and D. R. MacGorman, 1994: Observed lightning morphology relative to modeled space charge and electric field distributions in a tornadic storm. *J. Atmos. Sci.*, **51**, 833-851.

APPENDIX A

THE FUJITA TORNADO INTENSITY SCALE (F-SCALE)

Table A.1. Fujita scale.*

Category	Windspeed (mph/m s^{-1})	Definition/Damage Description
F0	40-72 18-32	Gale Tornado: Light damage. Some damage to chimneys; break branches off trees; push over shallow-rooted trees; damage sign boards
F1	73-112 33-49	Moderate Tornado: Moderate damage. The lower limit is the begining of hurricane wind speed; peel surface off roofs; mobile homes pushed off foundations or overturned; moving autos pushed off roads.
F2	113-157 50-69	Significant Tornado: Considerable damage. Roofs torn off frame houses; mobile homes demolished; boxcars pushed over; large trees snapped or uprooted; light-object missiles generated.
F3	158-206 70-92	Severe Tornado: Severe damage. Roofs and some walls torn off well-constructed houses; trains overturned; most trees in forest uprooted; heavy cars lifted off ground and thrown.
F4	207-260 93-116	Devasting Tornado: Devasting damage. Well-constructed houses leveled; structure with weak foundation blown off some distance; cars thrown and large missiles generated.
F5	261-318 117-142	Incredible Tornado: Incredible damage. Strong frame houses lifted off foundations and carried considerable distance to disintegrate; automobile-sized missles fly through the air in excess of 100 m; trees debarked; incredible phenomena will occur.
F6-F12	319-Mach 1 142-Mach 1	Inconceivable Tornado: The maximum wind speeds of tornadoes are not expected to reach the F6 wind speeds.

* From Fujita (1981)

VITA

William John Carle was born on 29 September 1968 in Tainan, Taiwan, Republic of China to Edward Russell and Pao-Chu Carle. As the son of an Air Force officer, he spent his childhood years living in a number of western states to include, California, Hawaii, Washington, and Utah, where he graduated from Brighton High School in Salt Lake City.

William started his military career by attending and graduating from the United States Air Force Academy in May 1990 with a Bachelor of Science degree. In December of the same year, he attended Texas A&M University under the supervision of the Air Force Institute of Technology (AFIT). After graduating from Texas A&M University in December 1992 with a Bachelor of Science degree in meteorology, he was assigned to Fort Ord, California to provide weather support to the Army's 7th Infantry Division (Light). Later, he was once again accepted by AFIT and Texas A&M University's Meteorology Department and returned to College Station in August of 1993. He conducted research under the direction of Dr. Richard E. Orville, Dr. John W. Nielsen-Gammon, and Dr. Jay N. Livingston. During his tenure at Texas A&M University, he wrote a paper with Dr. Orville for the American Meteorological Society's 14th Conference on Weather Analysis and Forecasting entitled, "The 21-23 November 1992 Severe Weather Outbreak: Correlation Between Lightning Flash Rate Tendencies and Tornadic Activity, and Shear Versus Bipolar Patterns."

William's permanent address is 2596 E. Dolphin Way, Salt Lake City, Utah 84121.